FIRST PRINCIPLES CALCULATION OF THE IMAGINARY PORTION OF THE DIELECTRIC FUNCTION FOR DIAMOND AND SILICON

By

DOYLE FRANK FOUQUET II

Bachelor of Science

Oklahoma State University

Stillwater, Oklahoma

1970

Submitted to the Faculty of the Graduate College
of the Oklahoma State University
in partial fulfillment of the requirements
for the Degree of
MASTER OF SCIENCE
July, 1973

FIRST PRINCIPLES CALCULATION OF THE IMAGINARY

PORTION OF THE DIELECTRIC FUNCTION

FOR DIAMOND AND SILICON

Thesis Approved:

Earl E. Lafon
Thesis Adviser

P. A. Westhaus

Richard C. Powell

N. N. Durham
Dean of the Graduate College

ACKNOWLEDGEMENTS

The author wishes to take this opportunity to express his gratitude to Dr. Earl E. Lafon for suggesting the problem and for his invaluable assistance and guidance in carrying out the research which is to be reported in this thesis.

The author also wishes to express his appreciation to the Aerospace Research Laboratories, Air Force Systems Command, United States Air Force, Wright-Patterson Air Force Base, Ohio, for partial support and funding this project.

Finally, special thanks is expressed to my wife, Pat, and daughter, Tessa, for their understanding, encouragement, and support.

TABLE OF CONTENTS

LIST OF TABLES

LIST OF FIGURES

CHAPTER I

INTRODUCTION

Because the imaginary portion of the dielectric function is important in describing the optical properties of semiconductors, the objective of this investigation is to extend the theoretical framework of tight-binding to a first principles calculation of the imaginary portion of the dielectric function as well as the density and joint density of states. Diamond and silicon are used to test the extended procedure. A tight-binding calculation of the electronic band structure is used as a starting point. The transition matrix elements as well as all other necessary quantities are evaluated from first principles.

Diamond and silicon are among the most studied of all materials, but the agreement between experiment and theory for their optical properties is still inconclusive. Silicon band structures have been calculated using Orthogonalized Plane Waves (1,2), pseudopotentials (3, 4,5), k·p techniques (6) and the tight-binding method (7), however, a first principles calculation of the dielectric function does not exist to date.

The best silicon work so far appears to be that of Stukel and Euwema (8) using the Self-Consistent Orthogonalized Plane Wave Method, but still some prominent features are not yet in complete agreement with experimental results (9).

In a recent study, Painter, Ellis and Lubinsky (10) have examined

the optical properties of diamond resulting from the electronic structure using the Discrete Variational Method. Their work is the first ab inito calculation of the dielectric function for diamond or any other material. This work represents another first principles calculation of the dielectric function using the framework of the tight-binding scheme.

A. Atomic Units

In this study, Hartree atomic units will be used. These units are defined in Table I. All numerical values, equations and data in this work will be given in these units unless otherwise specified.

TABLE I

HARTREE ATOMIC UNITS

Unit	Equivalent	Numerical Value
Mass	rest mass of the electron	9.1091×10^{-28} gm
Length	radius of first Bohr orbit of Hydrogen	0.529167×10^{-8} cm
Energy	twice the ionization energy of the ground state of Hydrogen	27.2106 eV
Charge	charge on the electron	1.6021×10^{-19} C

B. Symmetry and Structure

To describe the periodic structure of a crystal, it is convenient to define a set of linearly independent vectors $\bar{a}_1$, $\bar{a}_2$, $\bar{a}_3$, called primitive basis vectors, such that the atomic structure remains invariant under translations of integer combinations of these vectors. The combination is known as a translation vector and is of the form

$$\bar{R}_n = n_1\bar{a}_1 + n_2\bar{a}_2 + n_3\bar{a}_3, \tag{1-1}$$

where n_1, n_2 and n_3 are required to be integers. The set of points obtainable from various combinations of the n's are the lattice sites for a particular Bravais lattice.

Lattice sites need not be occupied by an atom of the crystal. Associated with each lattice site is an unit assembly of atoms, ions, etc., called the basis. A set of basis vectors then describes the positions of basis components with respect to the lattice site. This set of basis vectors is referred to as nonprimitive translations.

Of the fourteen Bravais lattices, silicon and one form of crystalline carbon, diamond, are of the face centered cubic type, but having two atoms per unit cell. The face centered cubic lattice is one where there is a lattice site at each corner of a cube and at the center of each face. The basis of both diamond and silicon consists of two atoms with nonprimitive translations of $+\sqrt{3}\ a_0/8$ and $-\sqrt{3}\ a_0/8$ along the (111) line. Where a_0 is the edge length of the face centered cube and (111) is the Miller indice notation. In terms of the atomic positions, the structure is two meshed faced centered cubic lattices, with atoms at the lattice sites, shifted $\sqrt{3}\ a_0/4$ along the (111) direction.

From the group theory standpoint, both the diamond and the silicon lattices belong to the point group O_h using the Schoenflies notation (11). The space group made by combining the rotations and reflections of the point group with the translations, $\overline{R_n}$, is O_h^7 and is nonsymmorphic. The individual atoms are in a tetrahedral environment of symmetry T_d.

Conceptually, the Wigner Seitz unit cell more clearly displays the rotational symmetry properties of the crystal. The Wigner Seitz cell is defined as the volume enclosed by planes which are perpendicular bisectors of the vectors from any chosen lattice site to all surrounding lattice sites.

A section of the Wigner Seitz cell is designated as a fundamental wedge. The fundamental wedge is selected such that each operation of T_d and the remaining operations of the point group with the nonprimitive translations maps a point inside the wedge onto an equivalent point inside the Wigner Seitz cell but outside the fundamental wedge. The point group for diamond and silicon has 48 elements, hence the fundamental wedge occupies 1/48th of the volume of the Wigner Seitz cell. Any numerical value or function which has the symmetry properties of the crystal and is associated with a position inside the wedge has the same value at the mapped location outside the wedge as the original position except for a phase factor. Only the contents of the fundamental wedge need be considered.

As a result of the translational invariance of the crystal potential and charge density, they have the periodicity of the lattice such that

$$f(\overline{r}) = f(\overline{r} + \overline{R_n}). \tag{1-2}$$

These functions can be described as a Fourier series given by

$$f(\bar{r}) = \Sigma_j A_{K_j} e^{i\bar{K}_j \cdot \bar{r}}, \tag{1-3}$$

where $\bar{K}_j$ is a reciprocal lattice vector such that

$$\bar{K}_j \cdot \bar{R}_n = 2\pi(\text{integer}). \tag{1-4}$$

To construct the reciprocal lattice vectors the reciprocal triad of the primitive basis vectors is taken giving

$$\bar{b}_1 = \frac{2\pi(\bar{a}_2 \times \bar{a}_3)}{\bar{a}_1 \cdot (\bar{a}_2 \times \bar{a}_3)}$$

$$\bar{b}_2 = \frac{2\pi(\bar{a}_3 \times \bar{a}_1)}{\bar{a}_1 \cdot (\bar{a}_2 \times \bar{a}_3)} \tag{1-5}$$

$$\bar{b}_3 = \frac{2\pi(\bar{a}_1 \times \bar{a}_2)}{\bar{a}_1 \cdot (\bar{a}_2 \times \bar{a}_3)} .$$

The vectors

$$\bar{K}_n = n_1\bar{b}_1 + n_2\bar{b}_2 + n_3\bar{b}_3, \tag{1-6}$$

define a reciprocal lattice spanned by the vectors $\bar{b}_1$, $\bar{b}_2$ and $\bar{b}_3$. The Wigner Seitz cell of the reciprocal cell is called the Brillouin zone. The reciprocal lattice for the face centered cubic lattice possessed by diamond and silicon is the body centered cubic.

CHAPTER II

BAND STRUCTURE CALCULATION

A. Bloch Sums

The tight-binding method demonstrates the concept of energy bands in crystalline materials. Consider N atoms in periodic array with one atom per unit cell, kept far apart so there is no orbital overlap. Each atom will have atomic levels ϕ_1, ϕ_2, ϕ_3, etc. given by the solution of the free atom problem. Each individual atom contributes a state for each electron, increasing the degeneracy N-fold.

As the atoms are brought closer together, the orbitals overlap and the degeneracy is split into a band of states. A complete band of states arises from each atomic level. If the atoms are not too close together, the bands retain their atomic nature and can be associated with the atomic states.

Figure 1 shows the bands arising from the 1s, 2s and 2p atomic states of diamond as a function of interatomic distance. Silicon diagrams are quite similar.

As the interatomic distance is decreased, the bands broaden and may eventually overlap. The change from a spherical to a periodic environment causes the bands to lose their atomic-like character and identity. The description of the bands must be modified from the isolated atom labeling scheme. The tight-binding model then prescribes, in a manner entirely similar to degenerate perturbation theory, the

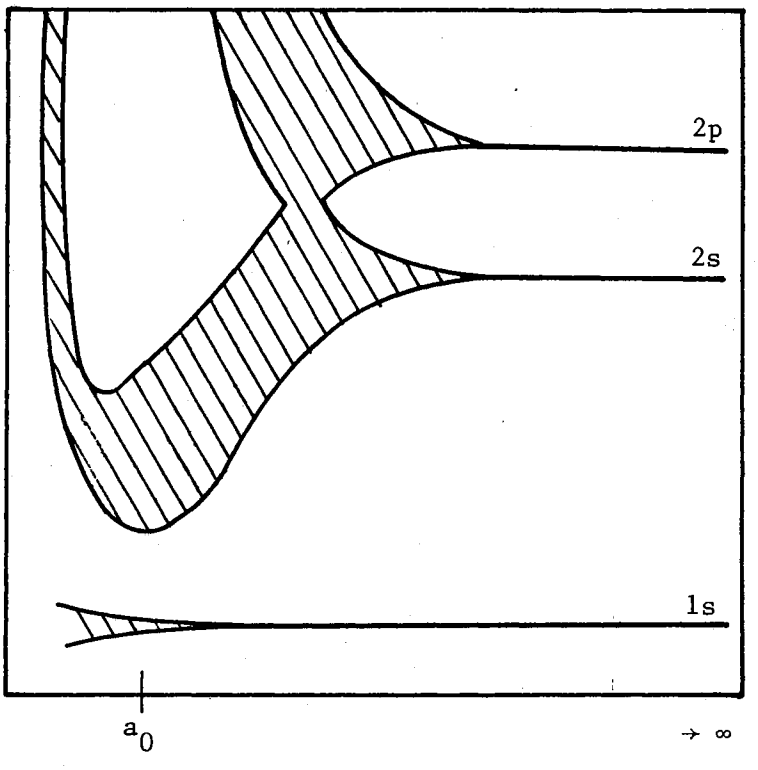

Figure 1. Bands Arising from the 1s, 2s and 2p Atomic States of Diamond as a Function of Interatomic Distance

isolated atomic states $\phi(\overline{r}-\overline{R}_n)$ are to be replaced by a linear combination of atomic orbitals of the form

$$b_i(\overline{K},\overline{r}) = \Lambda\Sigma_j\ C_j\phi_i(\overline{r} - \overline{R}_j), \tag{2-1}$$

where the $\phi(\overline{r} - \overline{R}_j)$ are atomic-like functions made of bound atomic orbitals and the C_j are chosen from symmetry considerations alone.

The periodicity of the crystal for a primitive translation and the cyclic or Born-Von Karmen boundary conditions require that the C_j's be a simple phase factor. The normalization requirement then gives a final form of

$$b_i(\overline{K},\overline{r}) = N^{-\frac{1}{2}}\Sigma_j e^{i\overline{K}\cdot\overline{R}_j}\ \phi_i(\overline{r} - \overline{R}_j), \tag{2-2}$$

where N represents the number of unit cells in the crystal. The normalization is so chosen that the $b_i(\overline{K},\overline{r})$ are normalized for the case of infinite lattice separation. The vector $\overline{K}$ defines the region of the Brillouin zone under consideration. This form of linear combination of atomic orbitals is known as Bloch sums and were first proposed as a model in 1928 by Bloch (12). The Bloch sums can be shown to have the required completeness under rotations and refelctions (13).

B. Solution for Eigenvalues and Eigenvectors

The trial wave function for the one electron model as given by a linear variation of parameters method is

$$\Psi_n(\overline{K}) = \Sigma_i C_{n,i}(\overline{K})b_i(\overline{K},\overline{r}), \tag{2-3}$$

where n is the band index and the $C_{n,i}(\overline{K})$ are the variational parameters. The sum i spans all occupied orbitals of the atom plus any additional excited states close enough to mix or required by group theory.

The one electron Schrodinger equation can then be written as

$$(H-E_m)\Psi_m(\bar{K},\bar{r}) = 0 \tag{2-4}$$

where the corresponding one-electron Hamiltonian is defined to be

$$H = -\tfrac{1}{2}\nabla^2 + V(\bar{r}). \tag{2-5}$$

Multiplying equation (2-4) by $\Psi^*_n(\bar{K},\bar{r})$ and integrating over $\bar{r}$ yields the equation

$$\Sigma_i\Sigma_j C^*_{n,i}C_{m,j}\{H_{ij}(\bar{K})-E_m(\bar{K})S_{ij}(\bar{K})\} = 0, \tag{2-6}$$

with normalization given by

$$\hat{C}^{\dagger}_{n\cdot}(\bar{K})S(\bar{K})\hat{C}_{n\cdot}(\bar{K}) = 1. \tag{2-7}$$

To find the values of the C's which make the energy a minimum, the derivative with respect to each $C_{n,i}$ is taken. The condition for a minimum,

$$\frac{\partial E}{\partial C_{n,i}} = 0, \tag{2-8}$$

leads to the set of equations,

$$\Sigma_j\{H_{ij}(\bar{K})-E_m(\bar{K})S_{ij}(\bar{K})\}C_{mj}(\bar{K}) = 0. \tag{2-9}$$

This equation describes a set of simultaneous homogenous linear equations in the independent variable C. The requirement for a non-trivial solution is that the determinant of the coefficients be equal to zero,

$$\det\left|H_{ij}(\bar{K}) - E_m(\bar{K})S_{ij}(\bar{K})\right| = 0. \tag{2-10}$$

The matrix elements $H_{ij}(K)$ and $S_{ij}(K)$ must be determined in order to solve the secular equation, and are defined as the integrals:

$$H_{ij}(\bar{K}) = \int b^*_i(\bar{K},\bar{r})\ H\ b_j(\bar{K},\bar{r})dv,$$

$$S_{ij}(\bar{K}) = \int b_i^*(\bar{K},\bar{r})\ b_j(\bar{K},\bar{r})dv. \tag{2-11}$$

These integrals can be reduced by using the Bloch sum definition given in equation (2-2).

$$H_{ij}(\bar{K}) = \frac{1}{N} \sum_{\bar{R}_q} \sum_{\bar{R}_p} e^{i\bar{K}\cdot(\bar{R}_p-\bar{R}_q)} \int \phi_i^*(\bar{r}-\bar{R}_q) H \phi_i(\bar{r}-\bar{R}_p)dv. \tag{2-12}$$

Since H is invariant under translations and $\bar{R}_p-\bar{R}_q$ is another translation vector, then the sum over $\bar{R}_q$ is just a sum over all N unit cells of the crystal. The matrix elements of equation (2-12) reduce to

$$H_{ij}(\bar{K}) = \sum_{\bar{R}_p} e^{i\bar{K}\cdot\bar{R}_p} \int \phi_i^*(\bar{r}) H \phi_j(\bar{r}-\bar{R}_p)dv. \tag{2-13}$$

In a similar manner the matrix elements of $S_{ij}(\bar{K})$ given in equation (2-10) can be simplified to

$$S_{ij}(\bar{K}) = \sum_{\bar{R}_p} e^{i\bar{K}\cdot\bar{R}_p} \int \phi_i^*(\bar{r}) \phi_j(\bar{r}-\bar{R}_p)dv. \tag{2-14}$$

Using the one electron Hamiltonian given in equation (2-5) and equation (2-13) two basic kinds of integrals can be written, namely,

$$KE_{ij}(\bar{K}) = -\Sigma_{R_p} e^{i\bar{K}\cdot\bar{R}_p} \int \phi_i^*(\bar{r}) \tfrac{1}{2}\nabla^2 \phi_j(\bar{r}-\bar{R}_p)dv, \tag{2-15}$$

$$PE_{ij}(\bar{K}) - \sum_{\bar{R}_p} e^{i\bar{K}\cdot\bar{R}_p} \int \phi_i^*(\bar{r}) V(\bar{r}) \phi_j(\bar{r}-\bar{R}_p)dv. \tag{2-16}$$

Equations (2-14) thru (2-16) define the overlap, kinetic energy and potential energy matrix elements, respectively.

Inspection of these matrix elements shows that the integrals are

independent of $\bar{K}$ and hence need be done only once. The entire matrix element is then a lattice sum of multi-centered integrals.

The potential $V(\bar{r})$ used in the potential energy matrix elements is assumed to have the same periodicity as the crystal. Ideally, the potential is the averaged effect of all electron-nuclei and electron-electron interactions. In practice the type of potential used is the Slater potential constructed from overlapping atomic potentials with the Slater approximation for exchange contributions (14). A result of the averaging process is that the potential experienced by each electron is the same and is a function of position only.

The analytical solutions of the multi-centered integrals for the matrix elements have been given in detail by Wang (13). The secular equation of equation (2-10) can now be solved for its eigenvalues and eigenvectors. The lowest eigenvalue, $E_m(\bar{K})$, is an upper limit to the energy of the lowest eigenstate (15). Also, the other eigenvalues given by this linear variation of parameters technique are upper bounds for the states described by the associated wave functions. The actual energy of the model problem may be lower but not higher than the calculated energies.

C. Representation of the Atomic-Like Functions

The tight-binding scheme is independent of the type orbital used. The orbitals ϕ_l, may be described in terms of optimized atomic orbitals, Slater orbitals, single gaussians or contracted gaussians.

In an earlier work (16) Slater type orbitals, (STO) were used with the tight-binding method. Later studies (17,18) have indicated that the gaussian type orbital, (GTO), which enables one to express all matrix

elements of the one electron crystal in analytic form, greatly reduces the computational effort required. Matrix elements to be presented later in this work have been done analytically using these gaussian type orbitals. This study uses contracted gaussians for the atomic-like functions, ϕ_l. A contracted gaussian is a linear sum of GTO's with predetermined combination and exponential coefficients. The general form is

$$\phi_i(\bar{r}) = \sum_j a_{ij} X^{\ell_i} Y^{m_i} Z^{n_i} e^{-\alpha_{ij} r^2} . \qquad (2\text{-}16)$$

CHAPTER III

OPTICAL PROPERTIES

A. Density and Joint Density of States

The first step in obtaining the imaginary portion of the dielectric function from the band structure is an evaluation of the density of states. The density of states is so defined that $D_n(E)dE$ is equal to the number of $\overline{K}$ points in band n per unit cell with energy between E and E+dE, or

$$D_n(E) = \int_{BZ} \delta\{E_n(\overline{K})-E\}(2/V_K)d^3K, \tag{3-1}$$

where $E_n(\overline{K})$ is the energy of the nth band at the point $\overline{K}$, and the volume of the Brillouin zone, V_K, is needed for normalization. A factor of two results from possible spin orientations.

The total density of states in an energy range is the sum of all individual band densities within the desired energy range such that

$$D(E) = \Sigma_n D_n(E). \tag{3-2}$$

A joint density of states, $J_{ij}(E)$, can also be defined such that $J_{ij}(E)dE$ represents the number of pairs of states with the same $\overline{K}$ and spin values, one in band i and one in band j per unit cell having an energy difference between E and E+dE, then

$$J_{ij}(E) = (2/V_K)\int_{BZ} \delta\{E_{ij}(\overline{K})-E\}d^3K, \tag{3-3}$$

where $E_{ij}(\overline{K})$ is the energy difference

$$E_{ij}(\bar{K}) = E_j(\bar{K}) - E_i(\bar{K}) \tag{3-4}$$

between the bands j and i.

A total joint density of states between the valence and conduction bands can be defined as the sum of all possible combinations of bands within the desired energy range such that

$$J(E) = \sum_{i,j} J_{ij}(E), \tag{3-5}$$

where i and j span the valence and conduction bands, respectively.

The cubic symmetry of diamond and silicon with the rotational and reflection invariance of the energy eigenvalues in $\bar{K}$-space under the operations of the point group allows a reduction of integrals over the complete Brillouin zone to integrals over the fundamental wedge with multiplication by the number of operations in the point group. Many different choices exist for the fundamental wedge, the one chosen is that portion of the Brillouin zone for which $K_x \geq K_y \geq K_z$. The expressions for the density and joint density of states then become

$$\begin{aligned} D_n(E) &= (96/V_K)\int \delta\{E_n(\bar{K}) - E\} d^3K, \\ J_{ij}(E) &= (96/V_K)\int \delta\{E_{ij}(\bar{K}) - E\} d^3K. \end{aligned} \tag{3-6}$$

B. Dielectric Function

Ehrenreich and Cohen's work (19) assuming direct transitions leads to a band theoretical prediction for the imaginary portion, $\varepsilon_2(\omega)$, of the dielectric function for insulators with a cubic point group given by

$$\varepsilon_2(\omega) = \frac{48e^2}{\pi m^2 \omega^2} \sum_i \sum_j \int_{FW} \delta\{E_{ij}(\bar{K}) - E(\omega)\} T_{ij}(\bar{K}) d^3K, \tag{3-7}$$

where $E(\omega)$ is the photon energy $\hbar\omega$ and the reduction to an integration over the fundamental wedge has been performed. The $T_{ij}(\bar{K})$ are the

transition matrix elements which are written as

$$T_{ij}(\bar{K}) = \frac{1}{3}\{|\langle i\bar{K}|P_x|j\bar{K}\rangle|^2+|\langle i\bar{K}|P_y|j\bar{K}\rangle|^2+|\langle i\bar{K}|P_z|j\bar{K}\rangle|^2\}. \qquad (3\text{-}8)$$

The transition matrix elements may be averaged in the manner shown in equation (3-8) because for materials possessing cubic point symmetry, as do diamond and silicon, the dielectric tensor can be reduced to a scalar and is independent of direction. The components are given in braket notation and are the integrals

$$\langle i\bar{K}|P_x|j\bar{K}\rangle = \int\Psi_i^*(\bar{K},\bar{r})P_x\Psi_j(\bar{K},\bar{r})dv, \qquad (3\text{-}9)$$

where P_x is the usual momentum operator for the x direction. Similar expressions exist for the y and z coordinates.

A complete first principles calculation requires evaluation of these transition probabilities. Using the equation (2-3) for the wave function the matrix elements of the momentum operator can be written as

$$\begin{aligned}\langle nK|-i\bar{h}\bar{\nabla}|mK\rangle &= \int\Psi_n^*(\bar{K},\bar{r})(-i\bar{h}\bar{\nabla})\Psi_m(\bar{K},\bar{r})dv \\ &= \hat{C}_{n\cdot}^{\dagger}(\bar{K})M\hat{C}_{m\cdot}(\bar{K}),\end{aligned} \qquad (3\text{-}10)$$

where the $\hat{C}_{n\cdot}$ are the variational coefficients defined in equation (2-1). The matrix elements, $M_{ij}(\bar{K})$, are obtained by using the Bloch sum definition given in equation (2-2) and can be expressed as

$$M_{ij}(\bar{K}) = -i\bar{h}\Sigma_\nu e^{i\bar{K}\cdot R_\nu}\int\phi_i^*(\bar{r})\nabla\phi_j(r-R_\nu)dv. \qquad (3\text{-}11)$$

This integral for the elements of M can be expressed as a linear combination of overlap integrals, which were previously calculated for the evaluation of the band structure.

CHAPTER IV

NUMERICAL METHOD OF COMPUTATION

The integrals for the density, joint density and the imaginary portion of the dielectric function as given by equations (3-6) and (3-7) have not yet been done analytically. The method of computation must be a numerical procedure. A numerical method which can sample a large number of $\overline{K}$ points within the Brillouin zone is needed.

A. Method of Gilat and Dolling

A numerical method that satisfies this condition has been presented by Gilat and Dolling (20). Their method utilizes the histogram approach, with discrete steps. Meshes are used to define the $\overline{K}$ points to be sampled. This method has been adapted to the present problem.

First the band energies are obtained by diagonalizing the secular equation, (2-10), for a small number of $\overline{K}$ points evenly distributed throughout the fundamental wedge. This distribution of points for which the secular equation is solved constitute the primary mesh. The fundamental wedge is separated into equal volume parallelopipeds centered on each primary mesh point.

Each of the parallelopipeds is covered with a secondary mesh of $\overline{K}$ points so chosen as to be uniformly spaced. The secondary mesh is also evenly distributed throughout the fundamental wedge. No secondary

points lying outside the fundamental wedge contributes to the density, joint density or the dielectric function.

The density, joint density and dielectric function are primarily dependent upon the band energies at each $\overline{K}$ point of the primary and secondary meshes. However, the secular equation is solved only for the primary mesh. The energies at a secondary mesh point are obtained by a linear extrapolation from the primary mesh point in the same parallelopiped. The necessary energy gradients, $\overline{\nabla}_K E_n(\overline{K})$, for this extrapolation are discussed in a later section.

B. Energy Mesh

A mesh of energy increments is used to divide the energy range of interest into small step sizes. If the step size is δE then the energy steps are defined so that

$$E_\lambda = E_0 + \lambda \delta E, \tag{4-1}$$

where E_0 is the lowest energy in the range of interest. The average of the density of states, $\overline{D_n}(E_\lambda)$, for a particular energy increment, λ, is given by

$$\begin{aligned} \overline{D_n}(E_\lambda) &= \frac{1}{\delta E} \int_{E_\lambda}^{E_\lambda+\delta E} \overline{D_n}(E)dE \\ &= \frac{96}{V_K \delta E} \int_{FW} \Delta\{E_n(\overline{K})-E_\lambda\}\, d^3K, \end{aligned} \tag{4-2}$$

where

$$\Delta(E_n(\overline{K})-E_\lambda) = \begin{cases} 1 & \text{if } E_\lambda \leq E_n(\overline{K}) \leq E_\lambda+\delta E \\ 0 & \text{otherwise} \end{cases}. \tag{4-3}$$

The integration can be further reduced to a sum over all parallelopipeds, ℓ, and an integration over the volume, V_p, of each parallelopiped,

such that

$$\overline{D_n}(E_\lambda) = \frac{96}{V_K \delta E} \sum_{\ell} \int_{V_p} \Delta\{E_n(\bar{K}) - E_\lambda\} d^3k. \tag{4-4}$$

The integration is done numerically by using the secondary mesh points and the extrapolation technique to obtain the band energies. Similar derivations exist for the joint density and dielectric function.

C. Primary and Secondary Mesh

The primary mesh of $\bar{K}$ points which separates the fundamental wedge into equal volume parallelopipeds is defined so that the center of the nth parallelopiped is given by

$$\bar{K}_n = \frac{2m_1+1}{N_1} \bar{\ell}_1 + \frac{2m_2+1}{N_2} \bar{\ell}_2 + \frac{2m_3+1}{N_3} \bar{\ell}_3, \tag{4-5}$$

where the $\bar{\ell}_i$ are vectors defining the edges of the fundamental wedge of are given by

$$\begin{aligned} \bar{\ell}_1 &= (2\pi/a_0)(1,0,0), \\ \bar{\ell}_2 &= (2\pi/a_0)(3/4,3/4,0), \\ \bar{\ell}_3 &= (2\pi/a_0)(1/2,1/2,1/2). \end{aligned} \tag{4-6}$$

The m_i are positive integers or zero, the combination of which must satisfy the boundary requirements given by

$$\begin{aligned} \frac{4m_1}{N_1} + \frac{3m_2}{N_2} + \frac{2m_3}{N_3} &< 4, \\ \frac{2m_1}{N_1} + \frac{3m_2}{N_2} + \frac{3m_3}{N_3} &< 3, \end{aligned} \tag{4-7}$$

in order to stay within the fundamental wedge, and where N_1, N_2, N_3 are

integers chosen so that

$$\frac{|\bar{\ell}_1|}{N_1} = \frac{|\bar{\ell}_2|}{N_2} = \frac{|\bar{\ell}_3|}{N_3}, \tag{4-8}$$

to keep the parallelopiped as cubical as possible.

The secondary mesh points are labeled according to the parallelopiped of which they are a member. The mth secondary mesh point in the nth parallelopiped is given by

$$\bar{K}_{n,m} = \bar{K}_n + \bar{\kappa}_m, \tag{4-9}$$

where

$$\bar{\kappa}_m = \frac{m_1 - \frac{1}{2}(M_1-1)}{M_1 N_1} \bar{\ell}_1 + \frac{m_1 - \frac{1}{2}(M_2-1)}{M_2 N_2} \bar{\ell}_2 + \frac{m_3 - \frac{1}{2}(M_3-1)}{M_3 N_3} \bar{\ell}_3, \tag{4-10}$$

with M_1, M_2, M_3 being odd integers of approximately equal magnitude.

D. Gradient of Energy

As suggested earlier, the energy at the secondary mesh points, $E(\bar{K}_{n,m})$, must be obtained. The energy at a secondary mesh point can be related to the energy at a nearby primary point by means of a first order Taylor series expansion, i.e.,

$$E(\bar{K}_{n,m}) = E(\bar{K}_n) + \nabla_K E(\bar{K}_n) \cdot \bar{\kappa}_m. \tag{4-11}$$

This gives the extrapolation formula for the energy at a secondary mesh point once the energy and gradient of energy have been found at the primary mesh point.

The gradient components can be found by examination of the tight-binding secular equation for adjacent points in $\bar{K}$ space, $\bar{K}$ and $\bar{K}+\delta\bar{K}$. The secular equation for these two points is given by

$$H(\bar{K})\hat{C}_{n\cdot}(\bar{K}) = E_n(\bar{K})S(\bar{K})\hat{C}_{n\cdot}(\bar{K}),$$

$$H(\bar{K}+\delta\bar{K})\hat{C}_{n\cdot}(\bar{K}+\delta\bar{K}) = E_n(\bar{K}+\delta\bar{K})S(\bar{K}+\bar{K})\hat{C}_{n\cdot}(\bar{K}+\delta\bar{K}), \tag{4-12}$$

where $S(\bar{K})$ is a square matrix and $\hat{C}_{n\cdot}$ is a column matrix using the Wigner notation as defined by equation (2-3). Expanding the last equation in a first order Taylor series about the primary mesh point yields

$$\begin{aligned}&\{H(\bar{K})-E_n(\bar{K})S(\bar{K})\}\hat{C}_{n\cdot}(\bar{K}) + \{H(\bar{K})-E_n(\bar{K})S(\bar{K})\}\bar{\nabla}_K\hat{C}_{n\cdot}(\bar{K})\cdot\delta\bar{K}\\ &+\{\bar{\nabla}_K H(\bar{K}) - E_n(\bar{K})\bar{\nabla}_K S(\bar{K})\}\cdot\delta K\hat{C}_{n\cdot}(\bar{K})\\ &\quad = \bar{\nabla}_K E_n(\bar{K})S(\bar{K})\hat{C}_{n\cdot}(\bar{K})\cdot\delta\bar{K}.\end{aligned} \tag{4-13}$$

Matrix multiplication on the left by $\hat{C}^{\dagger}_{n\cdot}(\bar{K})$ using equation (2-8) and the normalization requirement of equation (2-7) gives the desired result of

$$\bar{\nabla}_K E_n(\bar{K}) = \hat{C}^{\dagger}_{n\cdot}(\bar{K})\{\bar{\nabla}_K H(\bar{K}) - E_n(\bar{K})\bar{\nabla}_K S(\bar{K})\}\hat{C}_{n\cdot}(\bar{K}). \tag{4-14}$$

These matrix elements involving the gradient operation do not require any more multi-center integrals to be done since the integrals themselves are $\bar{K}$ independent. By applying the gradient operation to equations (2-12) and (2-13) for the Hamiltonian and Overlap matrix elements the needed matrix elements are again lattice sums of knows integrals, i.e.,

$$\begin{aligned}\nabla_K H_{ij}(\bar{K}) &= i\sum_q \bar{R}_q e^{i\bar{R}_q\cdot\bar{K}} \int\phi_i^*(\bar{K},\bar{r})H\phi_j(\bar{K},\bar{r})dv,\\ \nabla_K S_{ij}(\bar{K}) &= i\sum_q \bar{R}_q e^{i\bar{K}\cdot\bar{R}_q} \int\phi_i^*(\bar{K},\bar{r})\phi_j(\bar{K},\bar{r})dv.\end{aligned} \tag{4-15}$$

These elements allow quick evaluation at general primary $\bar{K}$ points, and hence the energies associated with each secondary mesh point are easily obtained.

CHAPTER V

RESULTS AND CONCLUSIONS

The band structure for diamond and silicon was calculated within the tight-binding framework using Gaussian orbitals as shown in equation (2-17) to construct the Bloch sums. The exponential and combinatorial coefficients for the five basis functions of diamond were obtained from Euwema (21) and are given in Table II. The silicon coefficients were taken from Veillard (22) and are found in Table III.

The resulting band structures are shown in Figures 2 and 3. The tight-binding band structure for diamond is nearly identical to other work. The band structure for silicon is in partial disagreement with earlier work, but agrees with recent calculations done by Stukel and Euwema (8) and by Chaney et al (7). The point of contention centers about the Γ-point. Earlier calculations predict that Γ_{15} lies at the bottom of the conduction, however more recent calculations and this one shows Γ_2' at the bottom of the conduction band. To date, no experimental data exist to resolve this conflict.

The density of states arising from the diamond and silicon band structures are shown in Figures 4 and 5, respectively. For silicon, Kunz (23) has investigated the soft x-ray absorbtion associated with this type of conduction density of states and has found it to be in better agreement with experiment than theoretical calculations which predict Γ_{15} to be the bottom of the conduction band.

TABLE II

DIAMOND ORBITAL COEFFICIENTS

Exponential Coefficients	Combinatorial Coefficients, a_{ij}		
	ϕ_{1s}	ϕ_{2s}	ϕ_{2p}
2.0480D 03	1.8623D 00	4.3321D-01	2.6885D-02
9.4363D 02	3.7934D-01	6.5761D-02	2.6128D-01
4.3479D 02	2.0885D-00	5.0311D-01	8.2331D-02
2.0033D 02	2.2360D 00	4.9202D-01	3.6352D-01
9.2304D 01	3.4434D 00	8.3260D-01	3.5867D-01
4.2530D 01	4.2920D 00	1.0228D 00	5.9984D-01
1.9596D 01	4.8625D 00	1.3109D 00	7.0235D-01
9.0290D 00	4.2603D 00	1.3049D 00	9.1637D-01
4.1602D 00	2.2324D 00	1.0169D 00	9.0379D-01
1.9168D 00	5.2777D-01	3.0897D-01	8.3474D-01
8.8320D-01	1.7426D-02	-4.1576D-01	5.8211D-01
4.0694D-01	1.3332D-03	-5.5204D-01	2.8885D-01
1.8750D-01	-4.8617D-04	-2.9243D-01	1.0563D-01
8.6393D-02	1.5422D-04	-5.6705D-01	2.5330D-02

TABLE III

SILICON ORBITAL COEFFICIENTS

Exponential	Combinatorial Coefficients, a_{ij}				
Coefficients	ϕ_{1s}	ϕ_{2s}	ϕ_{3s}	ϕ_{2p}	ϕ_{3p}
6.9989D 04	9.5070D-01	-2.4534D-01	6.1336D-02	0.0	0.0
1.0383D 04	1.8250D 00	-4.8374D-01	1.1727D-01	0.0	0.0
2.3300D 03	3.1144D 00	-8.4134D-01	2.1512D-01	0.0	0.0
6.5747D 02	4.8369D 00	-1.3131D 00	3.3776D-01	0.0	0.0
3.3749D 02	0.0	0.0	0.0	7.2992D 00	-1.5464D 00
2.1400D 02	6.4406D 00	-1.8997D 00	4.8969D-01	0.0	0.0
7.8687D 01	0.0	0.0	0.0	9.1999D 00	-1.9809D 00
7.7606D 01	6.4789D 00	-2.1391D 00	5.6036D-01	0.0	0.0
3.0639D 01	3.7539D 00	-1.8813D 00	5.0436D-01	0.0	0.0
2.4935D 01	0.0	0.0	0.0	9.2521D 00	-1.0380D 00
1.2816D 01	7.8411D-01	-3.1972D-01	9.2976D-02	0.0	0.0
9.2151D 00	0.0	0.0	0.0	6.7124D 00	-1.5123D 00
3.9271D 00	1.8172D 02	1.0806D 00	-3.6854D-01	0.0	0.0
3.6153D 00	0.0	0.0	0.0	3.0750D 00	-7.2728D-01
1.4522D 00	-6.3169D-04	5.4001D-01	-3.2235D-01	0.0	0.0
1.4520D 00	0.0	0.0	0.0	6.9457D-01	-1.6424D-01
5.0399D-01	0.0	0.0	0.0	2.7680D-02	1.2258D-01
2.5764D-01	6.4434D-05	8.0388D-03	1.5632D-01	0.0	0.0
1.8604D-01	0.0	0.0	0.0	-6.7748D-04	9.8923D-02
9.4404D-02	-1.3352D-05	-1.0548D-03	6.7650D-02	0.0	0.0
6.5432D-02	0.0	0.0	0.0	7.1229D-05	1.8144D-02

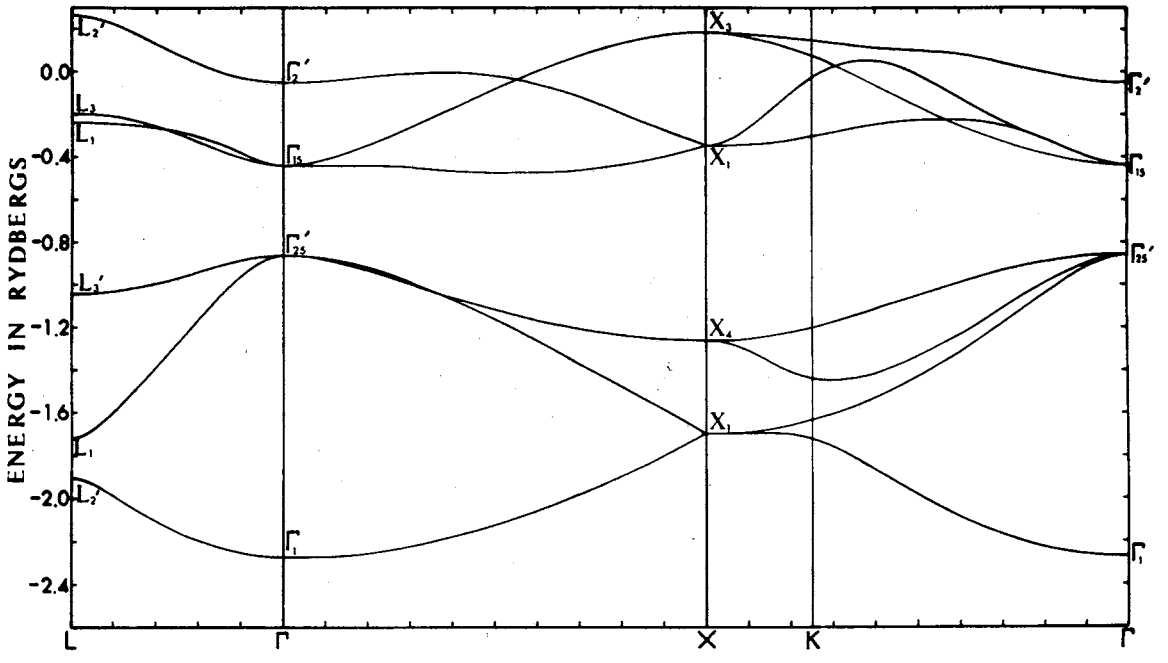

Figure 2. Tight-binding Band Structure of Diamond

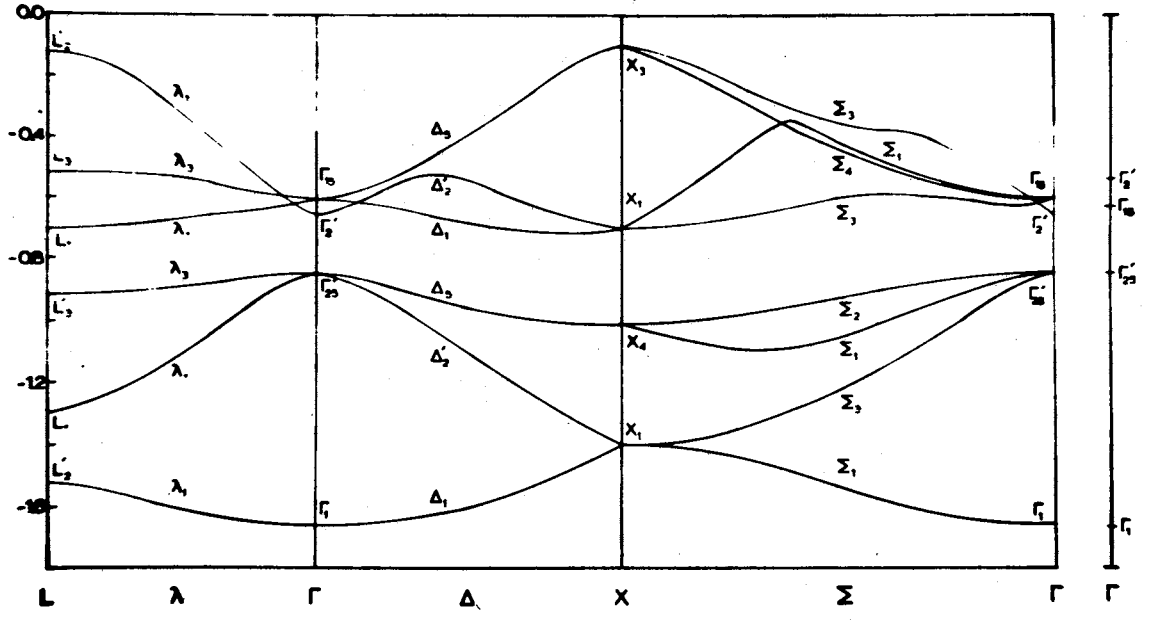

Figure 3. Tight-binding Band Structure of Silicon

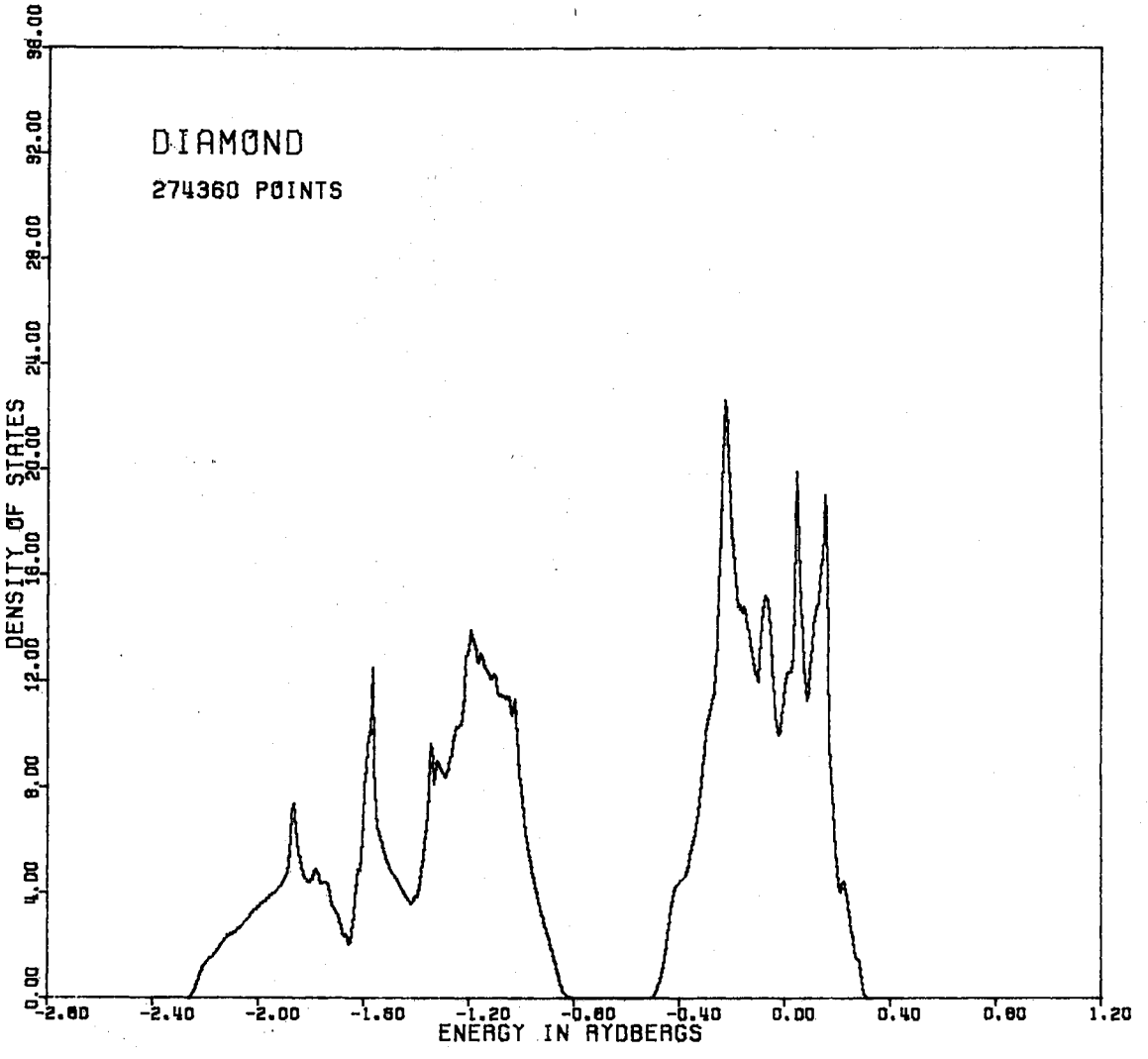

Figure 4. Density of States for Diamond

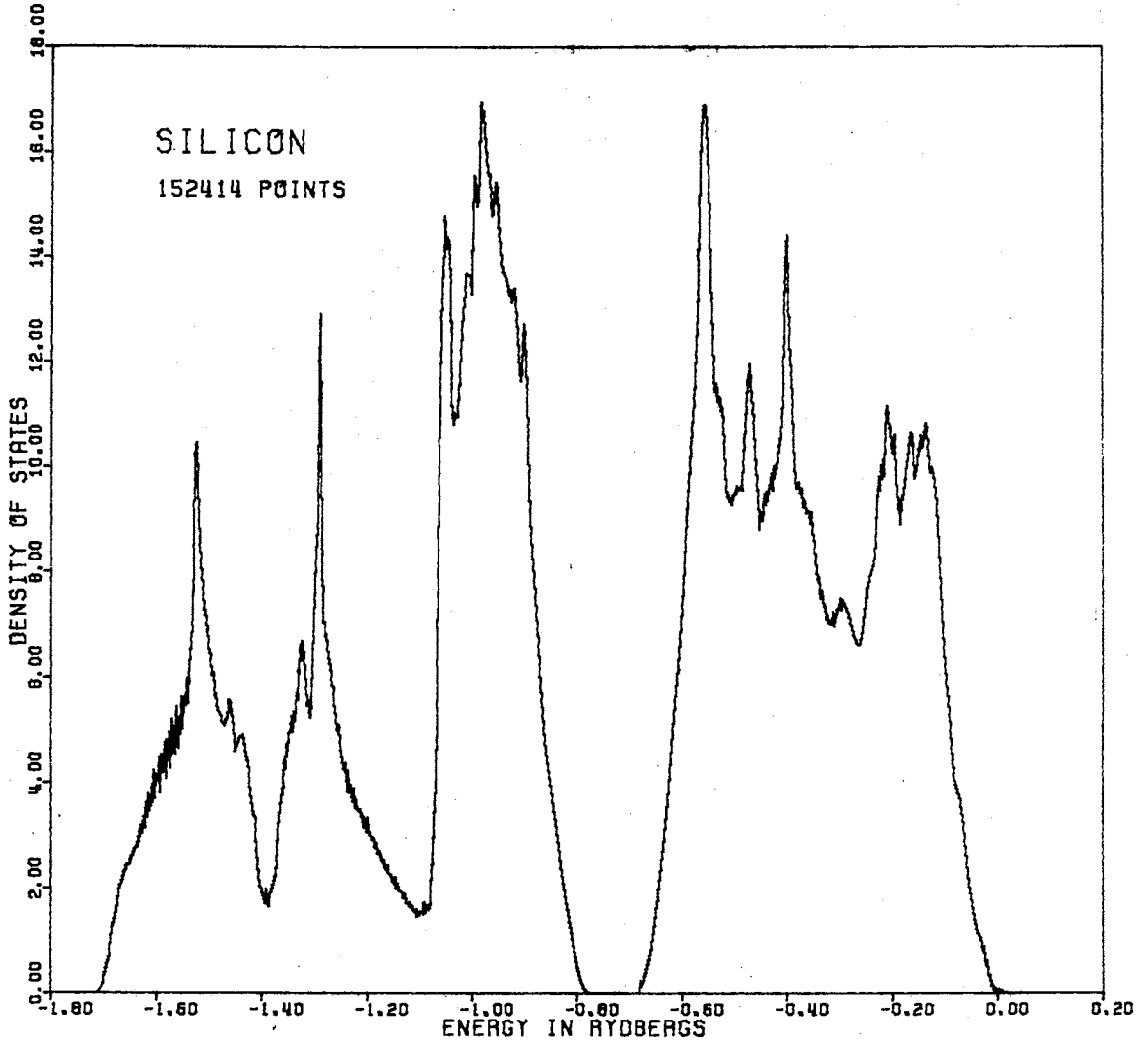

Figure 5. Density of States for Silicon

The graphs of appendixes A and B for diamond and silicon, respectively, show the joint density of states and the resulting dielectric function by band pairs. The notation used is a two digit symbol where the first digit is either a V for valence bands or a C for conduction bands. The second symbol is a number indicating the individual energy states within the conduction or valence bands. One refers to the bottom of a band and four refers to the top. Both diamond and silicon have four energy states making up the total valence or conduction bands with higher conduction states being ignored. A graph labeled "V2 to C3" represents the data connecting the second valence band to the third conduction band.

The variation of the transition matrix elements over $\overline{K}$-space has a pronounced effect upon the dielectric function. This is clearly demonstrated by examination of the band pair data given in appendixes A and B. In many band pairs a large joint density of states exist but because the transition probability is small the resulting contribution to the dielectric function is small. A classic example would be the band pair V2 to C4 of silicon.

The band to band data also displays the effect of the transition matrix elements on the final structure of the dielectric function. Band pairs, V4 to C1 and V4 to C2, among others, indicate that the transition matrix elements variation with energy for a particular band pair can significantly modify the shape and enhance features of the joint density data in yielding ε_2 for that particular band pair.

The calculated dielectric function for diamond is shown by the solid line in Figure 6, the experimental results of Roberts and Walker (24) are shown in the dashed line. The corresponding joint density of

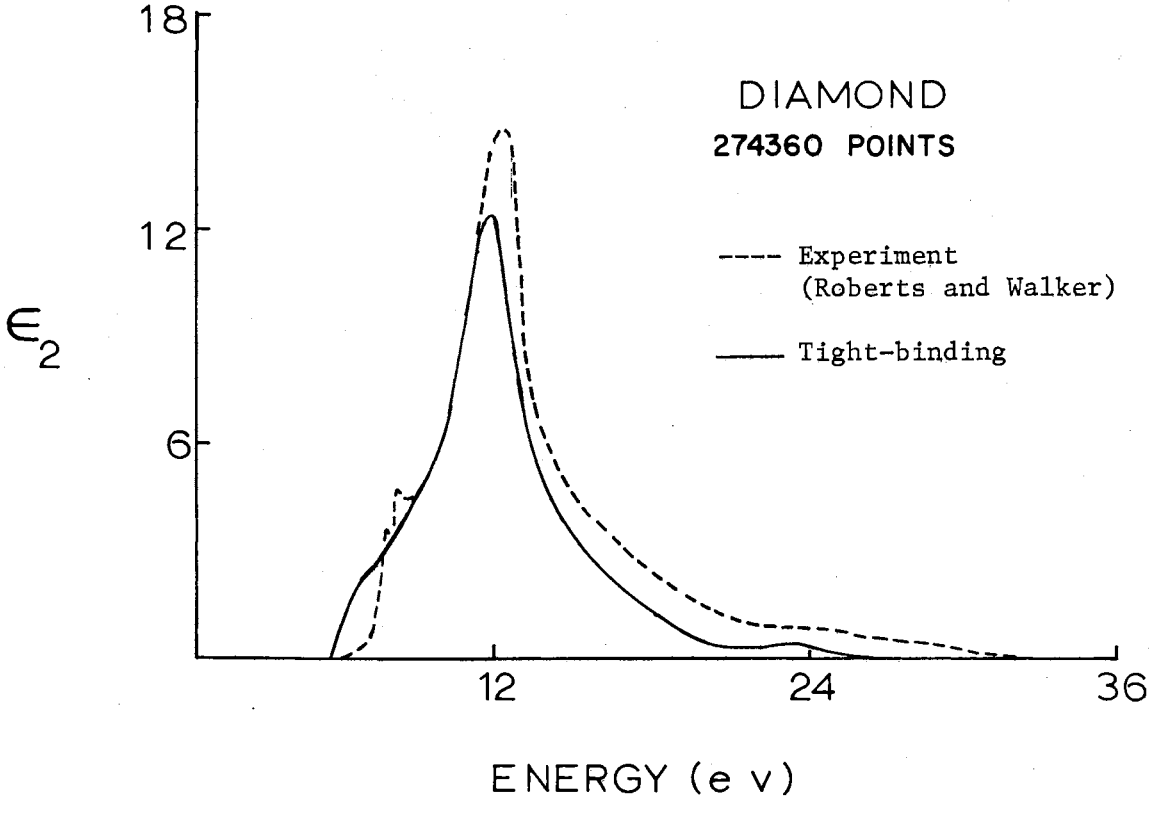

Figure 6. Experimental and Theoretical Results for the Imaginary Portion of the Dielectric Function of Diamond

states is shown in Figure 7. The diamond results are in good agreement with experiment having the properties of a fast rising leading edge and the maximum peak and a double shoulder occuring at the same energies as reported by Roberts and Walker (24). These results also agree with the theoretical work of Painter, Ellis and Lubinsky (10). These results seem to indicate that the experimental structure on the leading edge of diamond is due to band structure and is not excitonic in origin as previously suggested (25).

The calculated ε_2 for silicon, Figure 9, agrees with the qualitative features of the experimental data published by Ehrenreich and Philipp (26) and is shown in Figure 10. The silicon joint density of states is shown in Figure 8. The features obtained from this method and not by other ab inito calculations are the steep leading edge and the double peak. These features reinforce the concept that the leading peak is a result of band structure rather than excitonic properties.

A primary cell by primary cell analysis indicates there is good reason to believe that the double peak in the dielectric function of silicon is a direct result of Γ_2' rather than Γ_{15} being at the bottom of the conduction band and to additional symmetry related enhancement effectis of the matrix elements around the Γ-point.

In an attempt to improve the accuracy and determine the stability of the results, another calculation was performed for silicon using optimized orbitals. The set of optimized orbitals, ϕ_1', was constructed by beginning with Veillards coefficients and breaking the orbitals, ϕ_i, into a sum of contracted gaussians. This increases the number of basis functions and hence the variational freedom of the linear variation of parameters technique and generally improves the band energies.

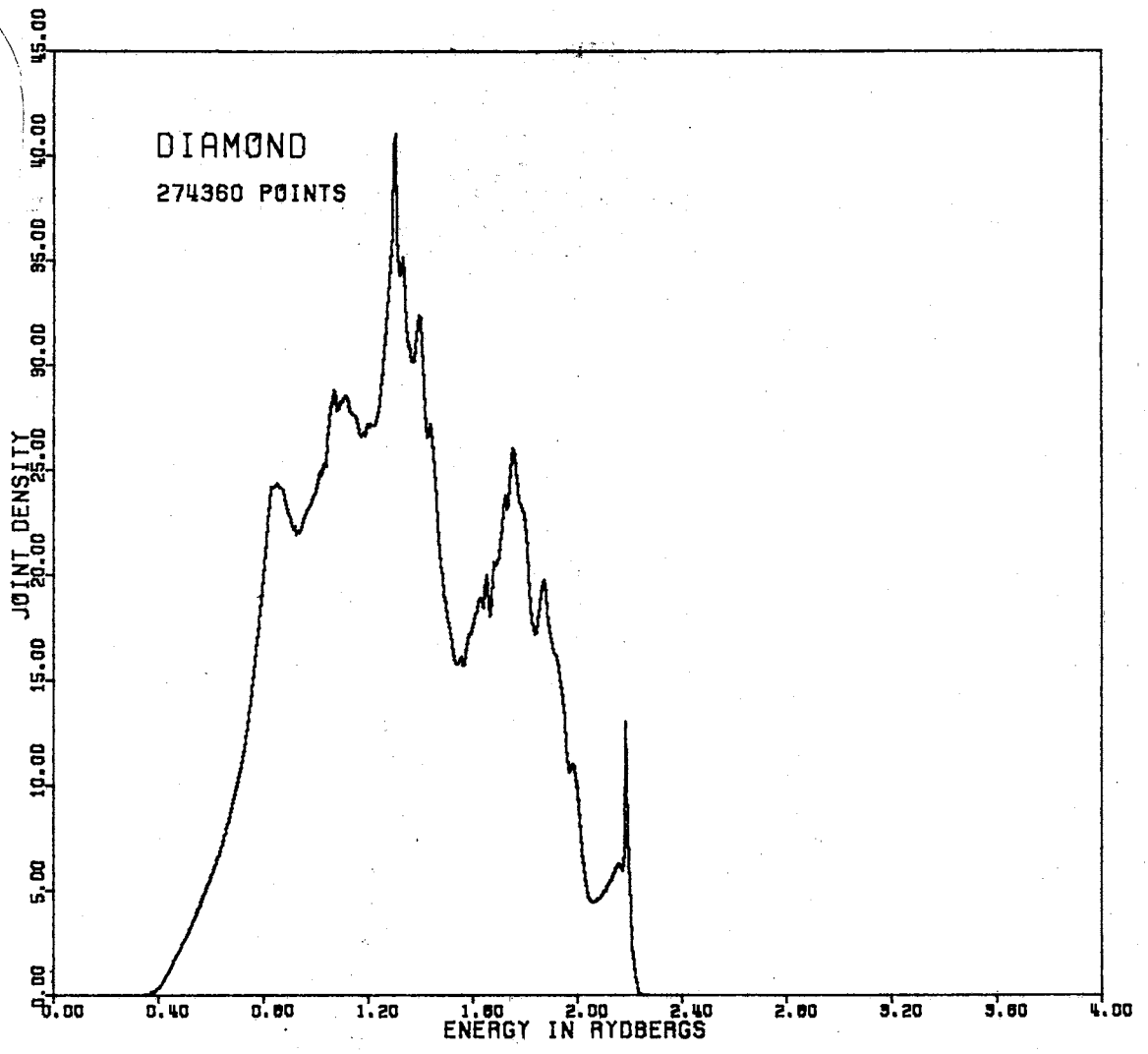

Figure 7. Joint Density of States of Diamond

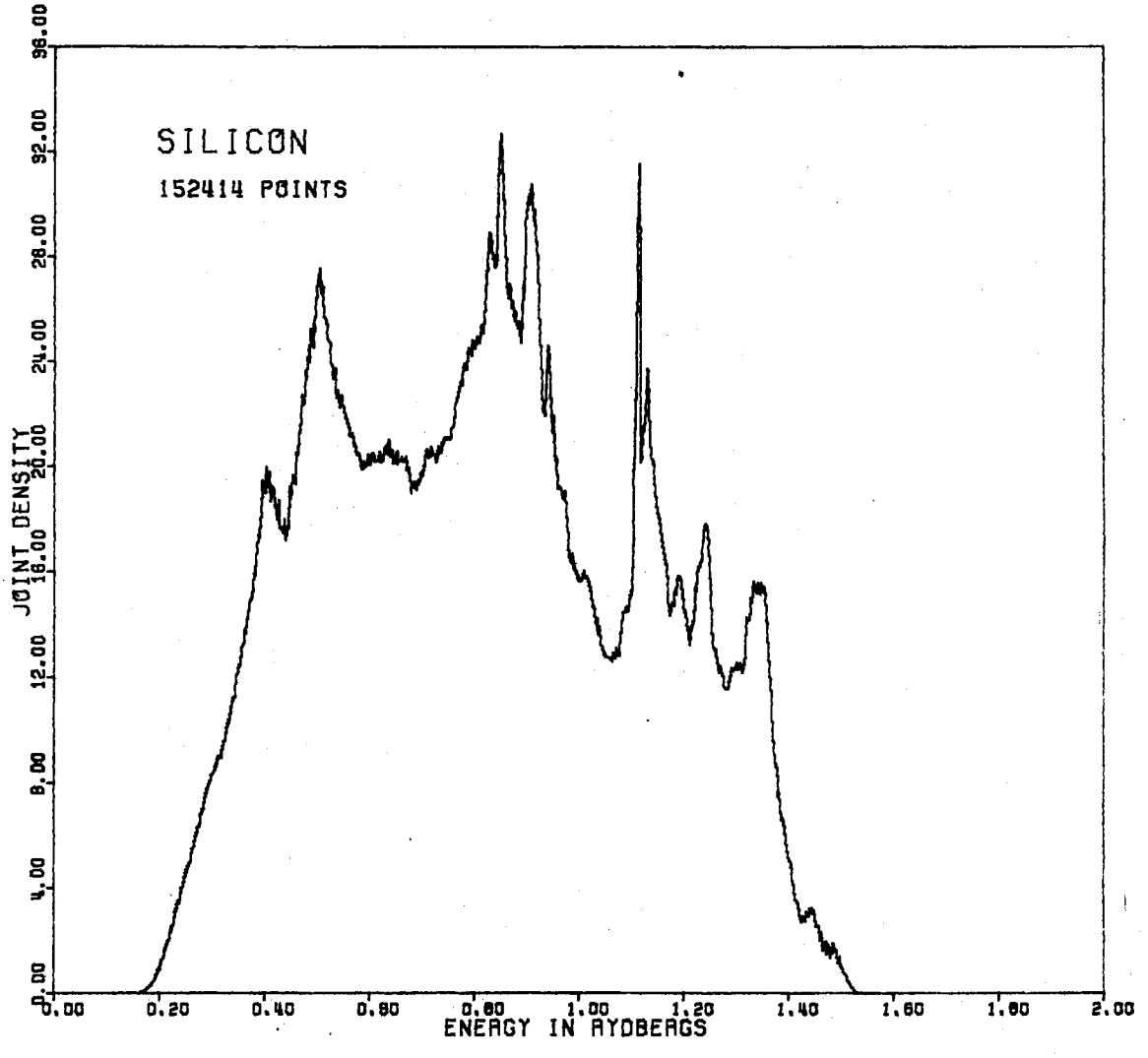

Figure 8. Joint Density of States of Silicon

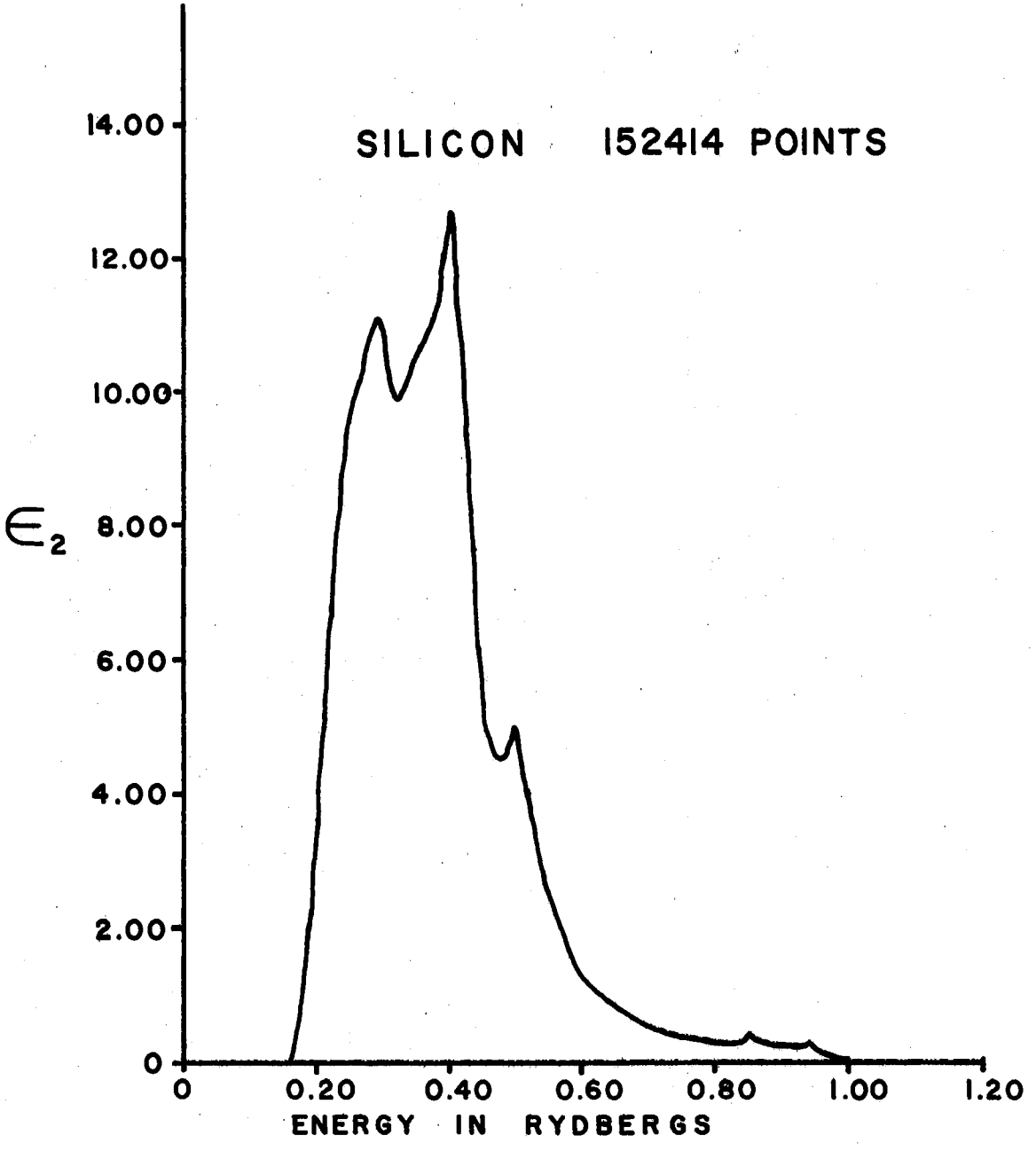

Figure 9. Calculated Dielectric Function for Silicon

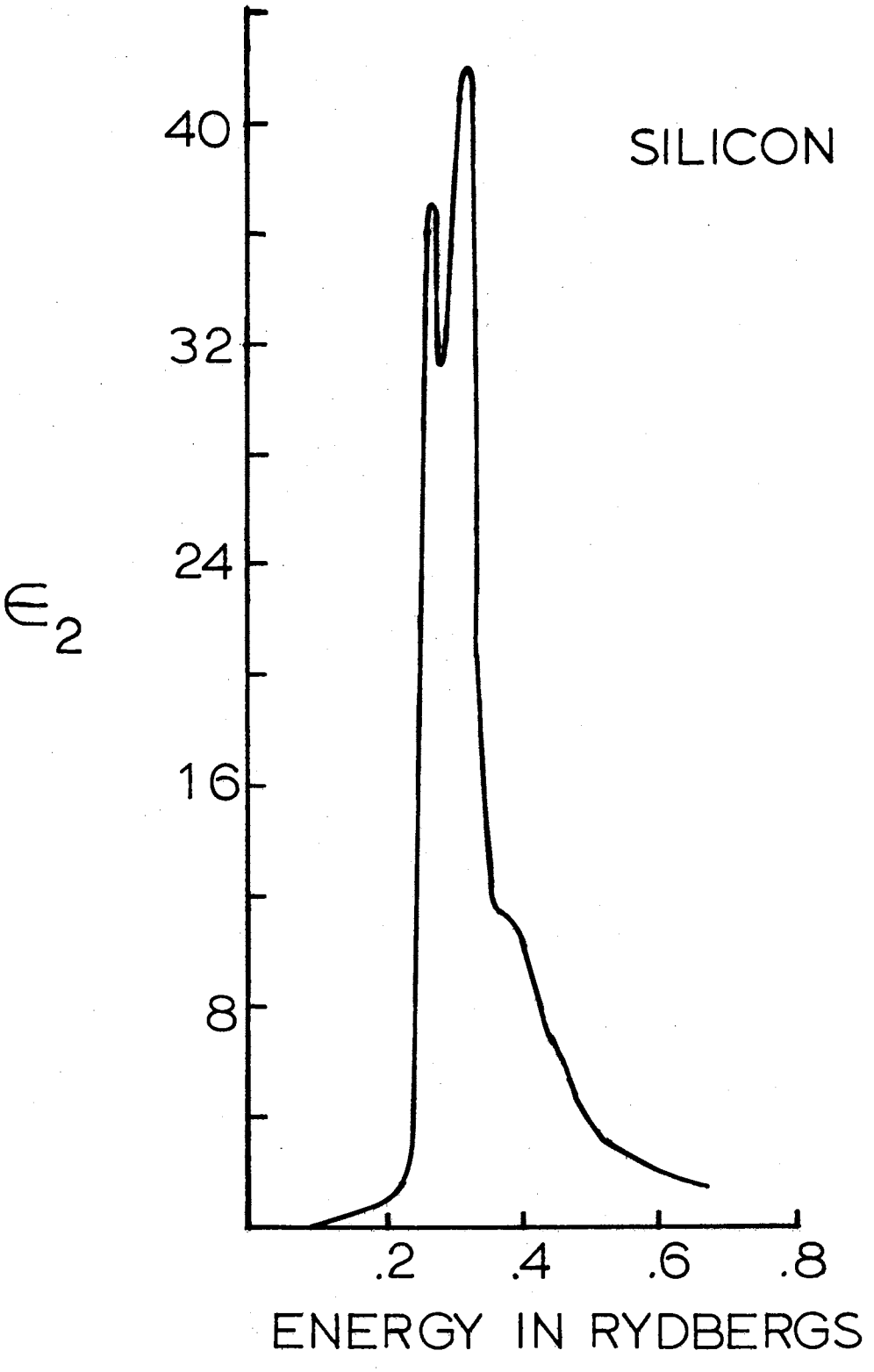

Figure 10. Ehrenreich and Phillipp's Experimental Dielectric Function for Silicon

The secular equation with the new basis functions is diagonalized for $\bar{K}$ being the gamma point. The eigenvectors then give the mixing of the separated orbitals. The mixing constants from the eigenvector are multiplied by the previous combinatorial coefficients to give the optimized orbitals. The coefficients are given in Table IV.

The resulting density of states and dielectric function from the comparison to the previous silicon calculation shows that the use of optimized orbitals and an increased number of basis functions leave the features in the same energy positions and heightens the peaks. This calculation confirms the stability of the previous calculation and tends to insure the accuracy of the model.

The results of this work indicate the importance of a first principles calculation of the optical properties of crystalline materials. The necessity of a first principles evaluation of the transition matrix elements has been demonstrated by the band pair analysis of the joint density and dielectric function. The results give reason to believe that some of the optical effects heretofore attributed to exciton states are in fact related to energy band structure. Other work (27) using this method on different materials tends to substantiate the findings of this investigation.

TABLE IV

OPTIMIZED SILICON ORBITAL COEFFICIENTS

Exponential	Combinatorial Coefficients, a_{ij}					
Coefficients	ϕ'_{1s}	ϕ'_{2s}	ϕ^1_s	ϕ^2_s	ϕ^3_s	ϕ'_{3s}
6.9989D 04	6.7107D-01	-1.6773D-01	6.1336D-02	0.0	0.0	4.2665D-02
1.0380D 04	1.2931D 00	-3.3665D-01	1.1727D-01	0.0	0.0	8.8425D-02
2.3300D 03	2.2126D 00	-5.6270D-01	2.1511D-01	0.0	0.0	1.5899D-01
6.5747D 02	3.4389D 00	-9.2791D-01	3.3776D-01	0.0	0.0	2.5022D-01
3.3749D 02	0.0	0.0	0.0	0.0	0.0	0.0
2.1400D 02	4.6366D 00	-1.4095D 00	4.8969D-01	0.0	0.0	4.1049D-01
7.8687D 01	0.0	0.0	0.0	0.0	0.0	0.0
7.7606D 01	4.5735D 00	-1.4910D 00	0.0	5.6036D-01	0.0	3.7405D-01
3.0639D 01	2.6514D 00	-1.3209D 00	0.0	5.0436D-01	0.0	4.1903D-01
2.4935D 01	0.0	0.0	0.0	0.0	0.0	0.0
1.2816D 01	5.5365D-01	-2.2376D-01	0.0	9.2976D-02	0.0	6.4442D-02
9.2151D 00	0.0	0.0	0.0	0.0	0.0	0.0
3.9271D 00	1.0410D-02	7.6951D-01	0.0	-3.6854D-01	0.0	-3.4143D-01
3.6153D 00	0.0	0.0	0.0	0.0	0.0	0.0
1.4522D 00	-1.6472D-03	3.8451D-01	0.0	-3.2235D-01	0.0	-1.7018D-01
1.4520D 00	0.0	0.0	0.0	0.0	0.0	0.0
5.0399D-01	0.0	0.0	0.0	0.0	0.0	0.0
2.5764D-01	3.3184D-04	2.0569D-03	0.0	0.0	1.5632D-01	1.1500D-01
1.8604D-01	0.0	0.0	0.0	0.0	0.0	0.0
9.4404D-02	-3.0087D-04	1.7826D-05	0.0	0.0	6.7651D-02	1.6853D-02
6.5432D-02	0.0	0.0	0.0	0.0	0.0	0.0

TABLE IV (Continued)

Combinatorial Coefficients, a_{ij}			
ϕ'_{2p}	ϕ^1_p	ϕ^2_p	ϕ^3_p
0.0	0.0	0.0	0.0
0.0	0.0	0.0	0.0
0.0	0.0	0.0	0.0
0.0	0.0	0.0	0.0
5.7975D 00	-1.5464D 00	0.0	0.0
0.0	0.0	0.0	0.0
7.3072D 00	-1.9809D 00	0.0	0.0
0.0	0.0	0.0	0.0
0.0	0.0	0.0	0.0
6.6347D 00	0.0	-2.0380D 00	0.0
0.0	0.0	0.0	0.0
4.8135D 00	0.0	-1.5123D 00	0.0
0.0	0.0	0.0	0.0
2.2051D 00	0.0	-7.2728D-01	0.0
0.0	0.0	0.0	0.0
4.9808D-01	0.0	-1.6424D-01	0.0
4.9728D-03	0.0	0.0	1.2258D-01
0.0	0.0	0.0	0.0
-1.2171D-04	0.0	0.0	9.8247D-02
0.0	0.0	0.0	0.0
1.2796D-05	0.0	0.0	1.8144D-02

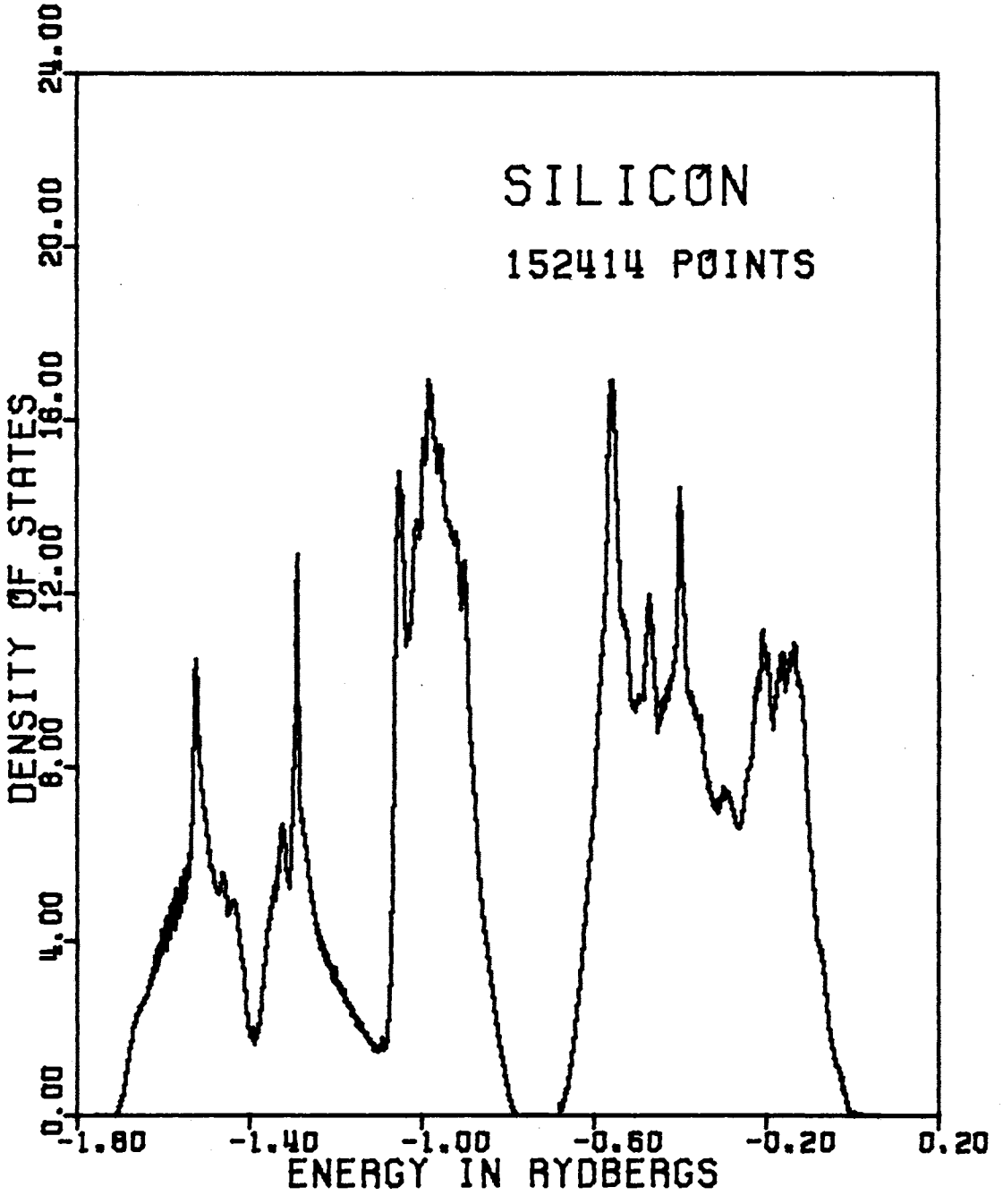

Figure 11. Silicon Density of States Using Optimized Orbitals

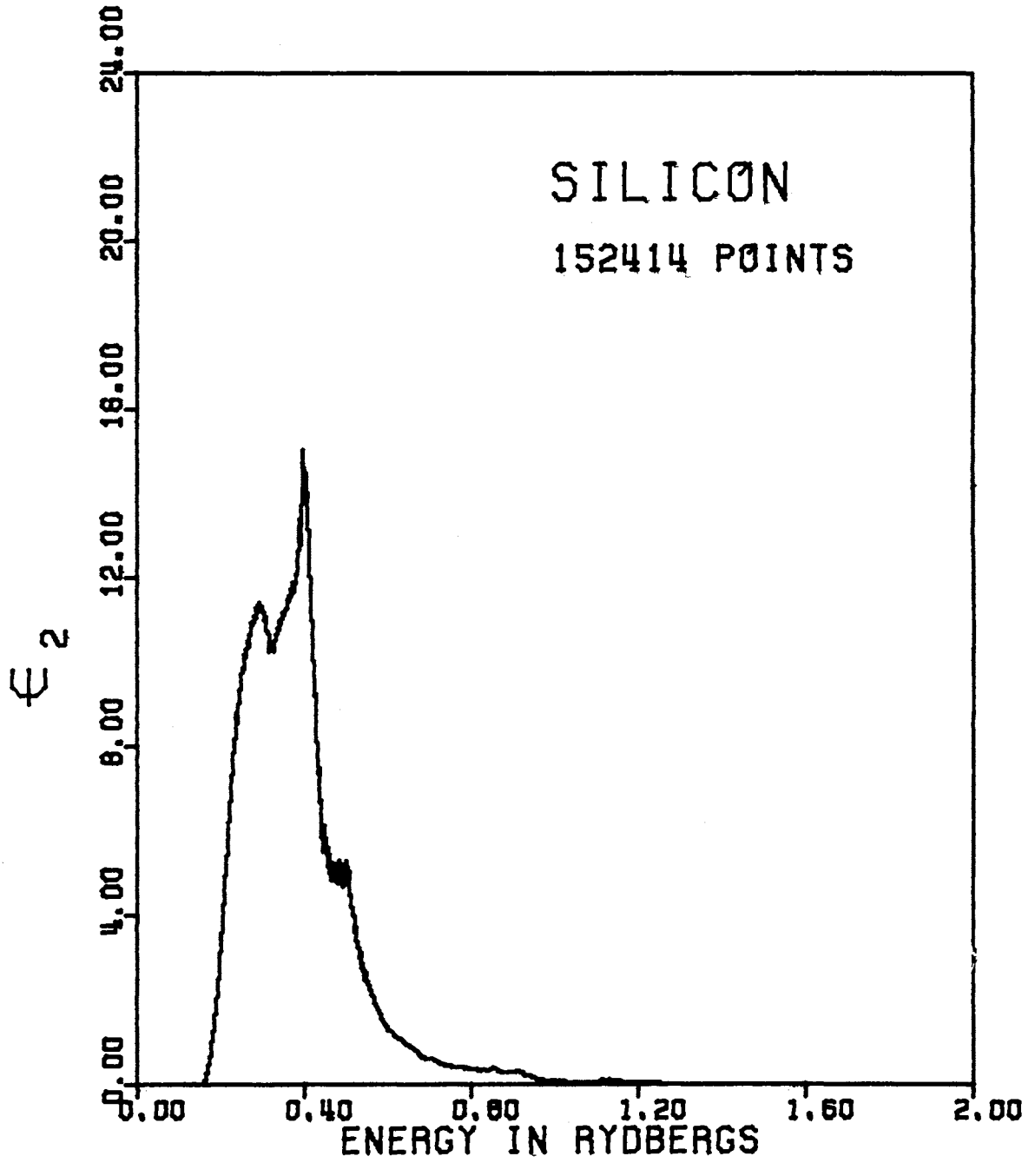

Figure 12. Silicon Dielectric Function Using Optimized Orbitals

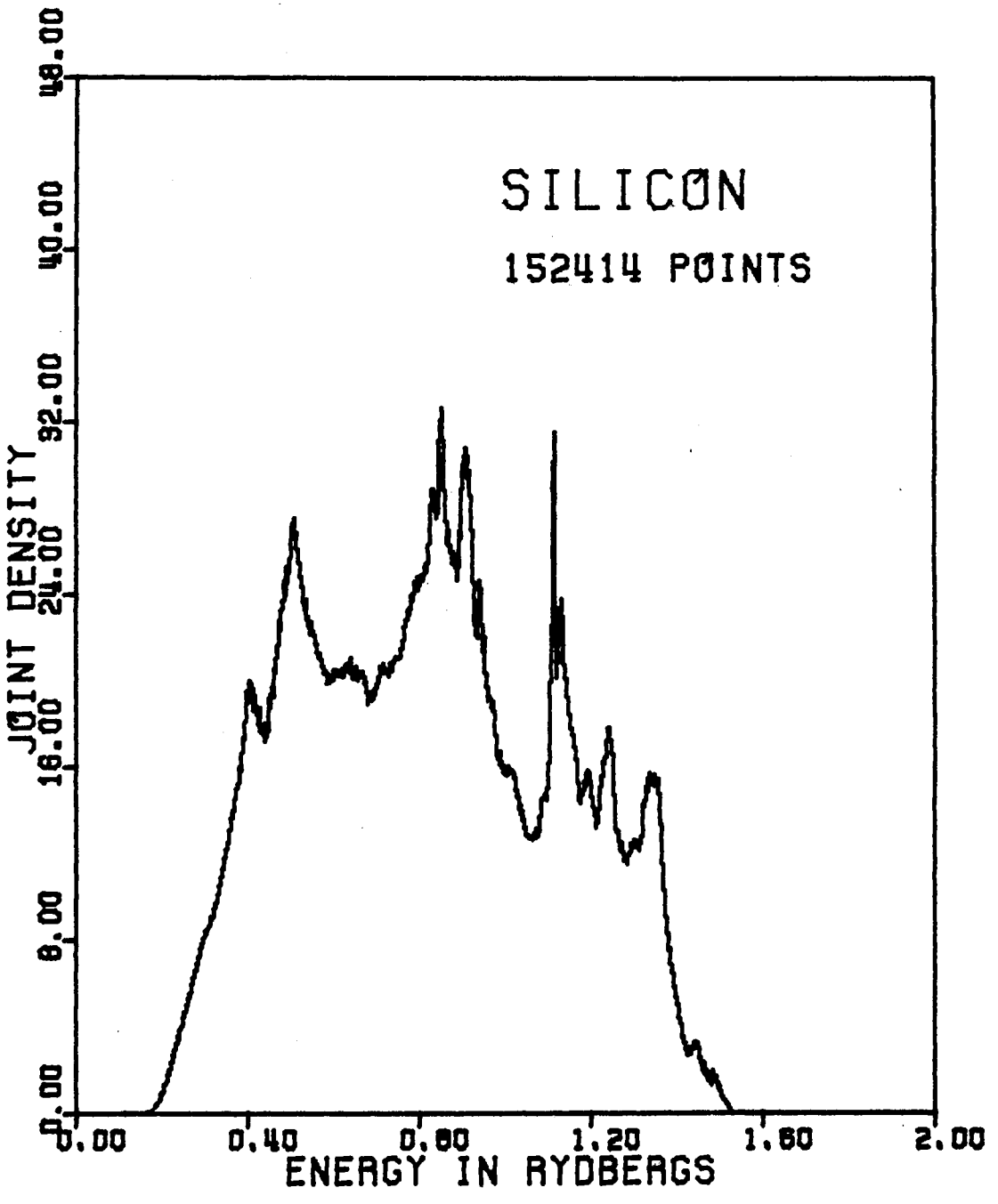

Figure 13. Silicon Joint Density of States
Using Optimized Orbitals

BIBLIOGRAPHY

(1) Herman, F., R. L. Kortum and C. D. Kuglin, Int. J. Quantum Chem. 15, 533 (1967).

(2) Herman, F., R. L. Kortum, C. D. Kuglin and R. A. Short, Quantum Theory of Atoms, Molecules and the Solid State, edited by Lowdin, P. O., Academic Press Inc., New York (1966).

(3) Brust, D., Phys. Rev., 134, A1337 (1964).

(4) Kane, E. O., Phys. Rev., 146, 558 (1966).

(5) Cohen, M. L. and T. K. Bergstresser, Phys. Rev., 141, 789 (1966).

(6) Cardona, M. and F. H. Pollak, Phys. Rev., 142, 530 (1966).

(7) Chaney, Roy C., Chun D. Lin and Earl E. Lafon, Phys. Rev., B3, 459 (1971).

(8) Stukel, D. J. and R. N. Euweme, Phys. Rev., B1, 1635 (1970).

(9) Philip, H. R. and H. Ehrenreich, Phys. Rev., 129, 1550 (1963).

(10) Painter, G. S., D. E. Ellis and A. R. Lubinsky, Phys. Rev., B4, 3610 (1971).

(11) Slater, John C., Quantum Theory of Molecules and Solids, McGraw-Hill Book Company, Inc., New York (1965), Vol. 2, p. 43.

(12) Bloch, F., Z. Physik, 52, 555 (1928).

(13) Wang, L., "Electronic Energy Band Structure of Copper by Tight-Binding Method." (Unpub. Ph.D. thesis, Oklahoma State University, 1971.)

(14) Slater, J. C. Phys. Rev., 81, 385 (1951).

(15) MacDonald, J. K. L., Phys. Rev., 43, 838 (1933).

(16) Lafon, E. E., and Chun C. Lin, Phys. Rev., 152, 579 (1966).

(17) Chaney, R. C., T. K. Tung, C. C. Lin and E. E. Lafon, J. Chem. Phys. 52, 361 (1970).

(18) Chaney, Roy C., Earl E. Lafon and Chun C. Lin, Phys. Rev., B4, 2734 (1971).

(19) Ehrenreich, H. and M. H. Cohen, Phys. Rev., 115, 786 (1959).

(20) Gilat, G. and G. Dolling, Phys. Lett. 8, 304 (1964).

(21) Euwema, R. N., (Private communication), (1972).

(22) Veillard, A., Theoret. Chim. Acta (Berl.), 12, 405 (1968).

(23) Kunz, A. B., Phys. Rev. Lett., 27, 567 (1971).

(24) Roberts, R. A. and W. C. Walker, Phys. Rev., 161, 730 (1967).

(25) Phillips, J. C., Phys, Rev., 139, A1291 (1965).

(26) Philipp, H. R. and H. Ehrenreich, Phys. Rev., 129, 1550 (1963).

(27) Menzel, P. W., C. C. Lin, D. F. Fouquet, E. E. Lafon and R. C. Chaney, "Optical Dielectric Function of the Lithium Fluoride Crystal," (submitted for publication) (1973).

APPENDIX A

DIAMOND BAND TO BAND DATA

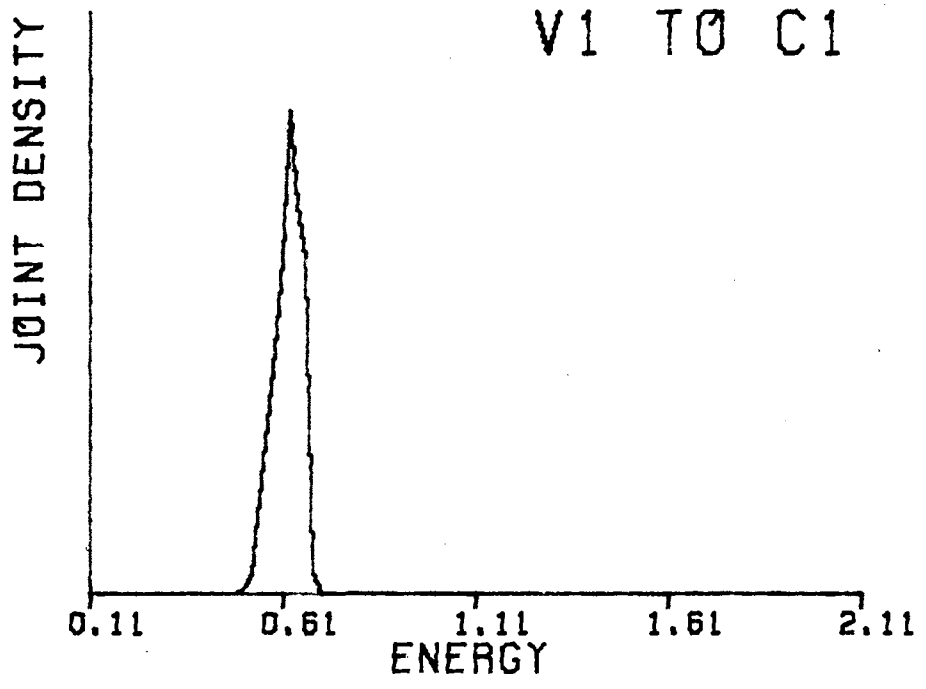
V1 TØ C1
JØINT DENSITY
0.11
0.61
1.11
1.61
2.11
ENERGY

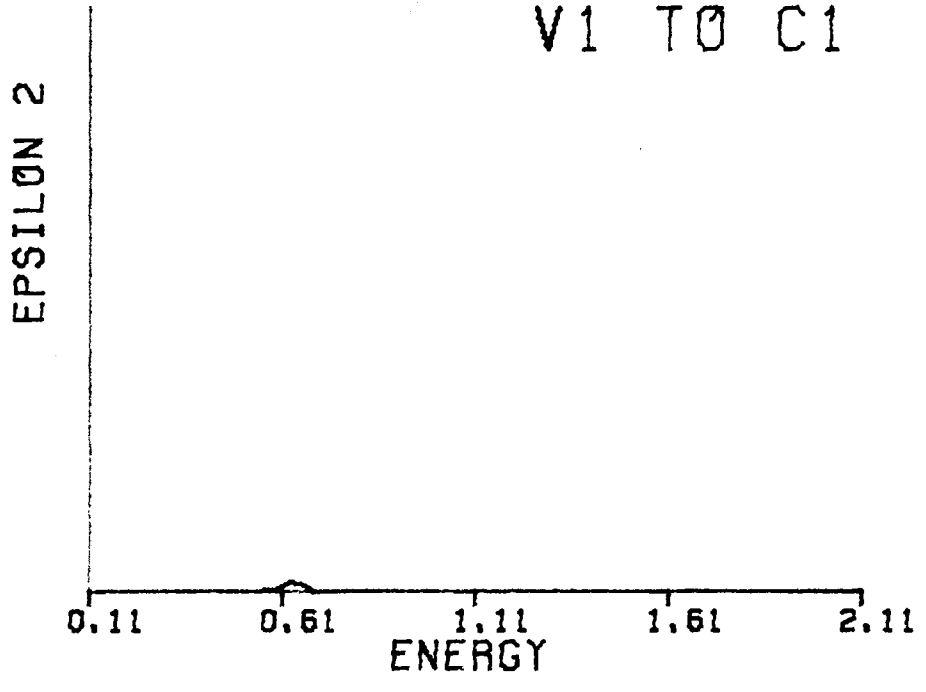
V1 TØ C1
EPSILØN 2
0.11
0.61
1.11
1.61
2.11
ENERGY

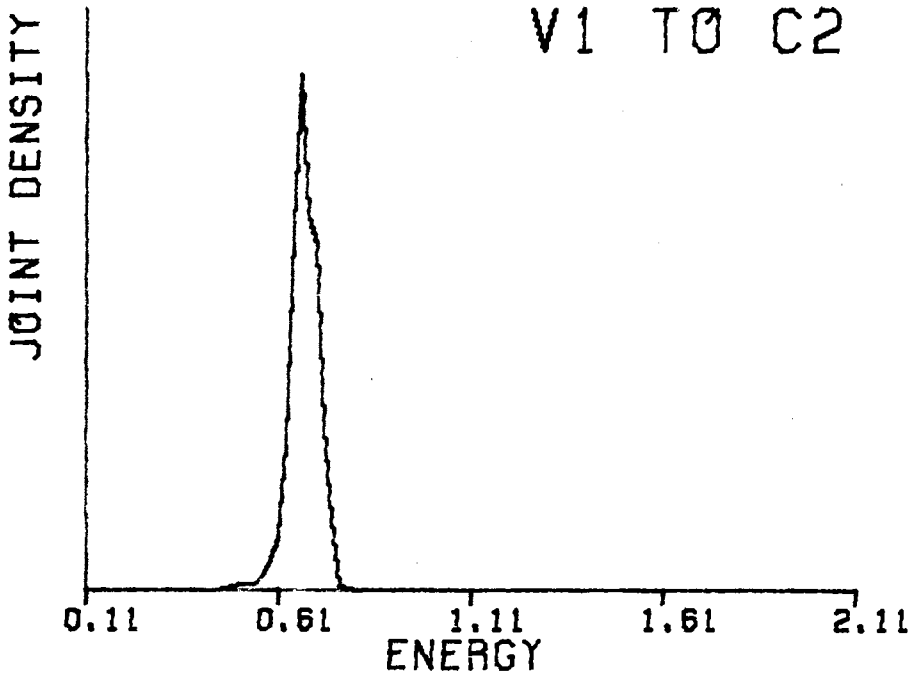
V1 TØ C2
JØINT DENSITY
0.11
0.61
1.11
1.61
2.11
ENERGY

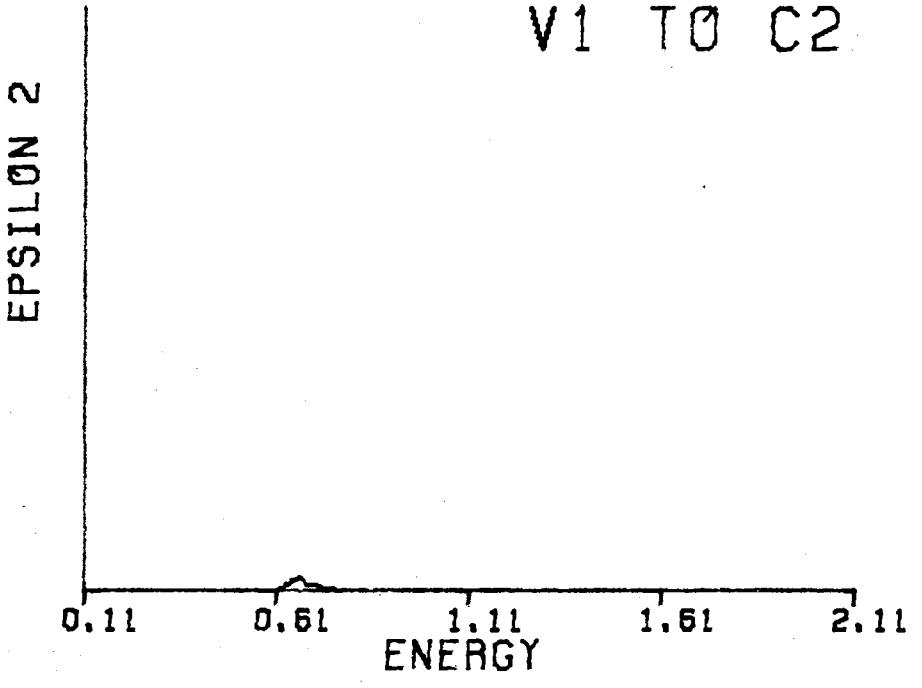
V1 TØ C2
EPSILØN 2
0.11
0.61
1.11
1.61
2.11
ENERGY

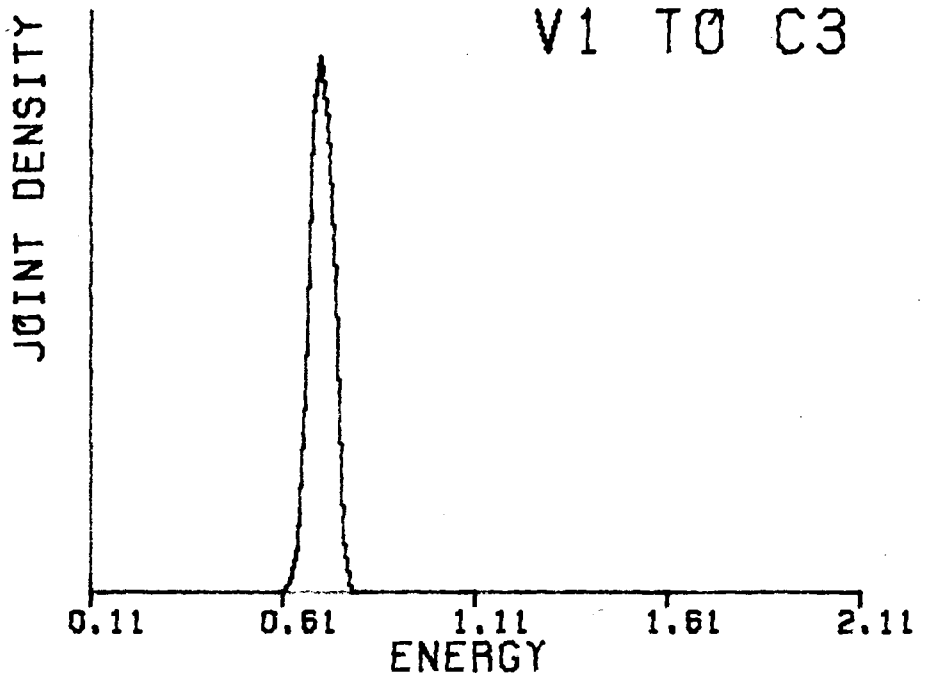
V1 TØ C3
JØINT DENSITY
0.11
0.61
1.11
1.61
2.11
ENERGY

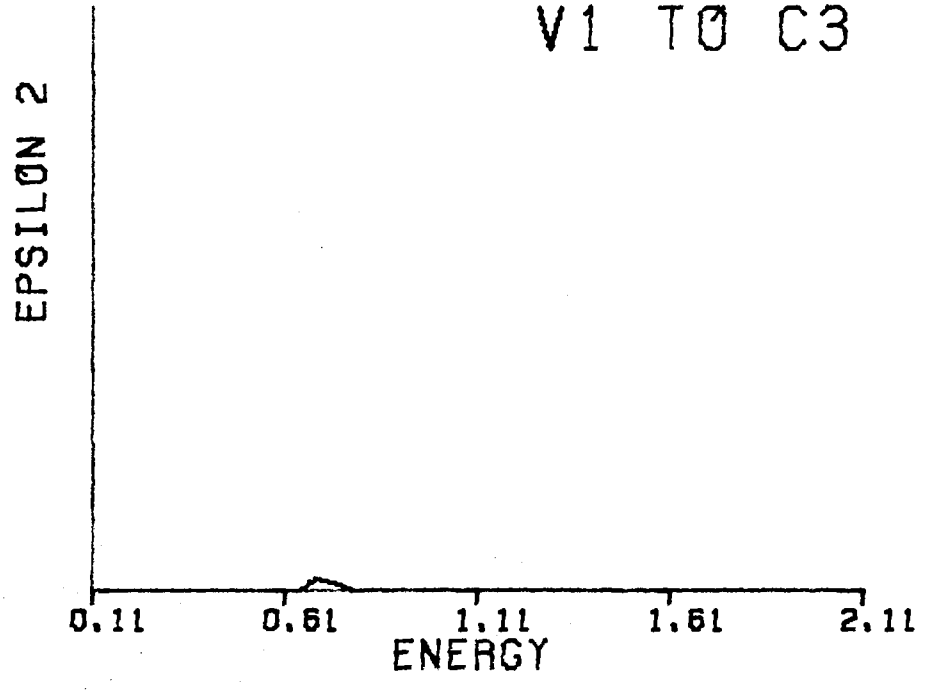
V1 TØ C3
EPSILØN 2
0.11
0.61
1.11
1.61
2.11
ENERGY

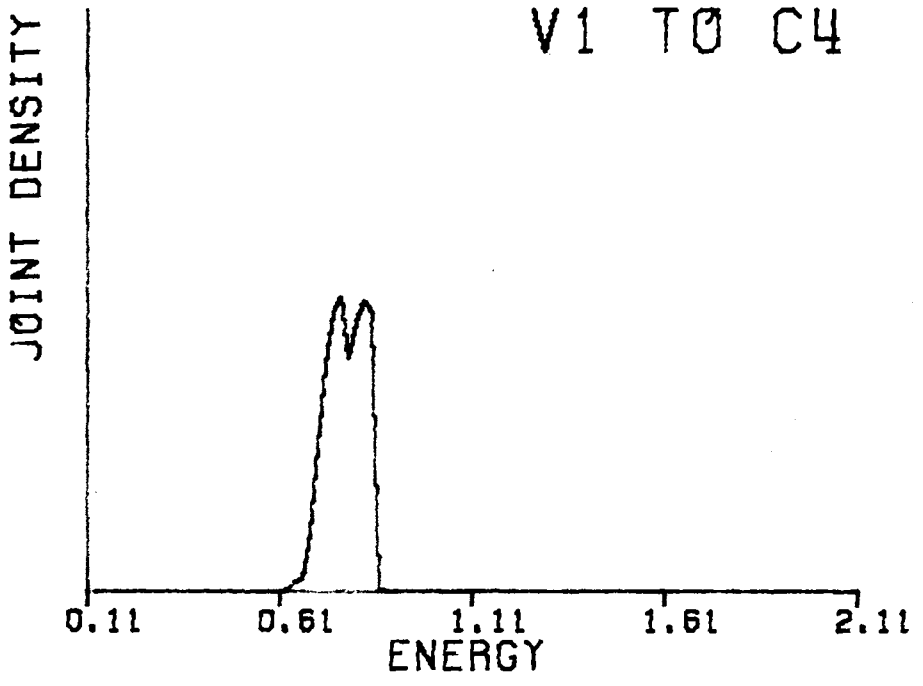
V1 TØ C4
JØINT DENSITY
0.11
0.61
1.11
1.61
2.11
ENERGY

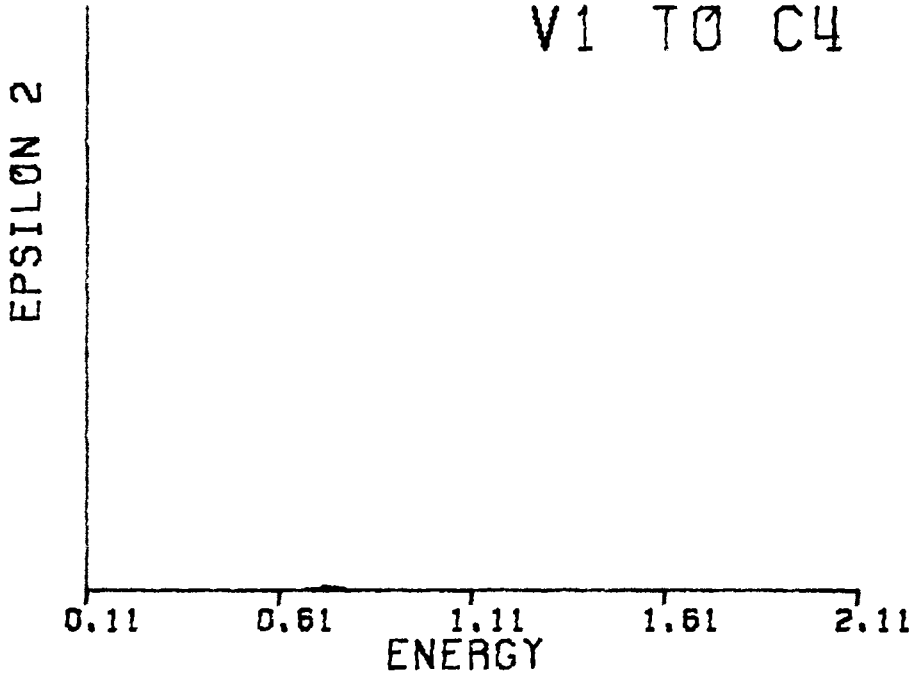
V1 TØ C4
EPSILØN 2
0.11
0.61
1.11
1.61
2.11
ENERGY

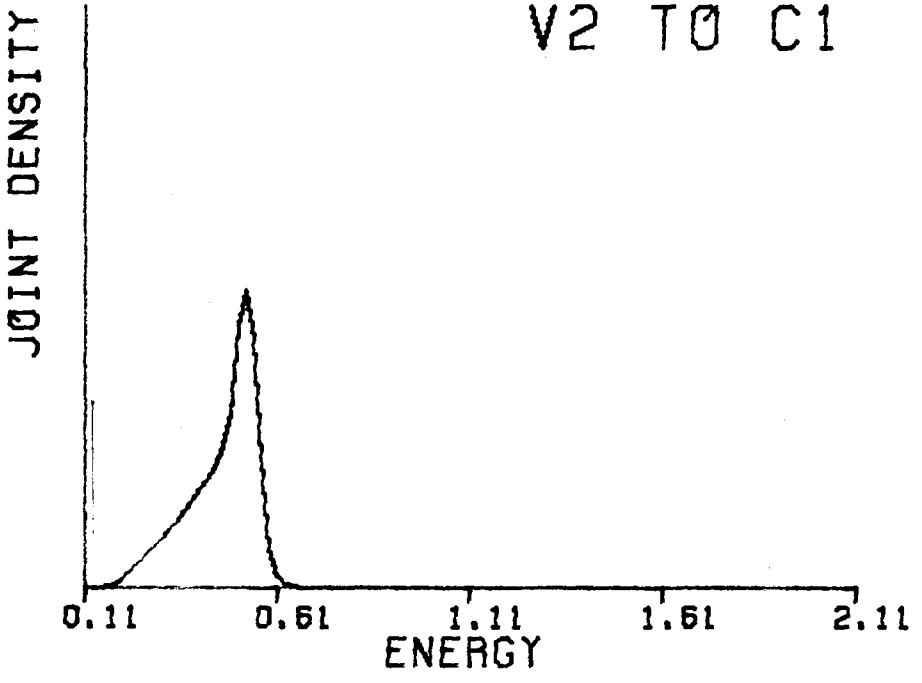
V2 TØ C1
JØINT DENSITY
0.11
0.61
1.11
1.61
2.11
ENERGY

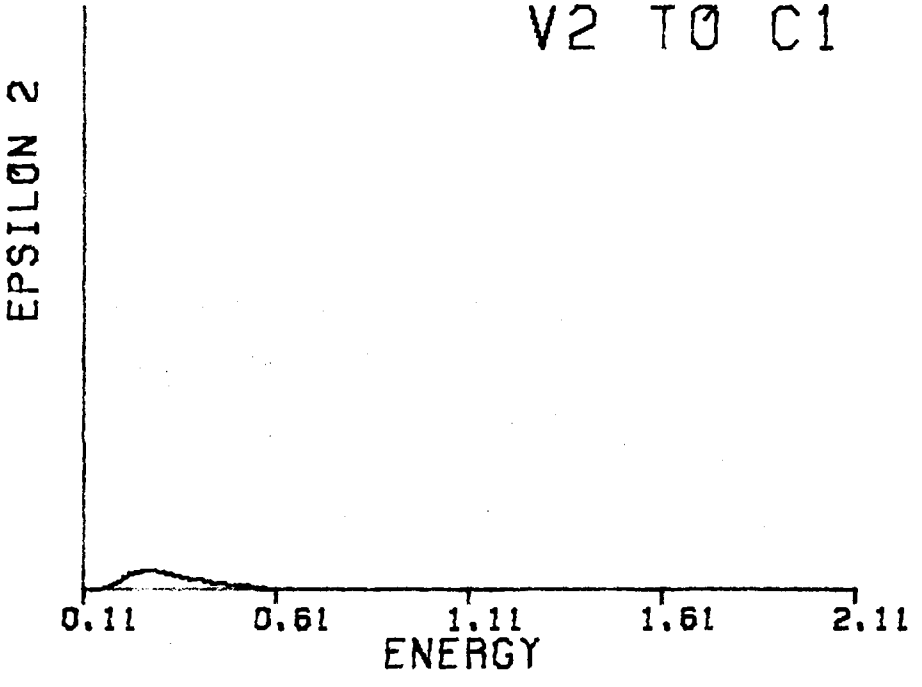
V2 TØ C1
EPSILØN 2
0.11
0.61
1.11
1.61
2.11
ENERGY

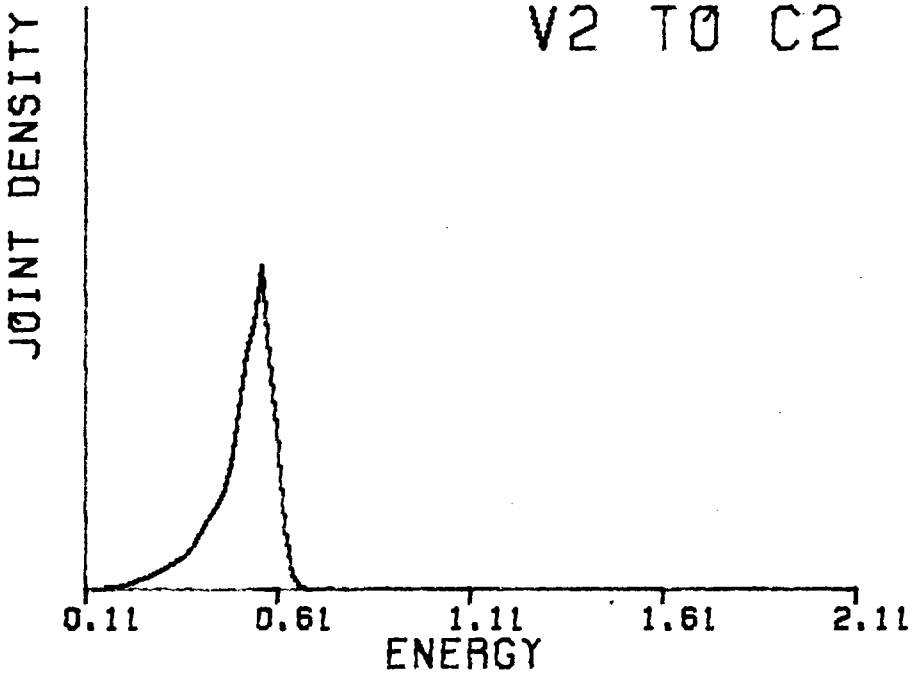
V2 TO C2
JOINT DENSITY
0.11
0.61
1.11
1.61
2.11
ENERGY

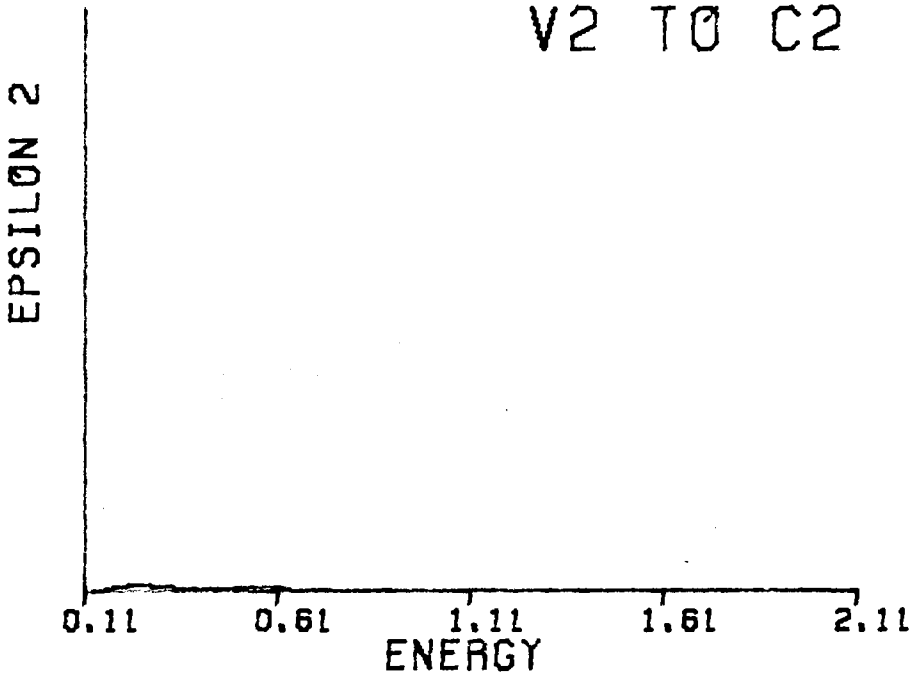
V2 TO C2
EPSILON 2
0.11
0.61
1.11
1.61
2.11
ENERGY

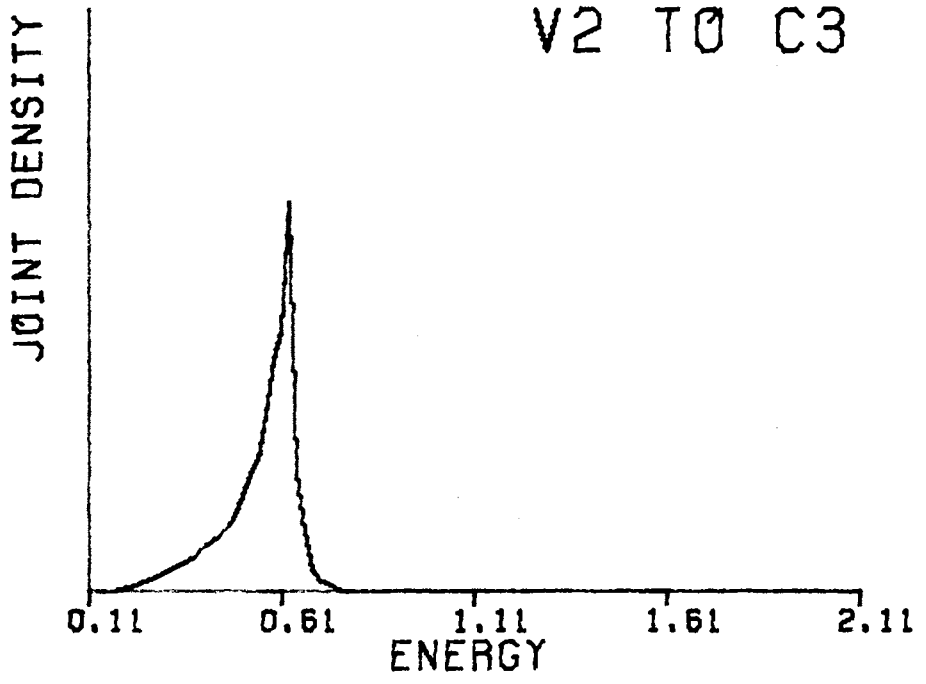
V2 TØ C3
JØINT DENSITY
0.11
0.61
1.11
1.61
2.11
ENERGY

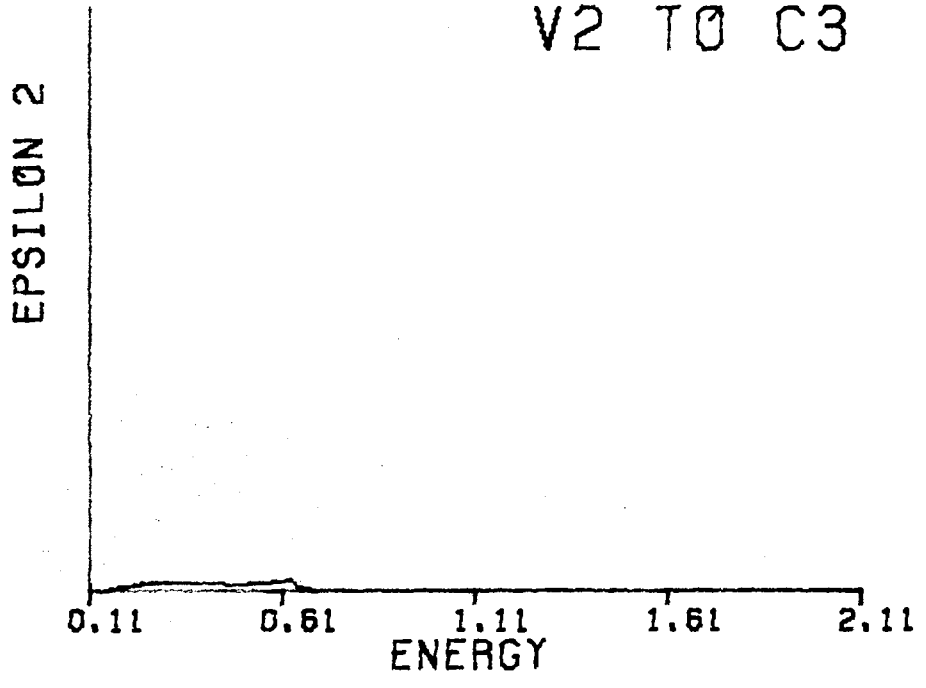
V2 TØ C3
EPSILØN 2
0.11
0.61
1.11
1.61
2.11
ENERGY

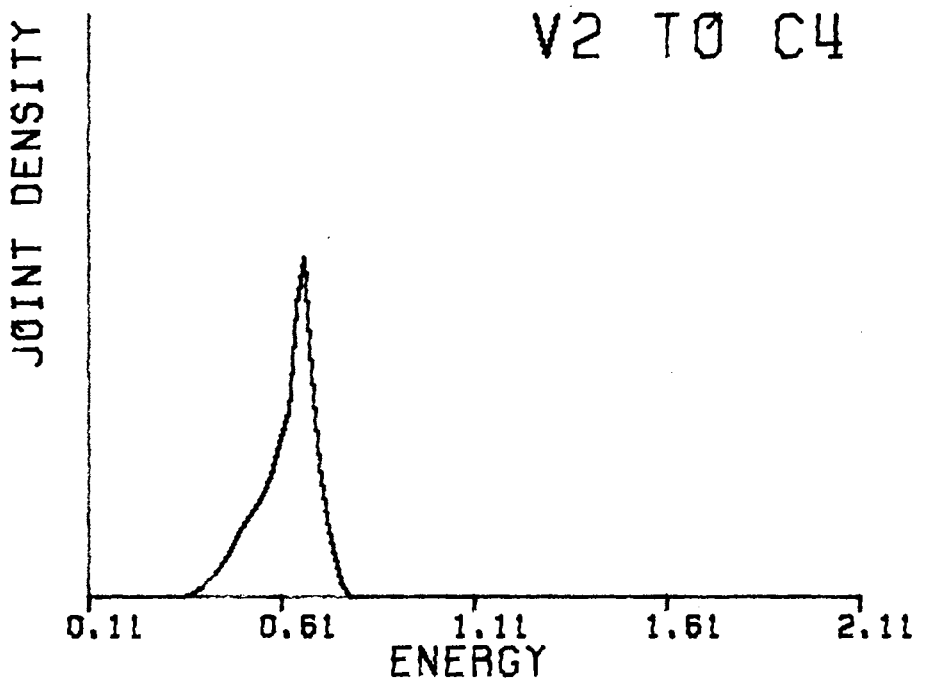
V2 TO C4
JOINT DENSITY
0.11
0.61
1.11
1.61
2.11
ENERGY

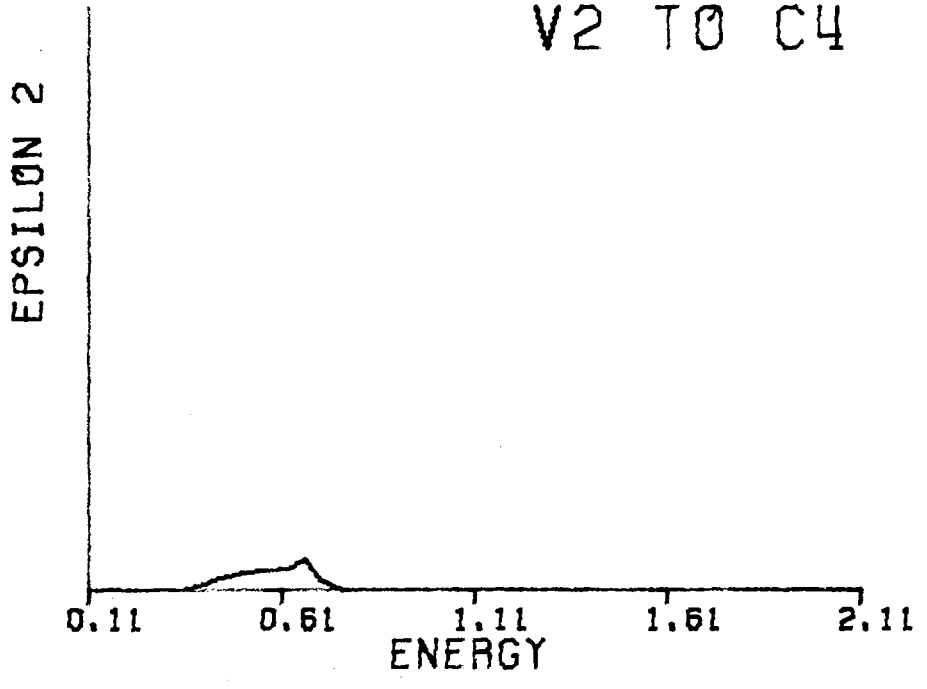
V2 TO C4
EPSILON 2
0.11
0.61
1.11
1.61
2.11
ENERGY

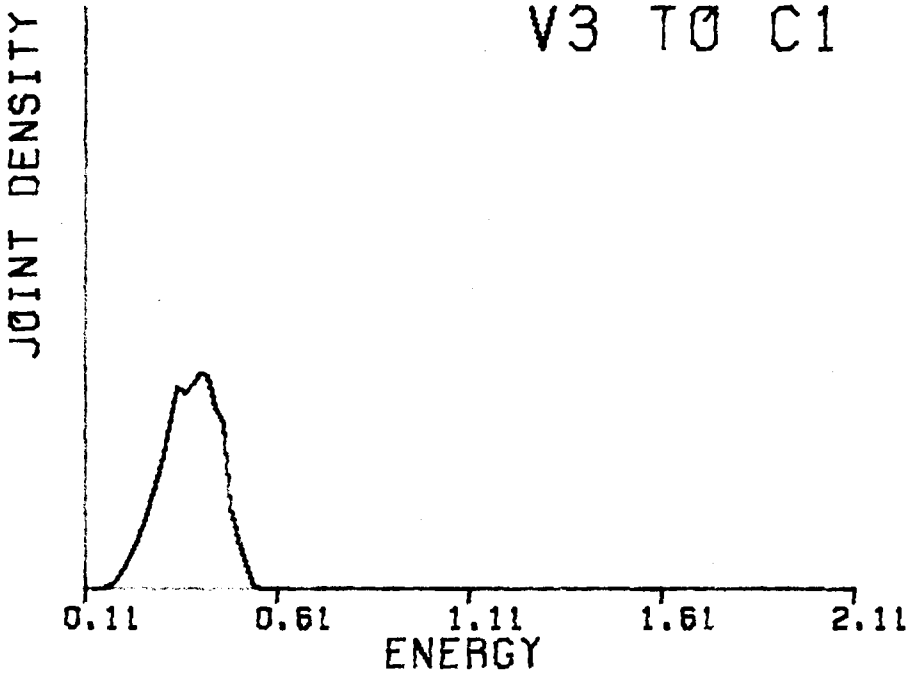
V3 TØ C1
JØINT DENSITY
0.11
0.61
1.11
1.61
2.11
ENERGY

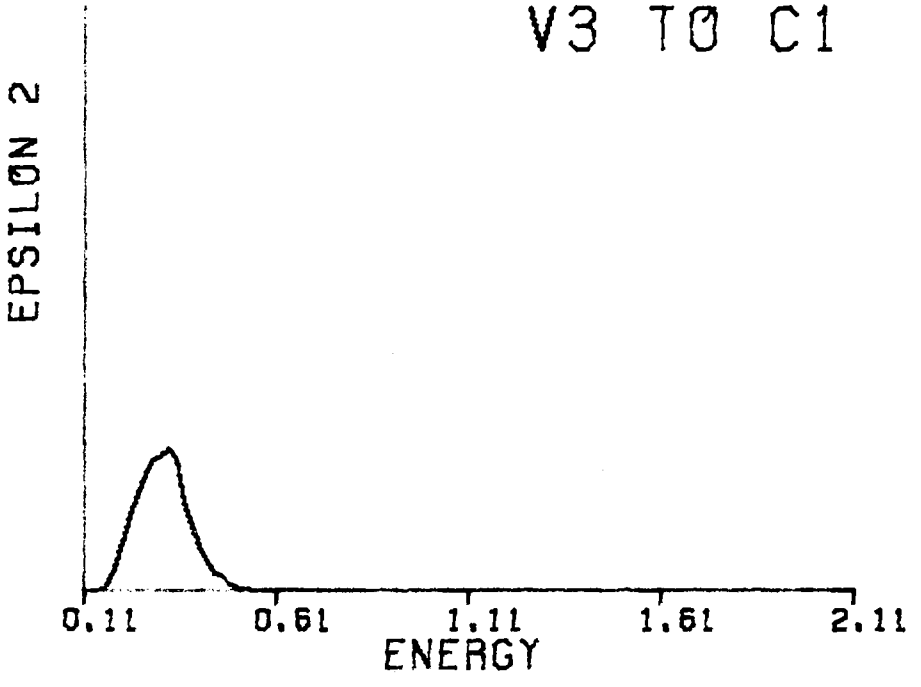
V3 TØ C1
EPSILØN 2
0.11
0.61
1.11
1.61
2.11
ENERGY

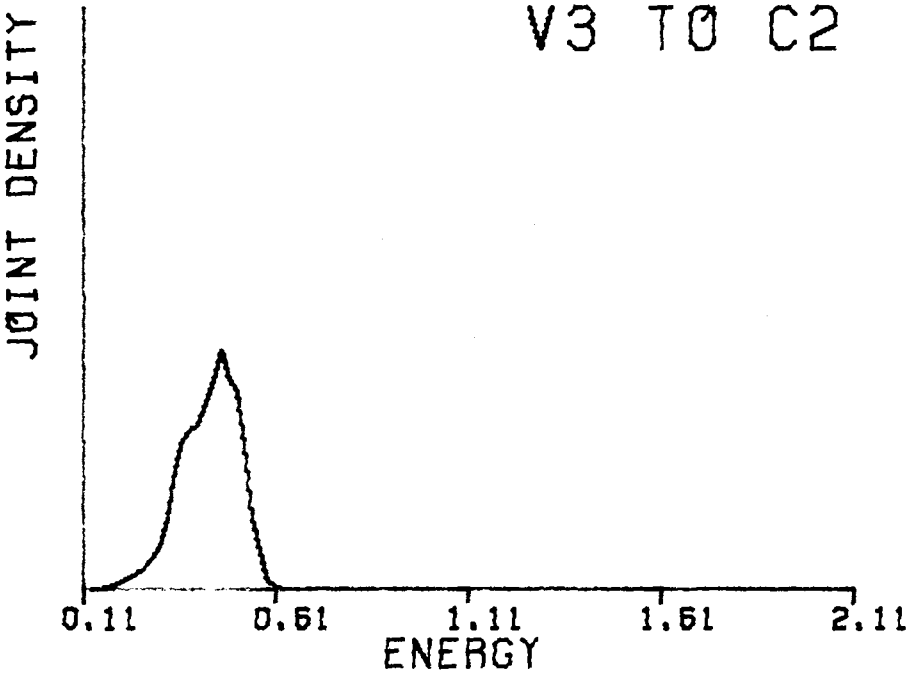
V3 TØ C2
JØINT DENSITY
0.11
0.61
1.11
1.61
2.11
ENERGY

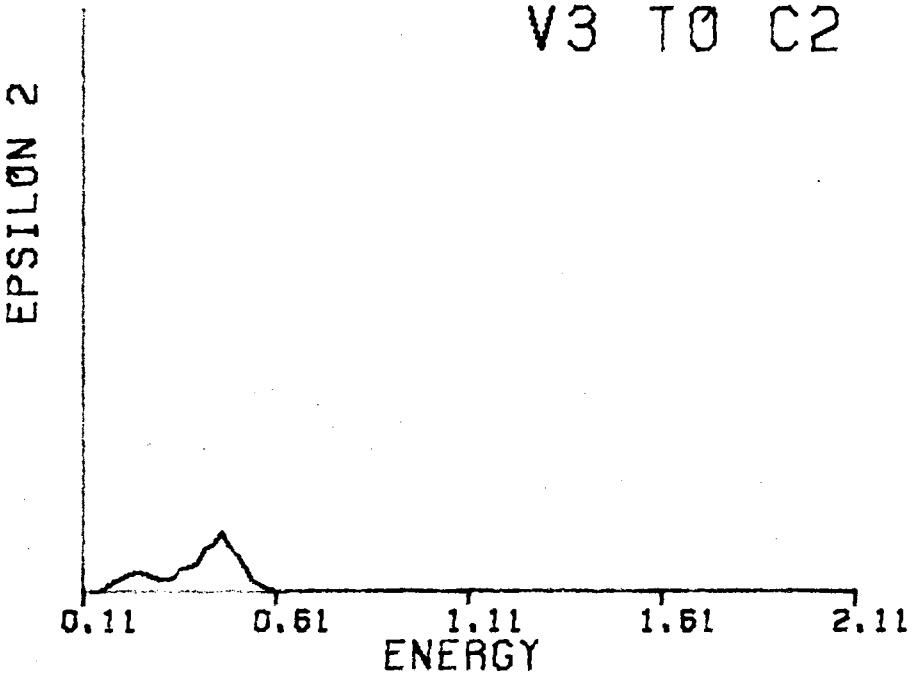
V3 TØ C2
EPSILØN 2
0.11
0.61
1.11
1.61
2.11
ENERGY

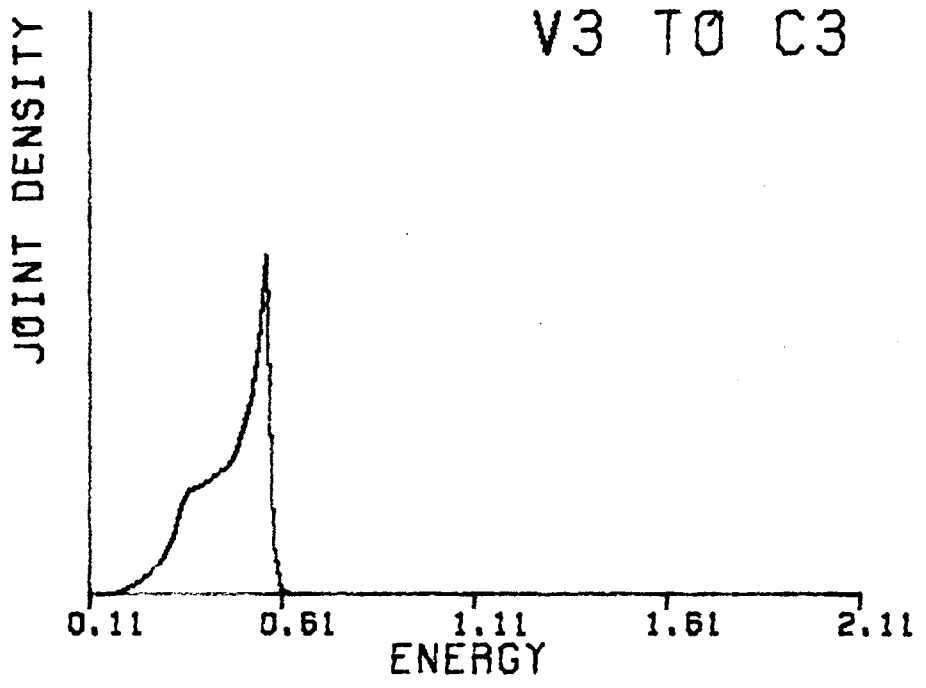
V3 TØ C3
JØINT DENSITY
0.11
0.61
1.11
1.61
2.11
ENERGY

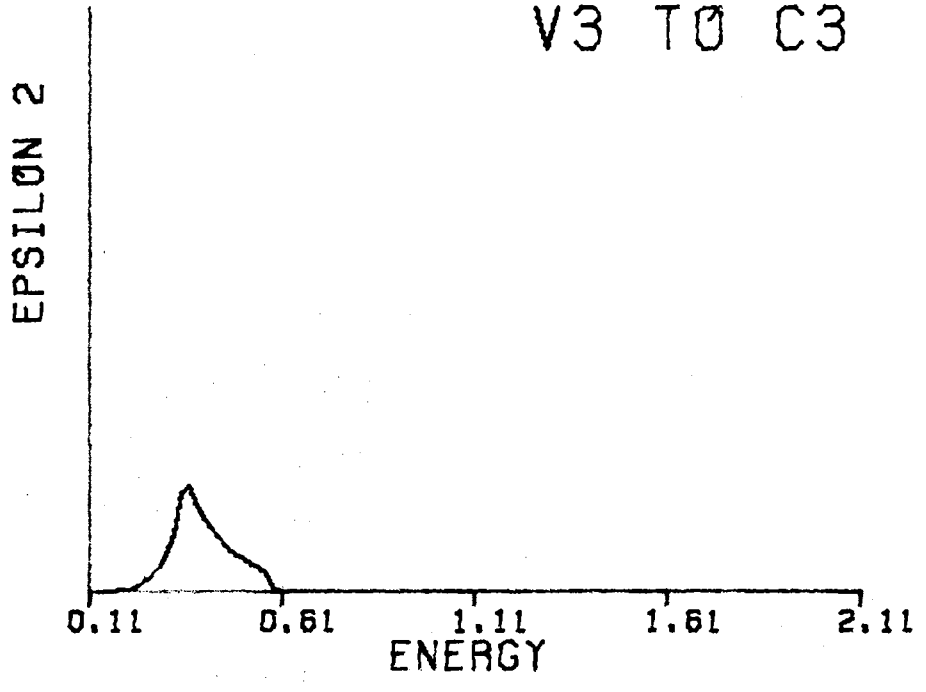
V3 TØ C3
EPSILØN 2
0.11
0.61
1.11
1.61
2.11
ENERGY

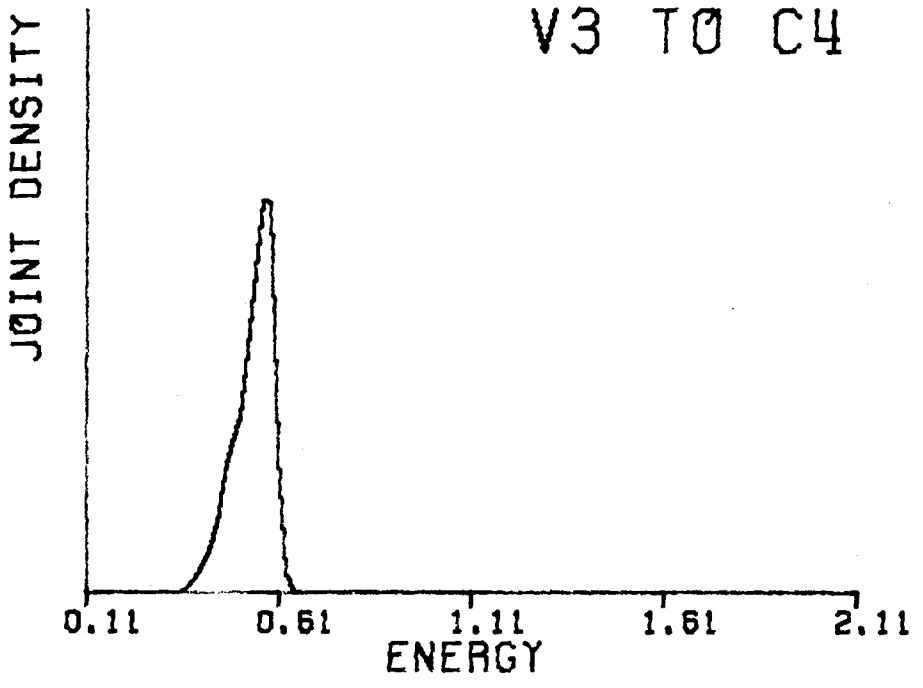
V3 TØ C4
JØINT DENSITY
0.11
0.61
1.11
1.61
2.11
ENERGY

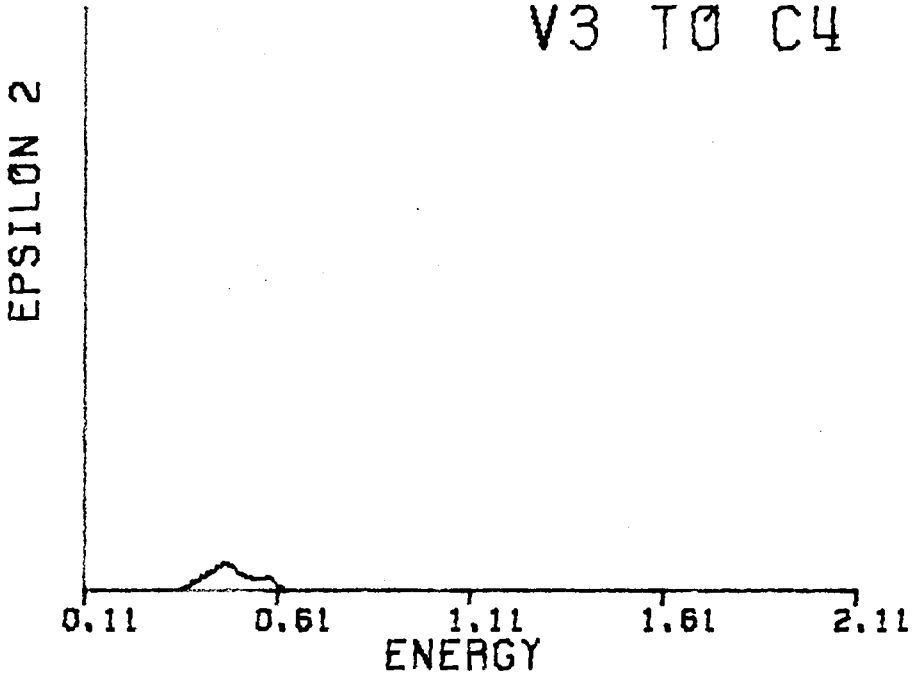
V3 TØ C4
EPSILØN 2
0.11
0.61
1.11
1.61
2.11
ENERGY

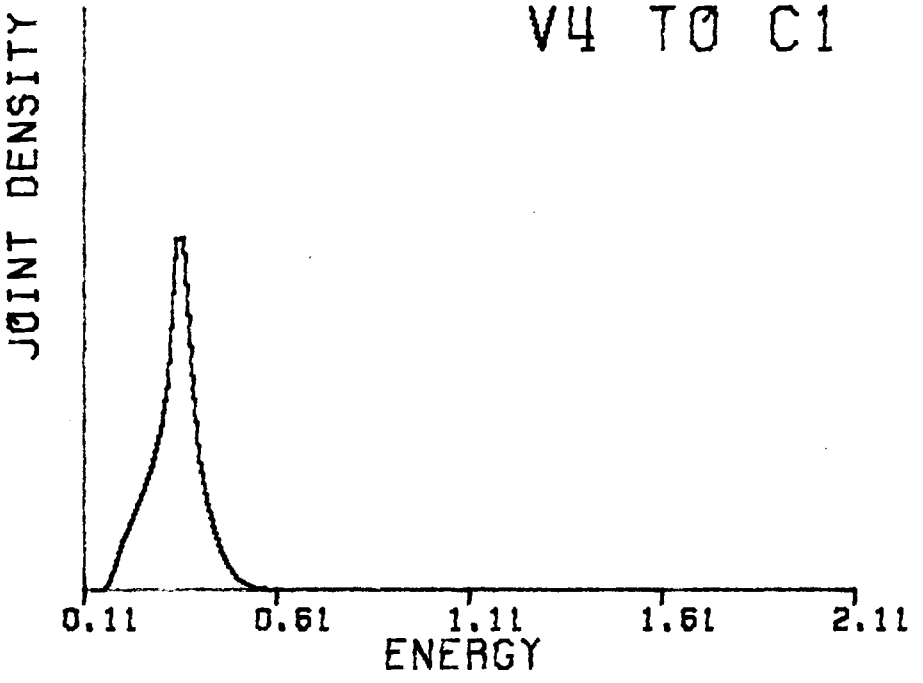
V4 TØ C1
JØINT DENSITY
0.11
0.61
1.11
1.61
2.11
ENERGY

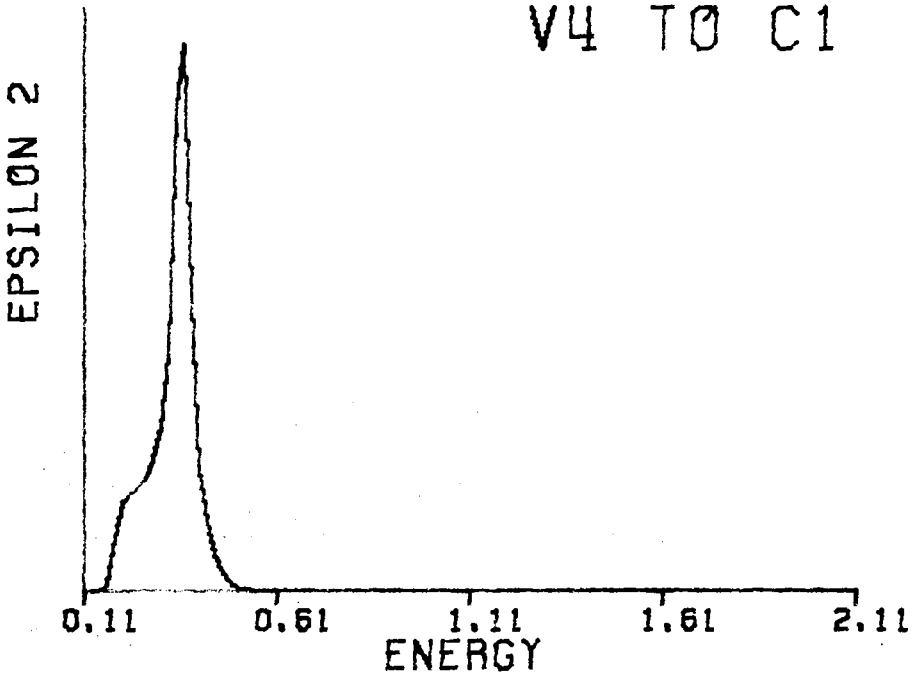
V4 TØ C1
EPSILØN 2
0.11
0.61
1.11
1.61
2.11
ENERGY

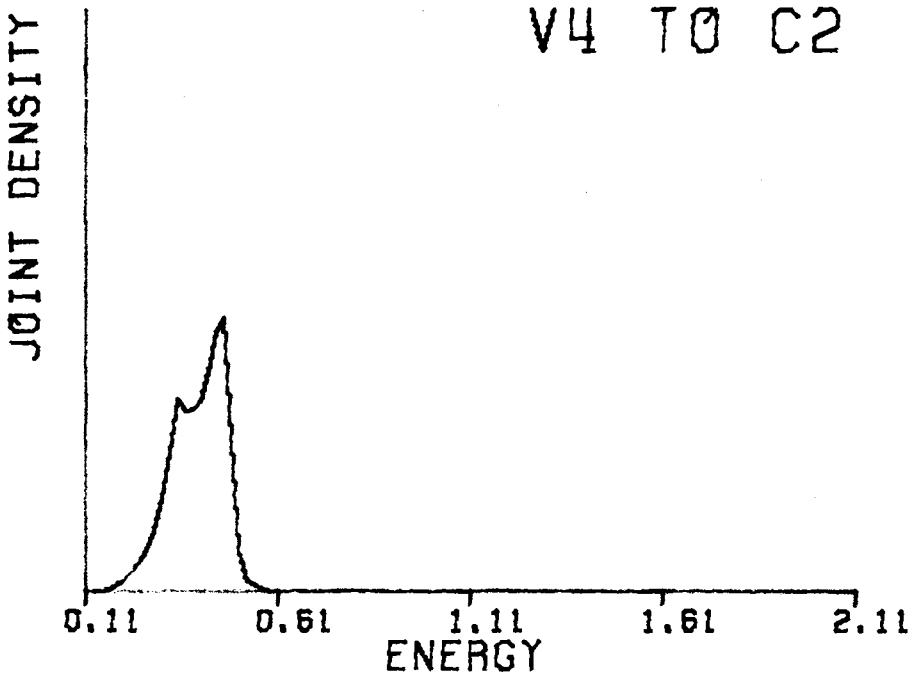
V4 TO C2
JOINT DENSITY
0.11
0.61
1.11
1.61
2.11
ENERGY

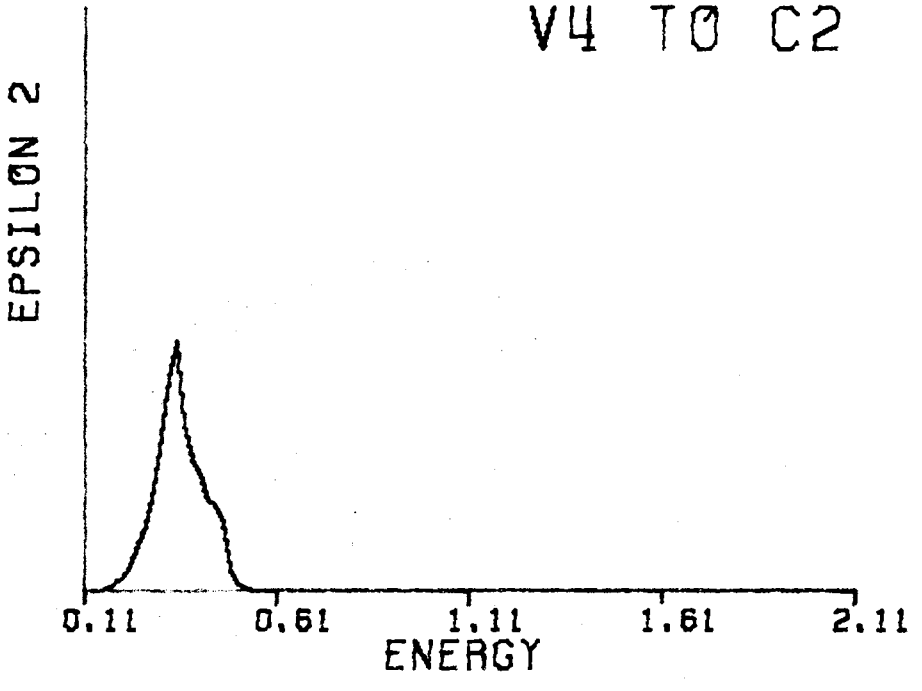
V4 TO C2
EPSILON 2
0.11
0.61
1.11
1.61
2.11
ENERGY

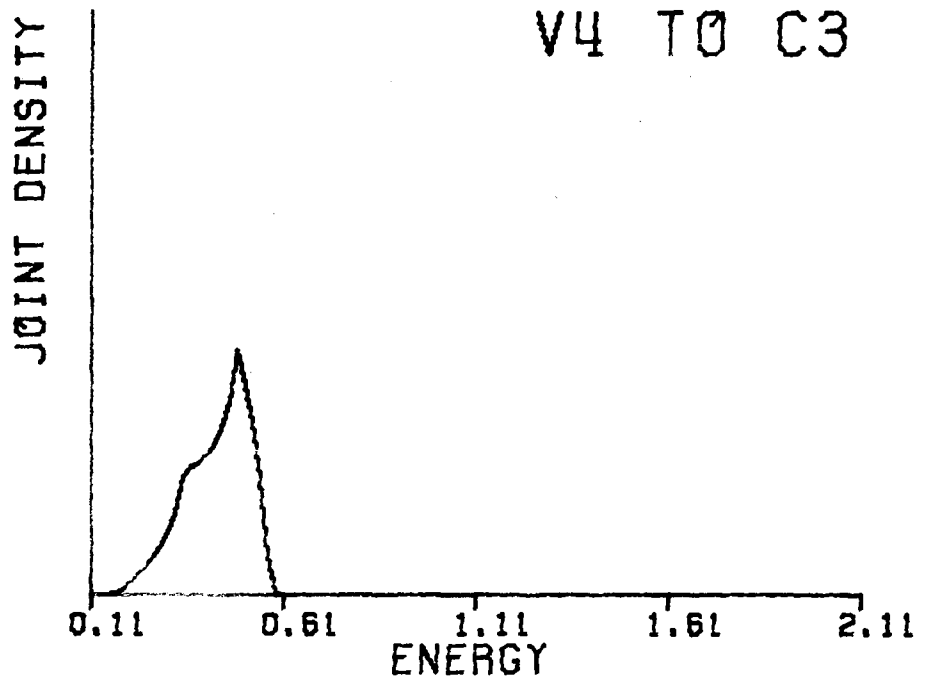
V4 TO C3
JOINT DENSITY
0.11
0.61
1.11
1.61
2.11
ENERGY

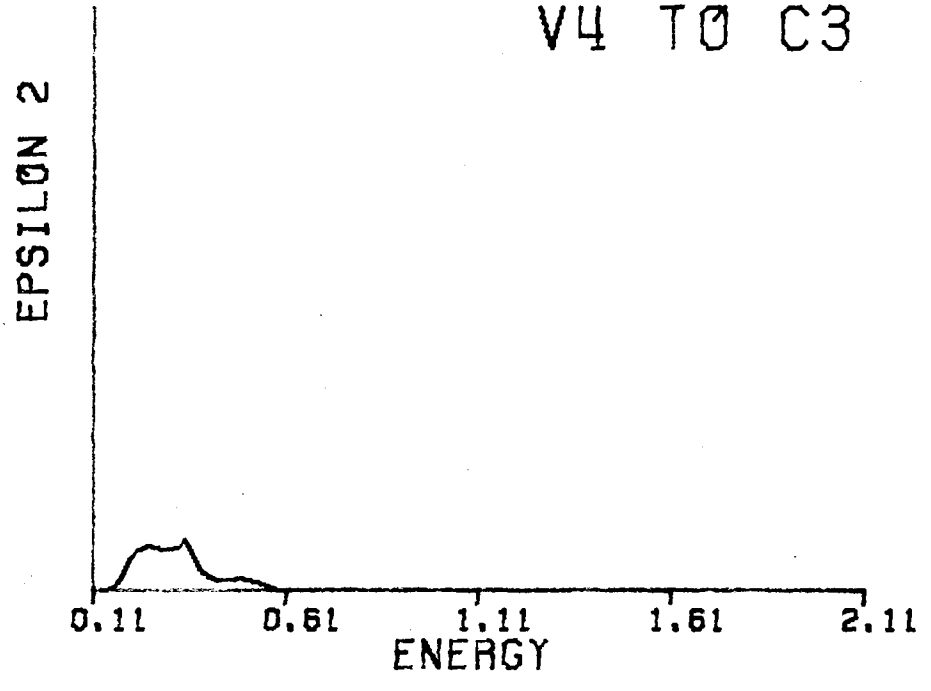
V4 TO C3
EPSILON 2
0.11
0.61
1.11
1.61
2.11
ENERGY

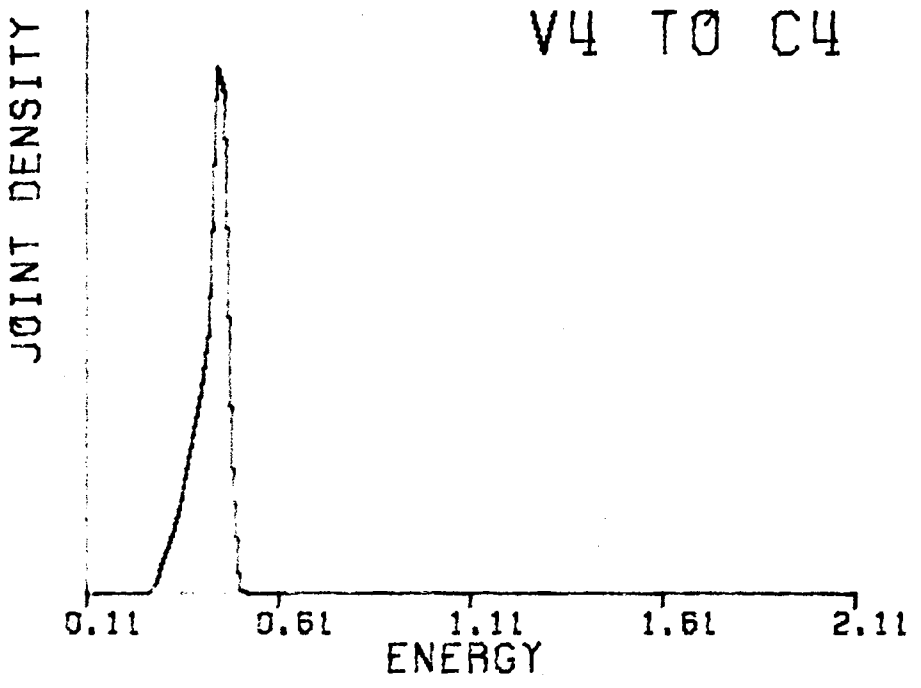
V4 TØ C4
JØINT DENSITY
0.11
0.61
1.11
1.61
2.11
ENERGY

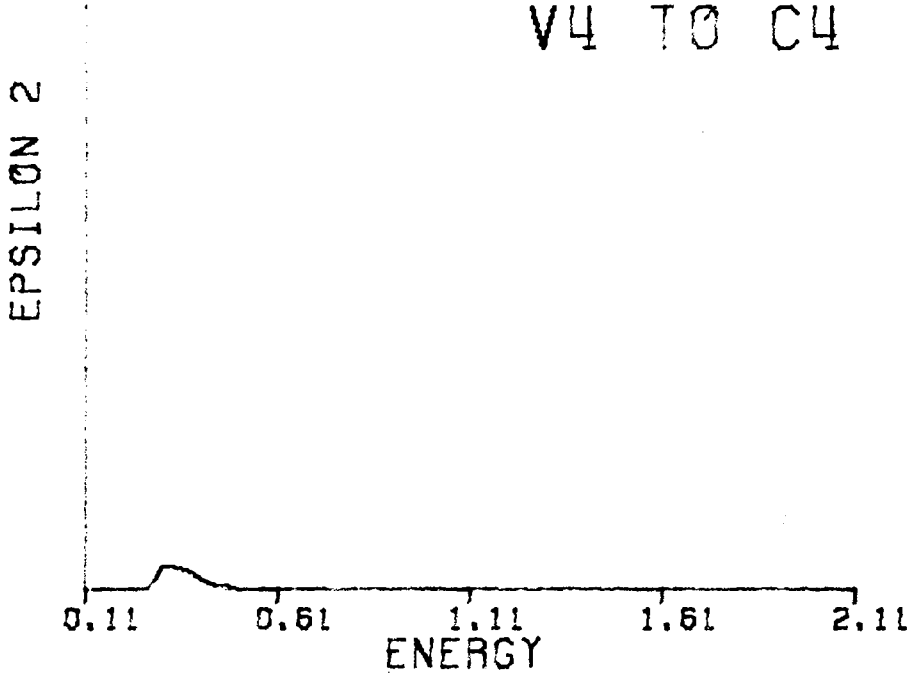
V4 TØ C4
EPSILØN 2
0.11
0.61
1.11
1.61
2.11
ENERGY

APPENDIX B

SILICON BAND TO BAND DATA

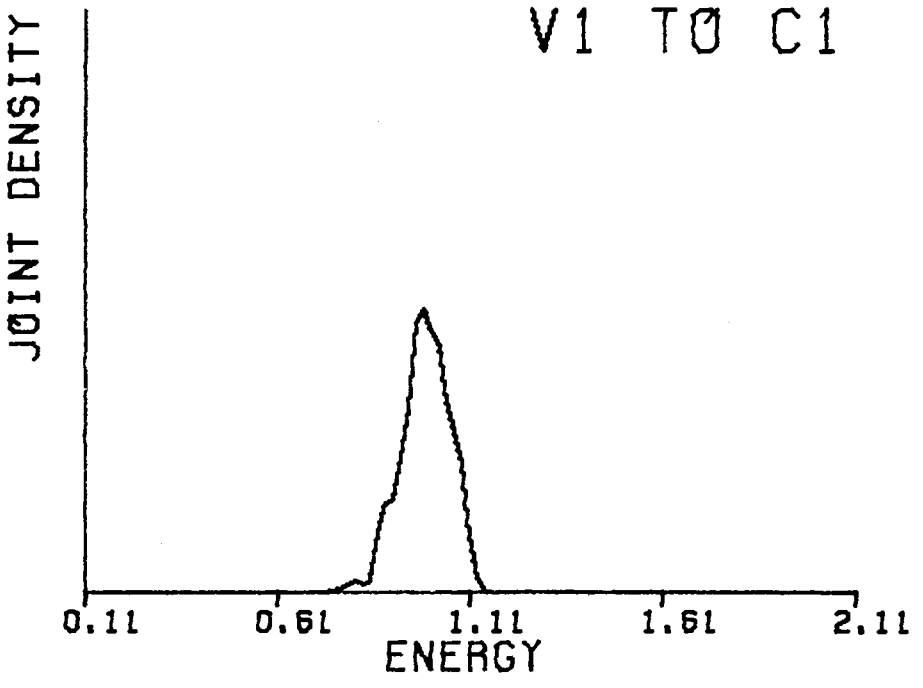
V1 TØ C1
JØINT DENSITY
0.11
0.61
1.11
1.61
2.11
ENERGY

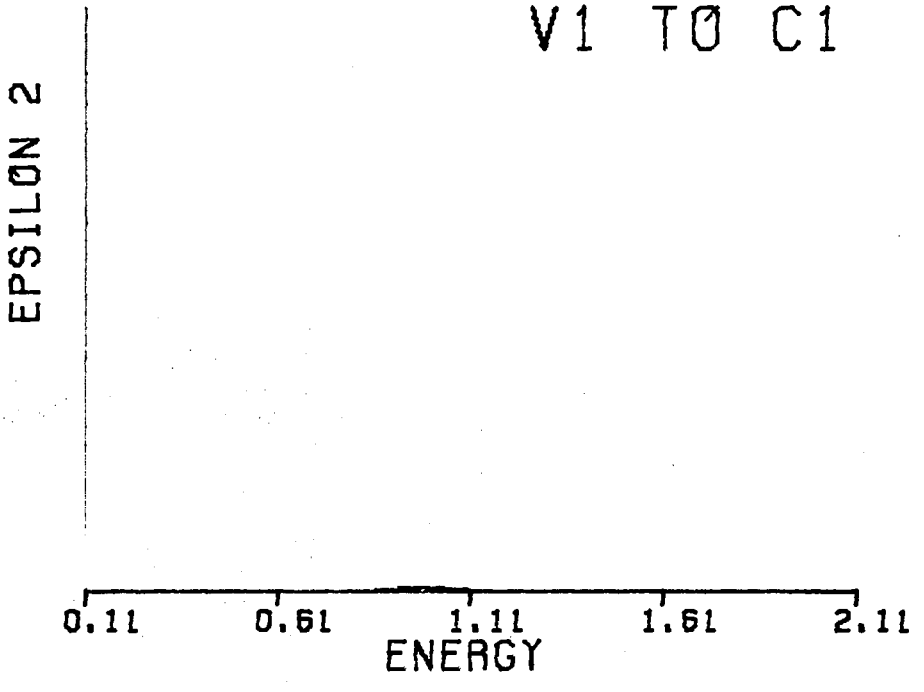
V1 TØ C1
EPSILØN 2
0.11
0.61
1.11
1.61
2.11
ENERGY

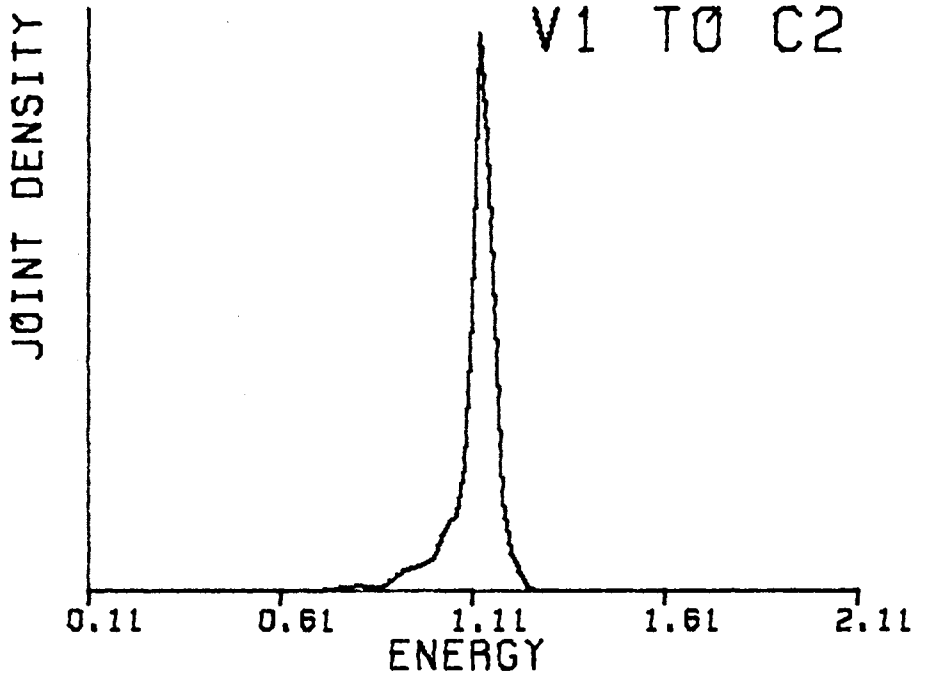
V1 TØ C2
JØINT DENSITY
0.11
0.61
1.11
1.61
2.11
ENERGY

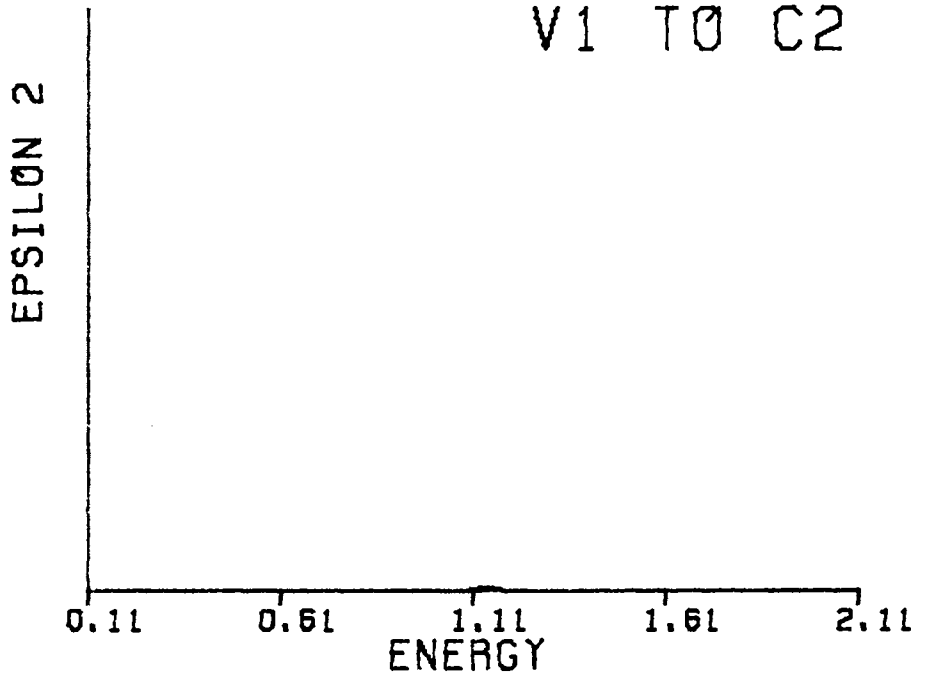
V1 TØ C2
EPSILØN 2
0.11
0.61
1.11
1.61
2.11
ENERGY

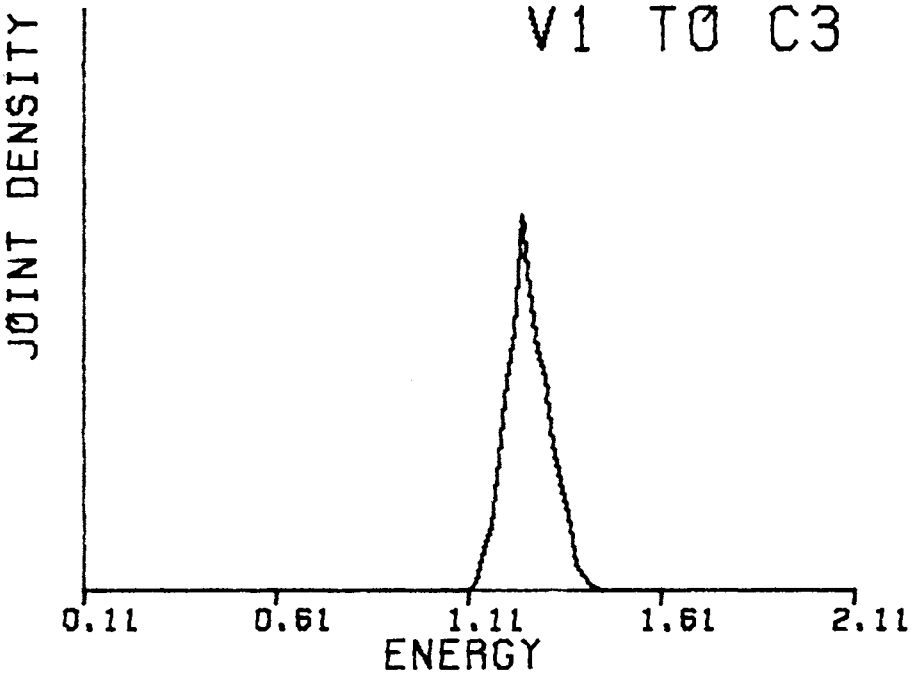
V1 TØ C3
JØINT DENSITY
0.11
0.61
1.11
1.61
2.11
ENERGY

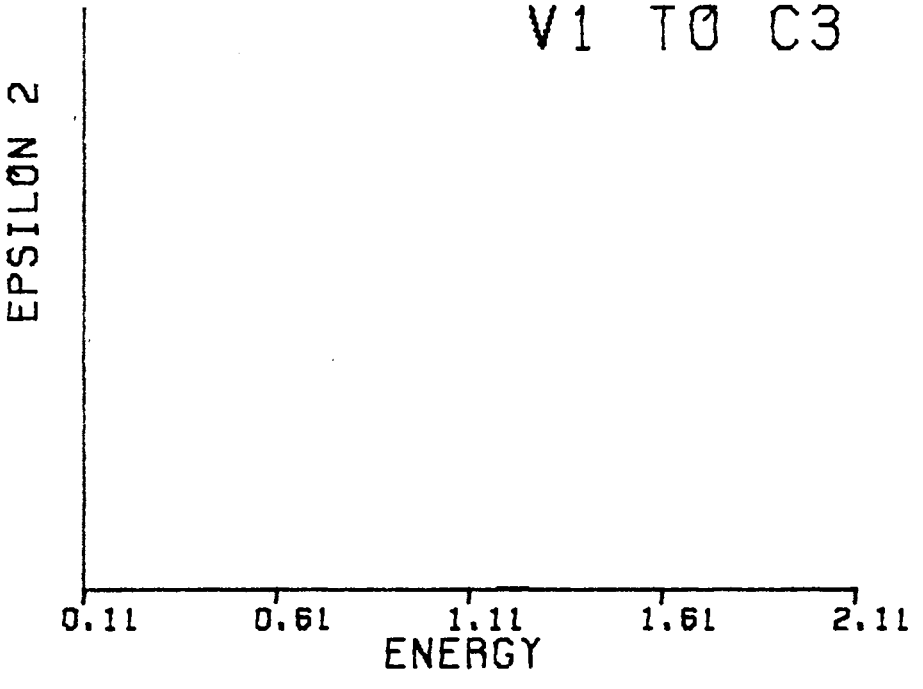
V1 TØ C3
EPSILØN 2
0.11
0.61
1.11
1.61
2.11
ENERGY

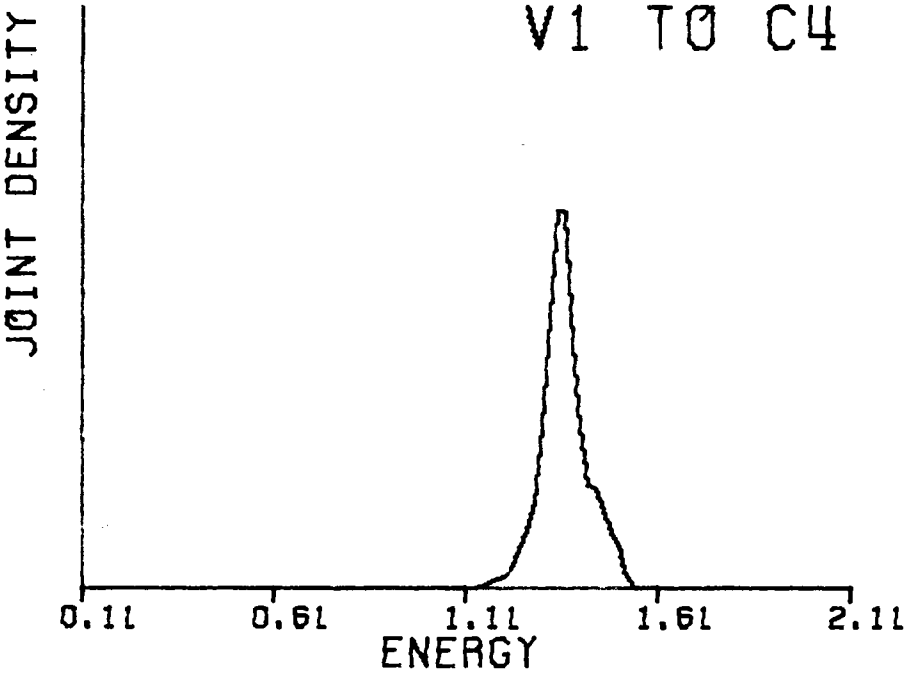
V1 TO C4
JOINT DENSITY
0.11
0.61
1.11
1.61
2.11
ENERGY

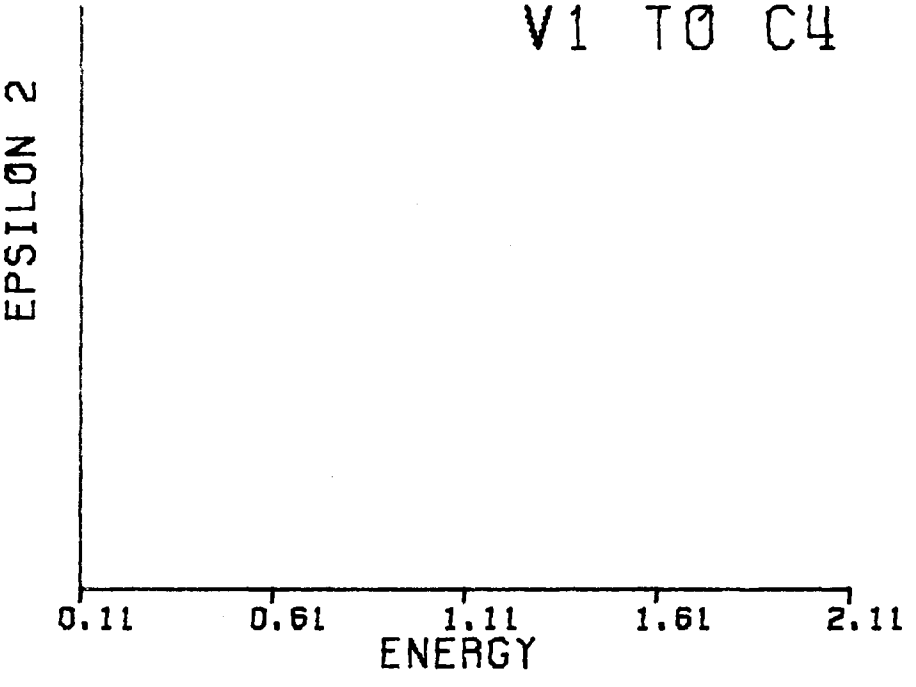
V1 TO C4
EPSILON 2
0.11
0.61
1.11
1.61
2.11
ENERGY

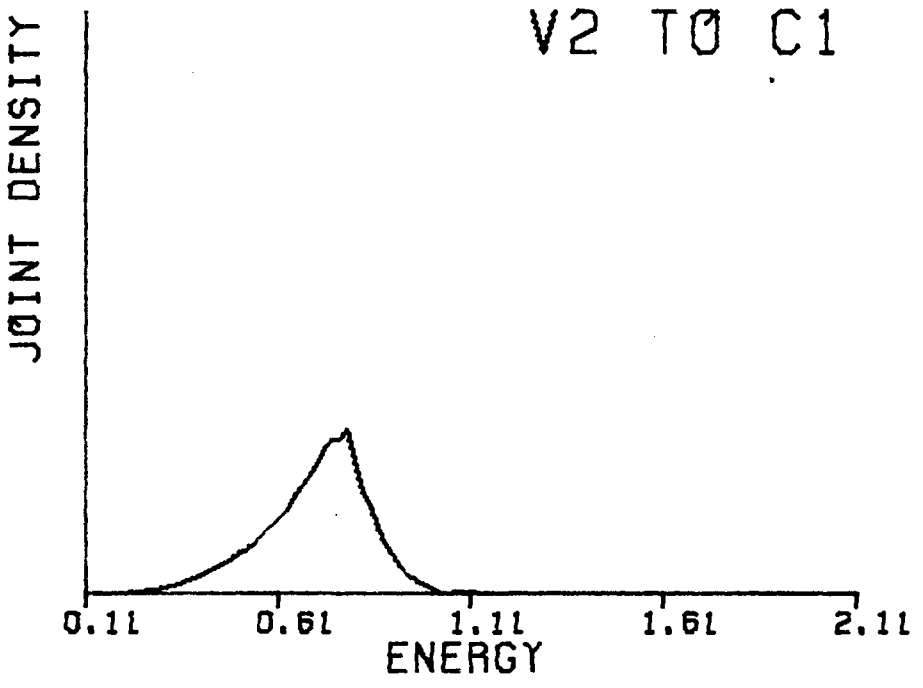
V2 TØ C1
JØINT DENSITY
0.11
0.61
1.11
1.61
2.11
ENERGY

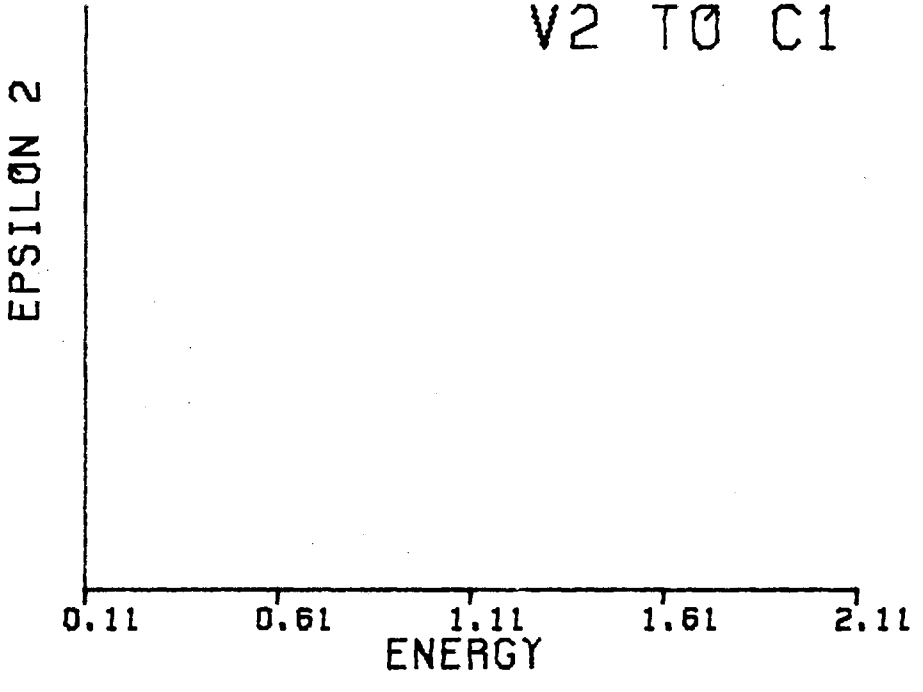
V2 TØ C1
EPSILØN 2
0.11
0.61
1.11
1.61
2.11
ENERGY

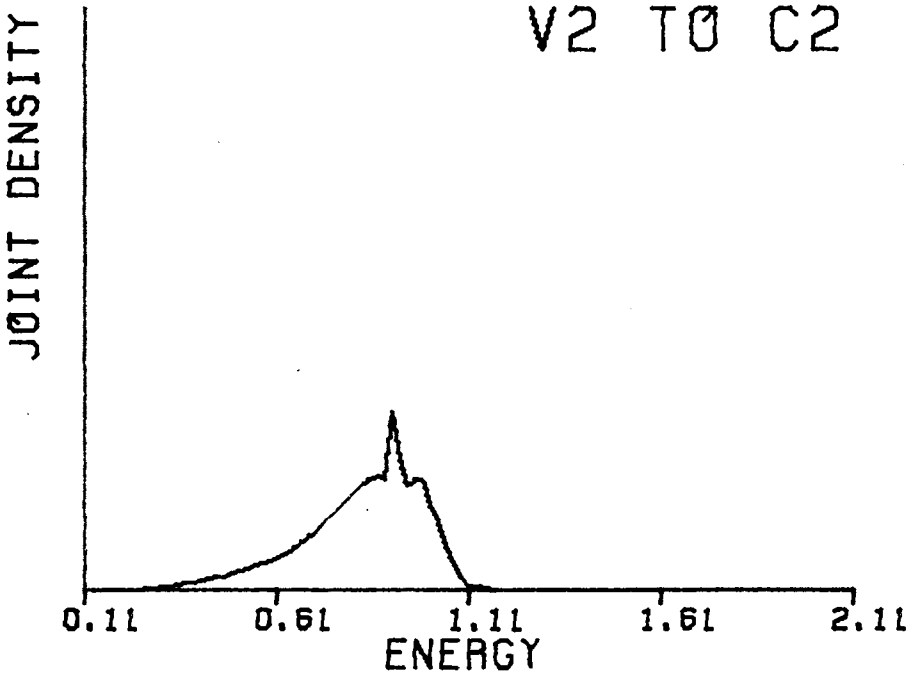
V2 T0 C2
JOINT DENSITY
0.11
0.61
1.11
1.61
2.11
ENERGY

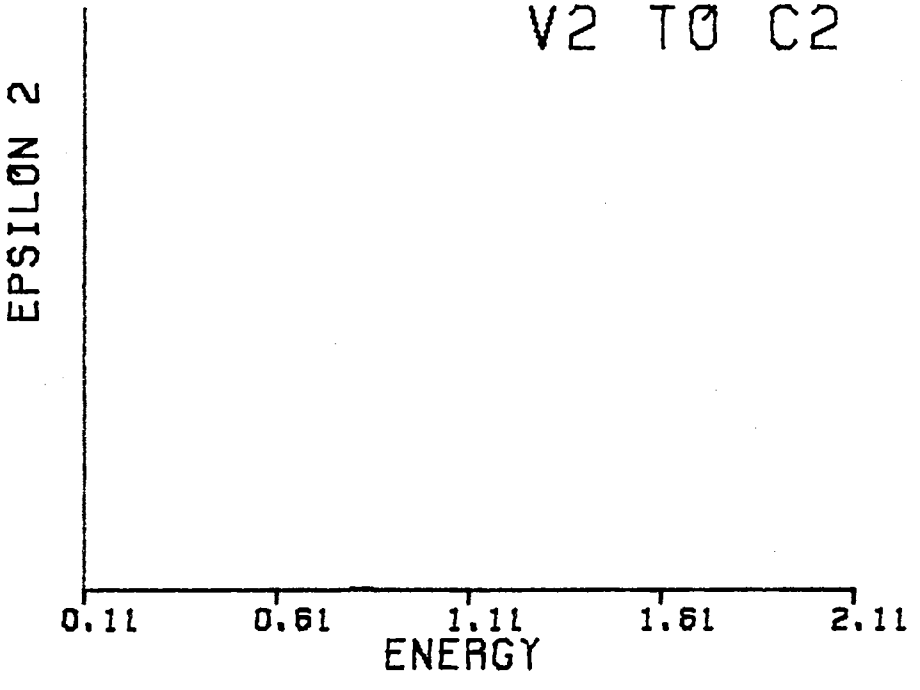
V2 T0 C2
EPSILON 2
0.11
0.61
1.11
1.61
2.11
ENERGY

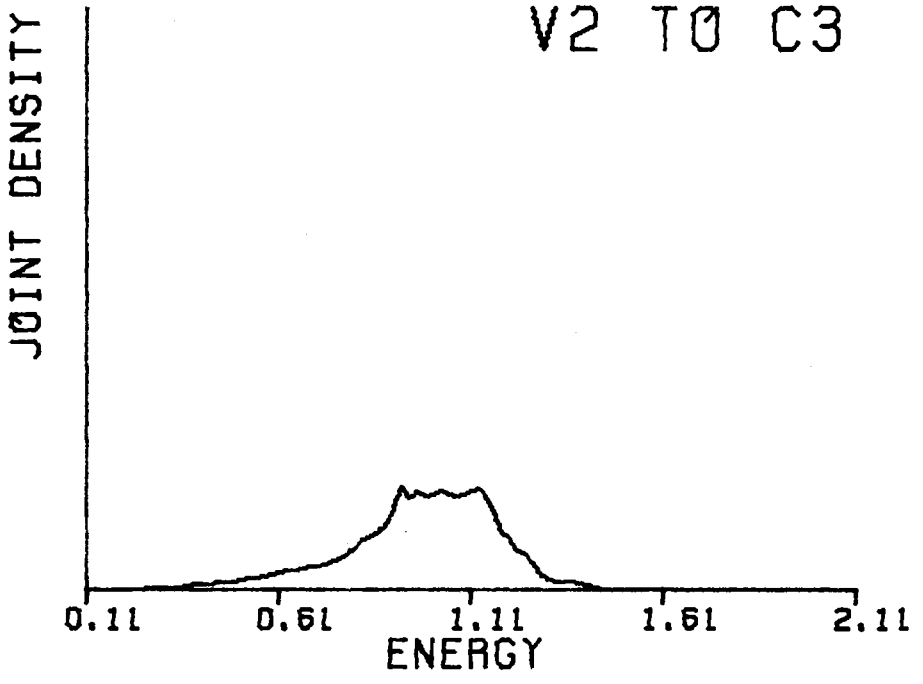
V2 T0 C3
JOINT DENSITY
0.11
0.61
1.11
1.61
2.11
ENERGY

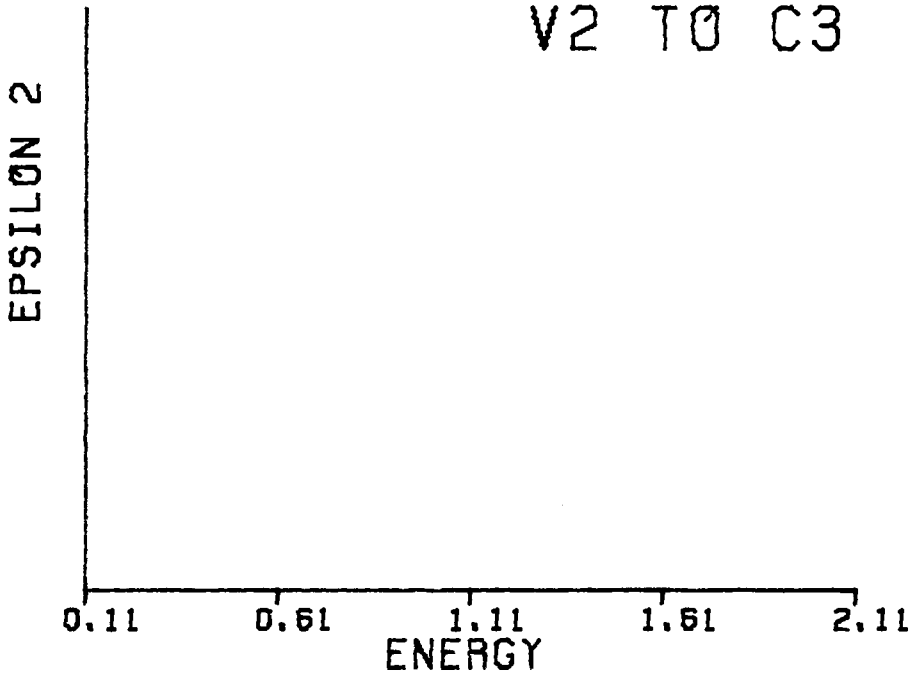
V2 T0 C3
EPSILON 2
0.11
0.61
1.11
1.61
2.11
ENERGY

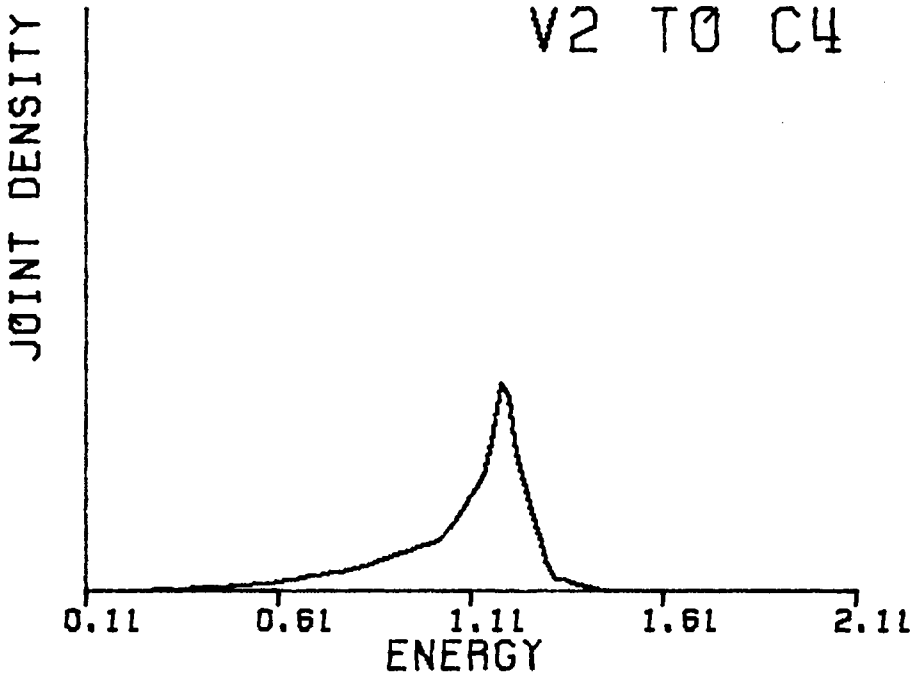
V2 TO C4
JOINT DENSITY
0.11
0.61
1.11
1.61
2.11
ENERGY

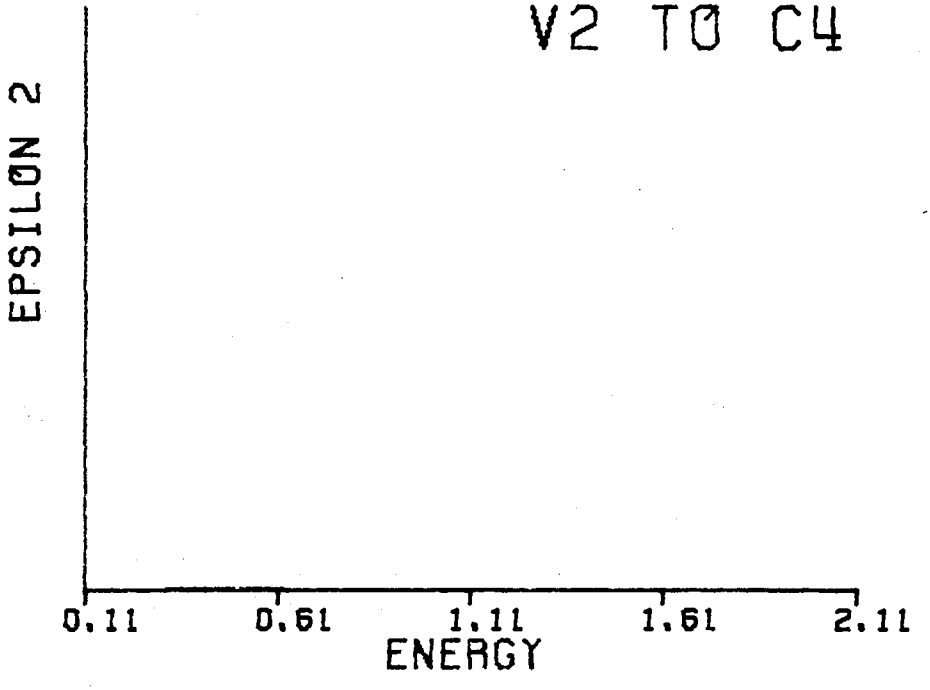
V2 TO C4
EPSILON 2
0.11
0.61
1.11
1.61
2.11
ENERGY

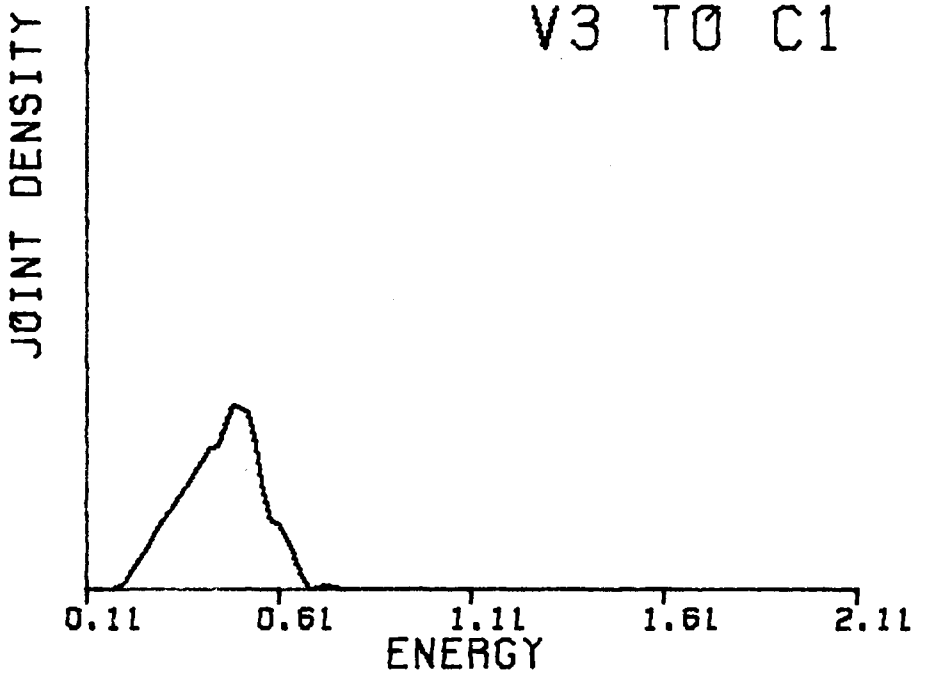
V3 T0 C1
JOINT DENSITY
0.11
0.61
1.11
1.61
2.11
ENERGY

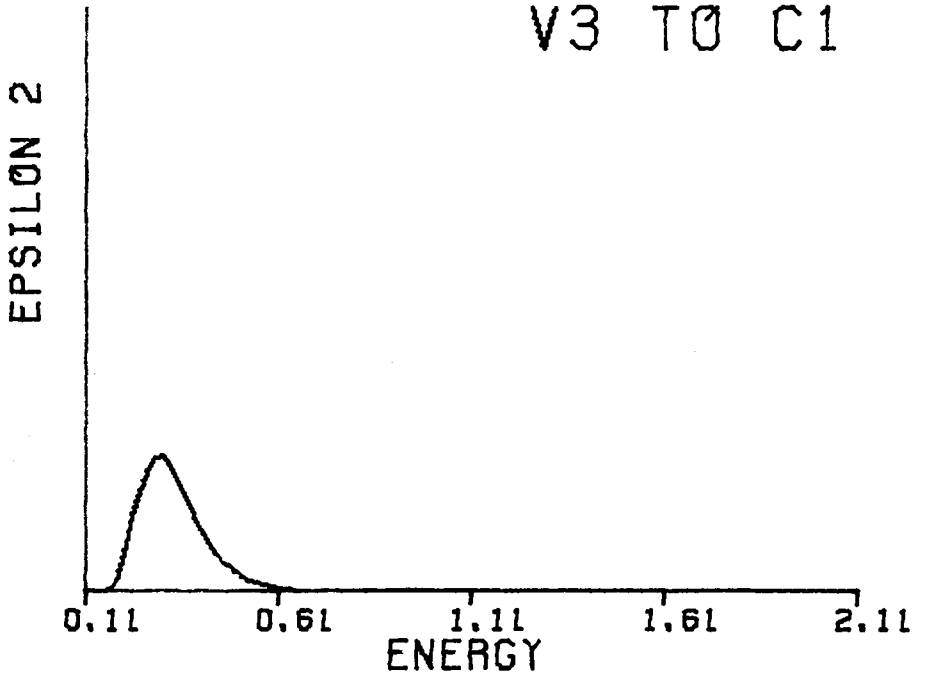
V3 T0 C1
EPSILON 2
0.11
0.61
1.11
1.61
2.11
ENERGY

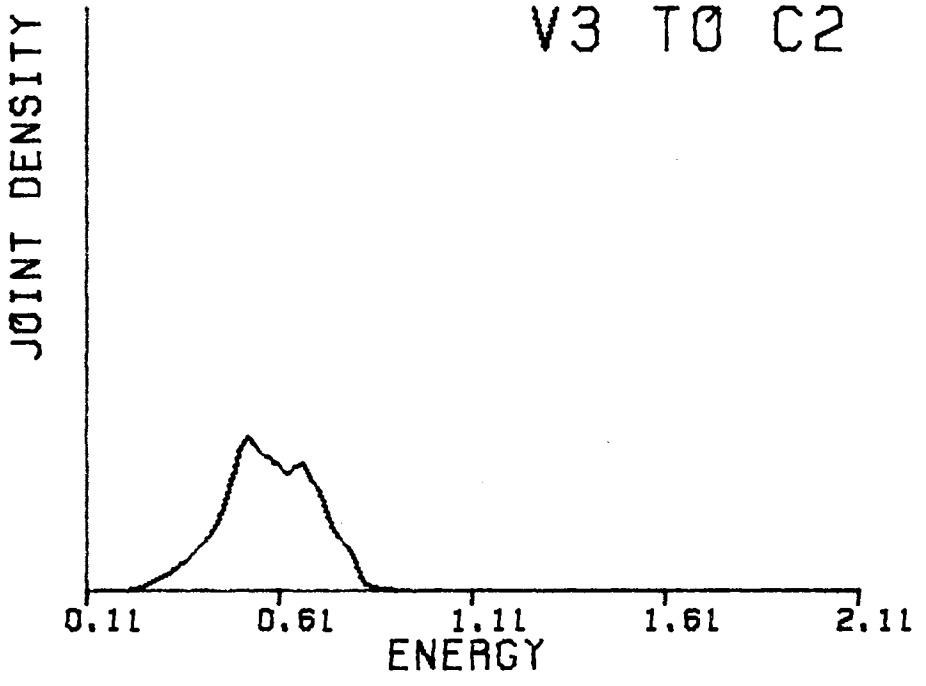
V3 TØ C2
JØINT DENSITY
0.11
0.61
1.11
1.61
2.11
ENERGY

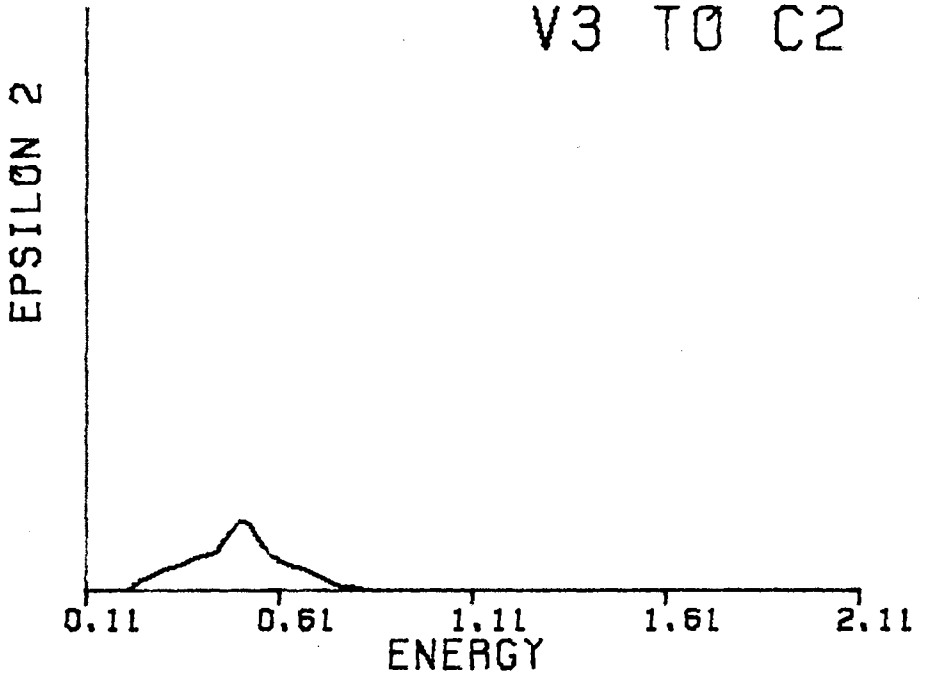
V3 TØ C2
EPSILØN 2
0.11
0.61
1.11
1.61
2.11
ENERGY

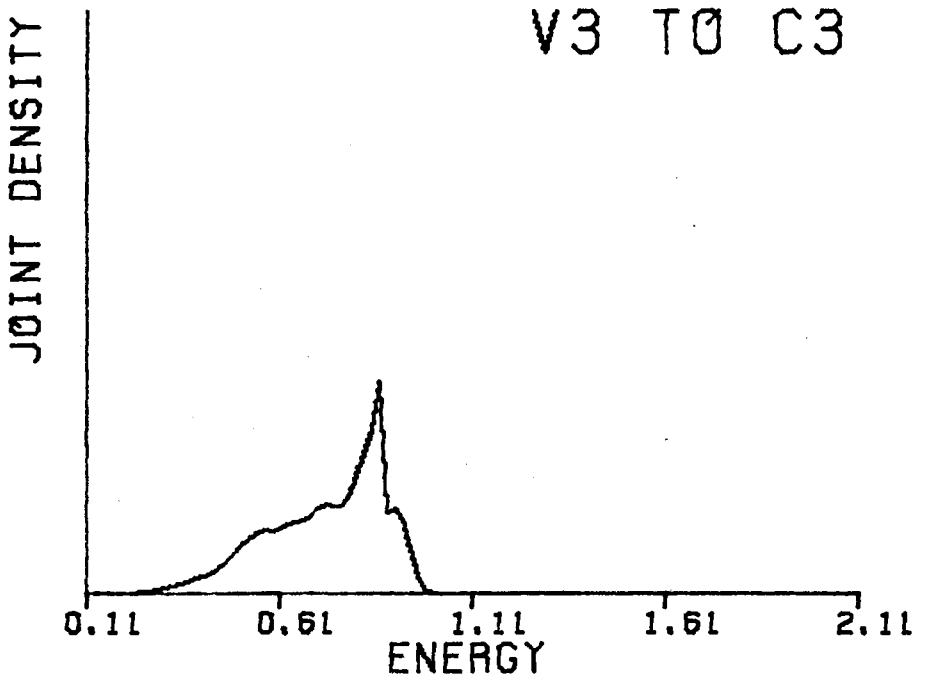
V3 T0 C3
JOINT DENSITY
0.11
0.61
1.11
1.61
2.11
ENERGY

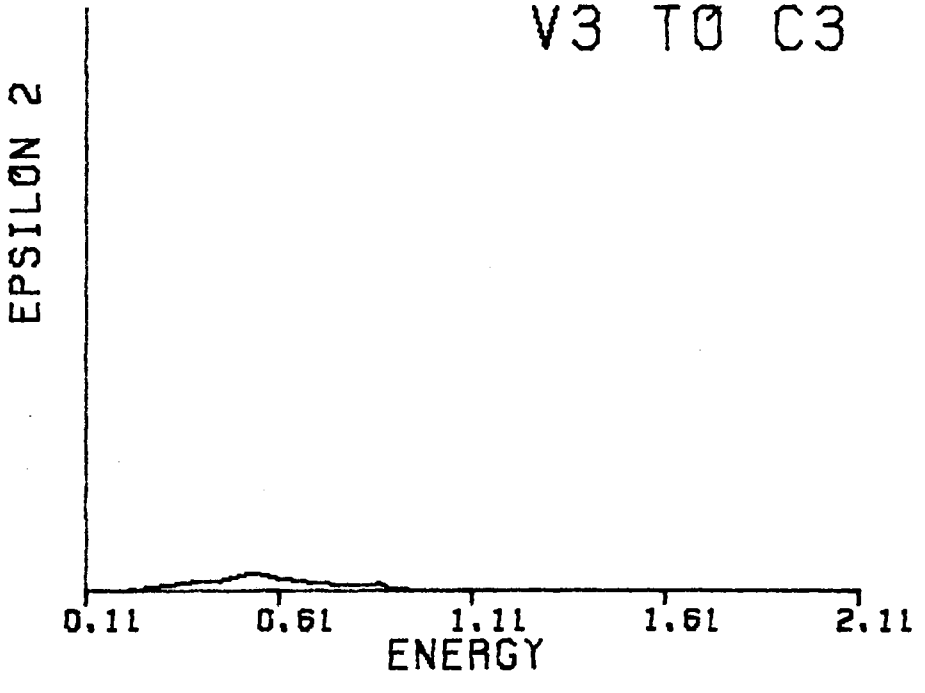
V3 T0 C3
EPSILON 2
0.11
0.61
1.11
1.61
2.11
ENERGY

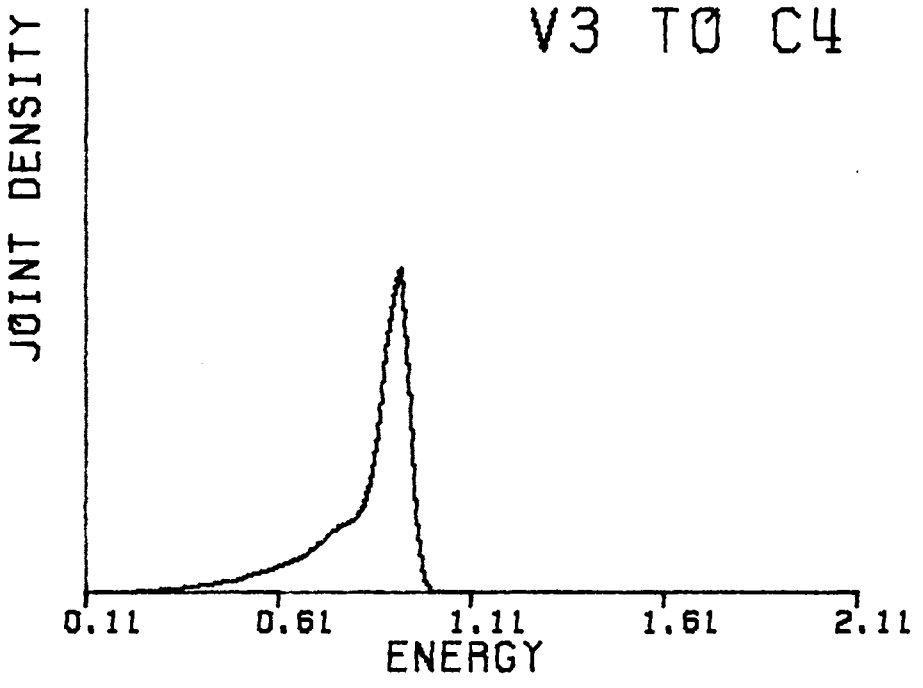
V3 TØ C4
JØINT DENSITY
0.11
0.61
1.11
1.61
2.11
ENERGY

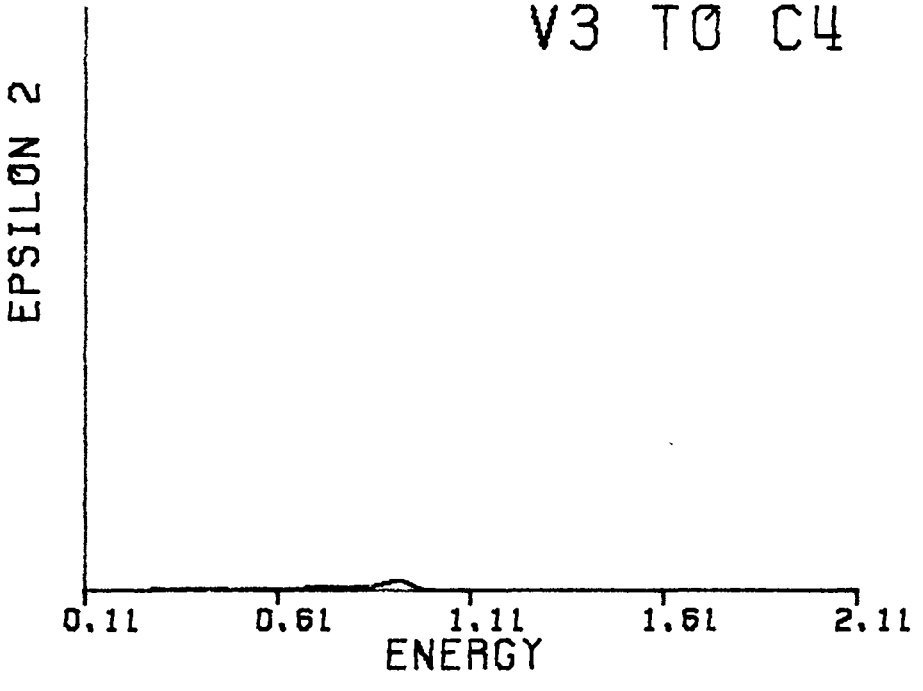
V3 TØ C4
EPSILØN 2
0.11
0.61
1.11
1.61
2.11
ENERGY

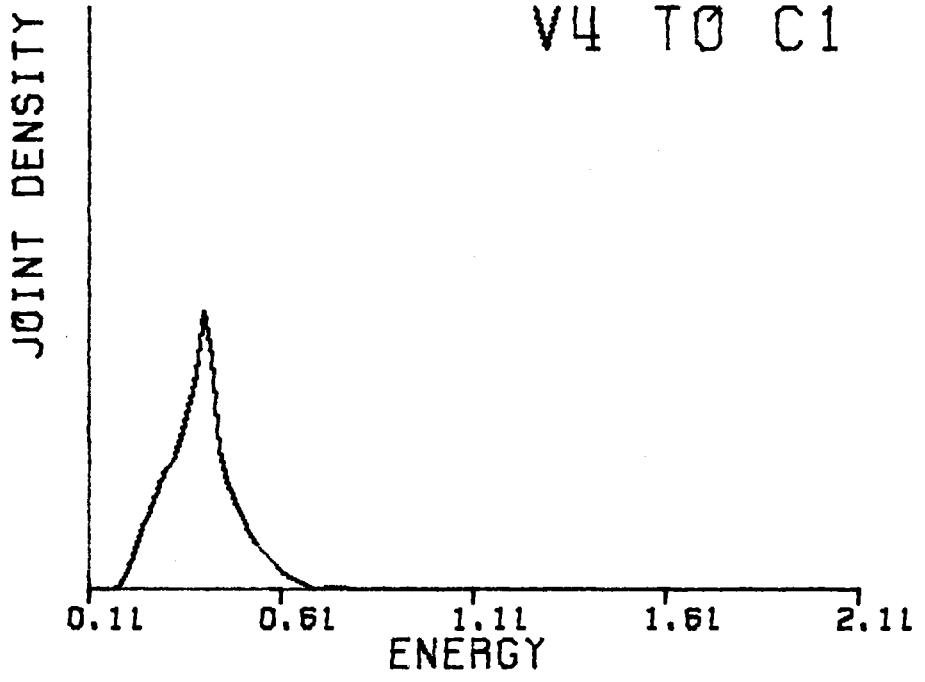
V4 TØ C1
JØINT DENSITY
0.11
0.61
1.11
1.61
2.11
ENERGY

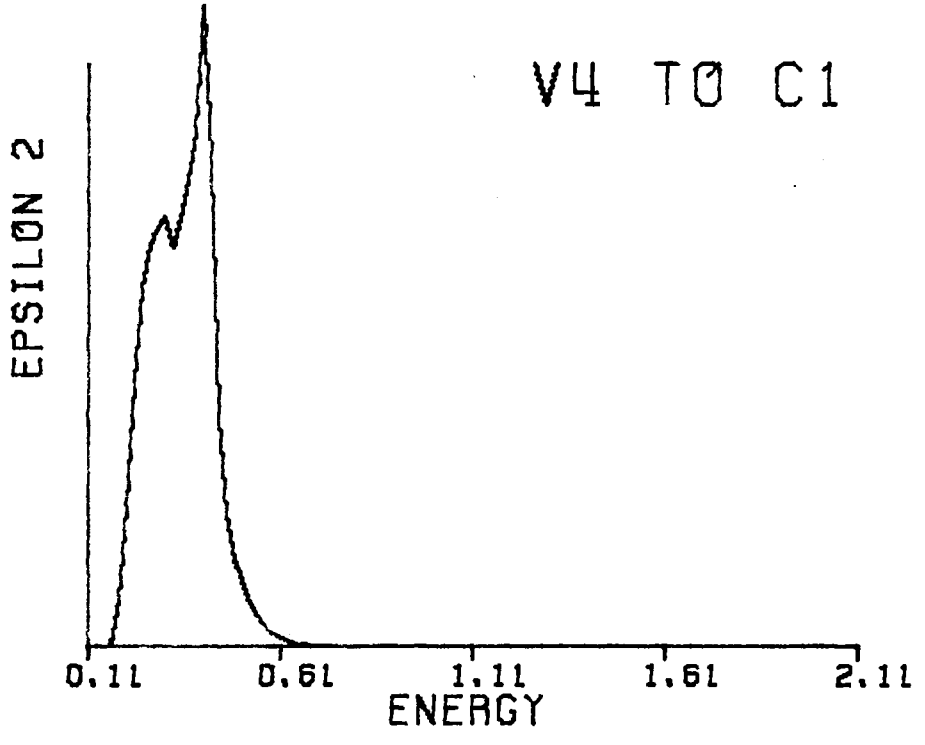
V4 TØ C1
EPSILØN 2
0.11
0.61
1.11
1.61
2.11
ENERGY

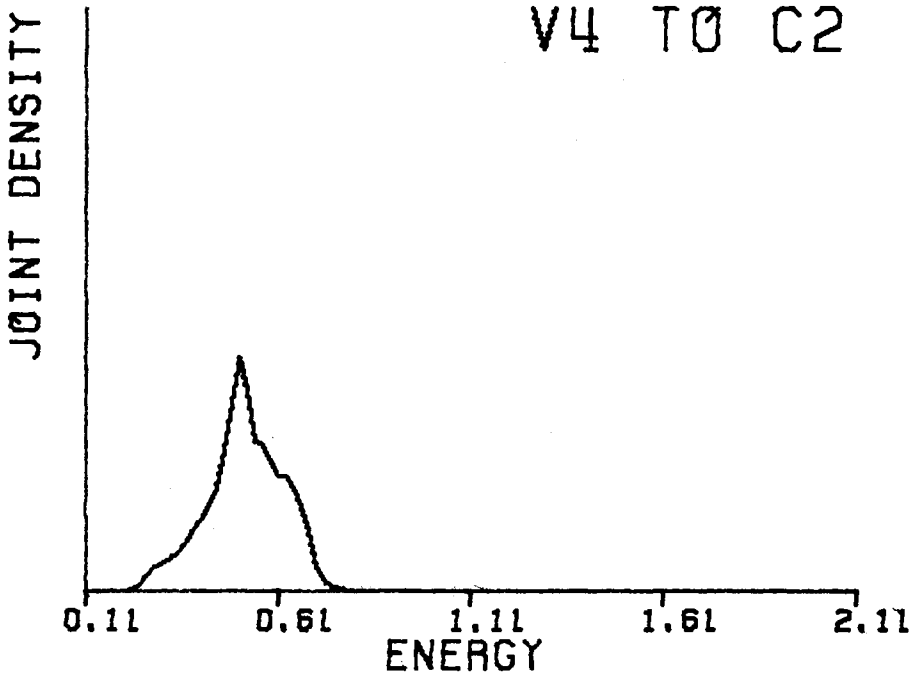
V4 TØ C2
JØINT DENSITY
0.11
0.61
1.11
1.61
2.11
ENERGY

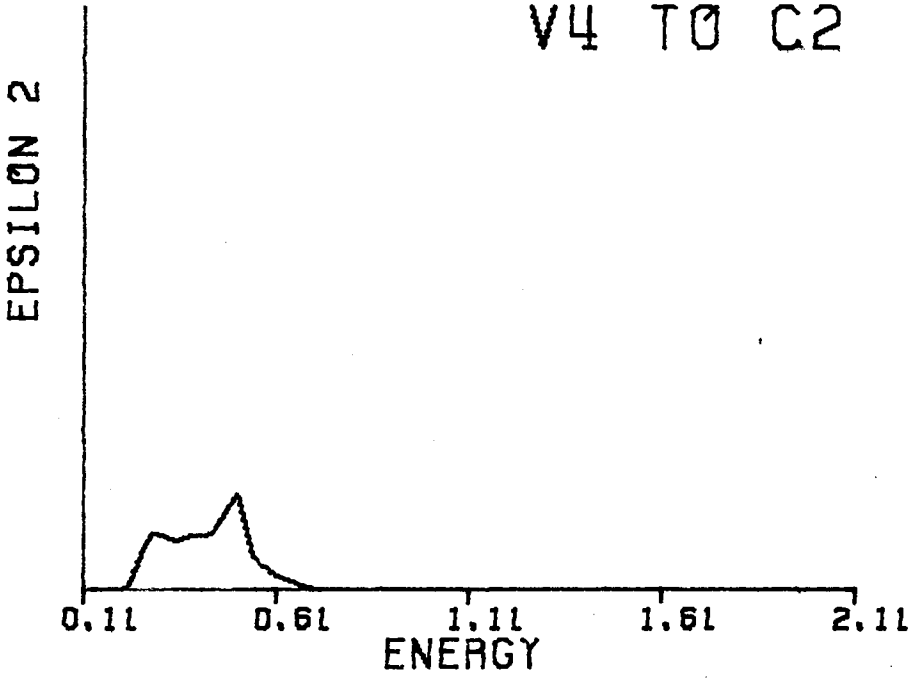
V4 TØ C2
EPSILØN 2
0.11
0.61
1.11
1.61
2.11
ENERGY

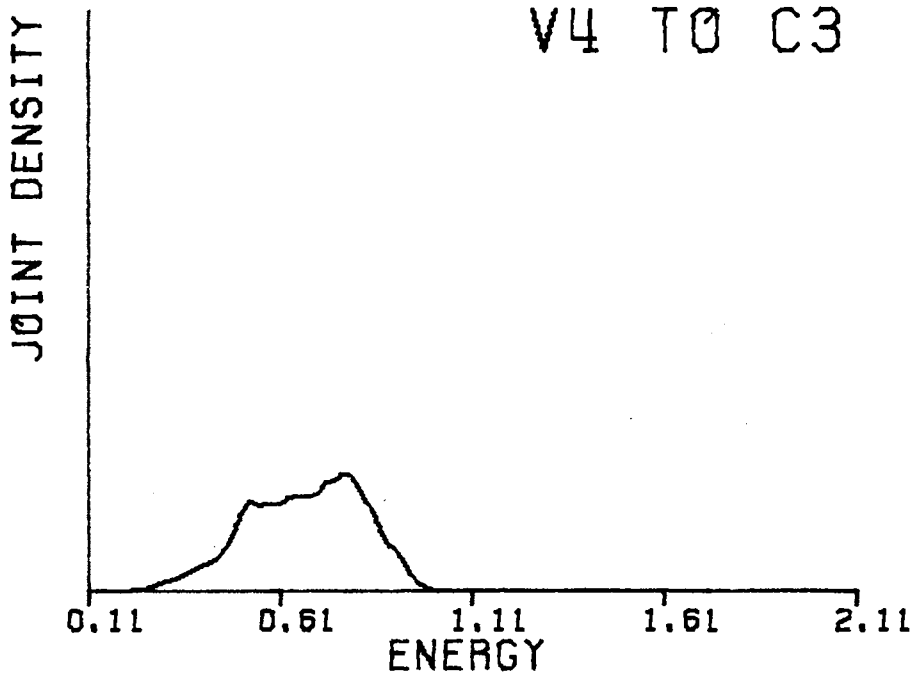
V4 TØ C3
JØINT DENSITY
0.11
0.61
1.11
1.61
2.11
ENERGY

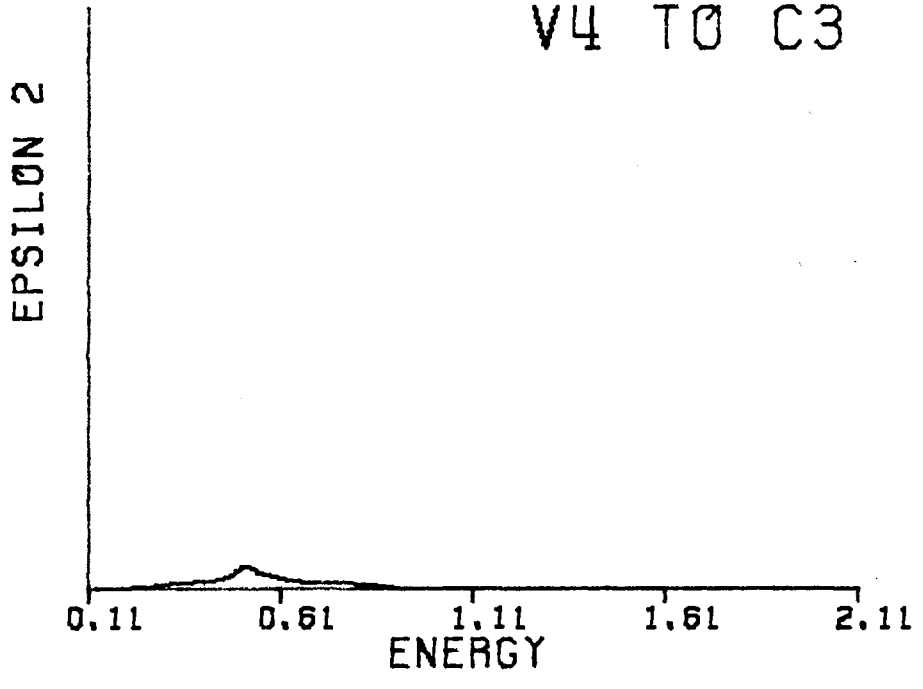
V4 TØ C3
EPSILØN 2
0.11
0.61
1.11
1.61
2.11
ENERGY

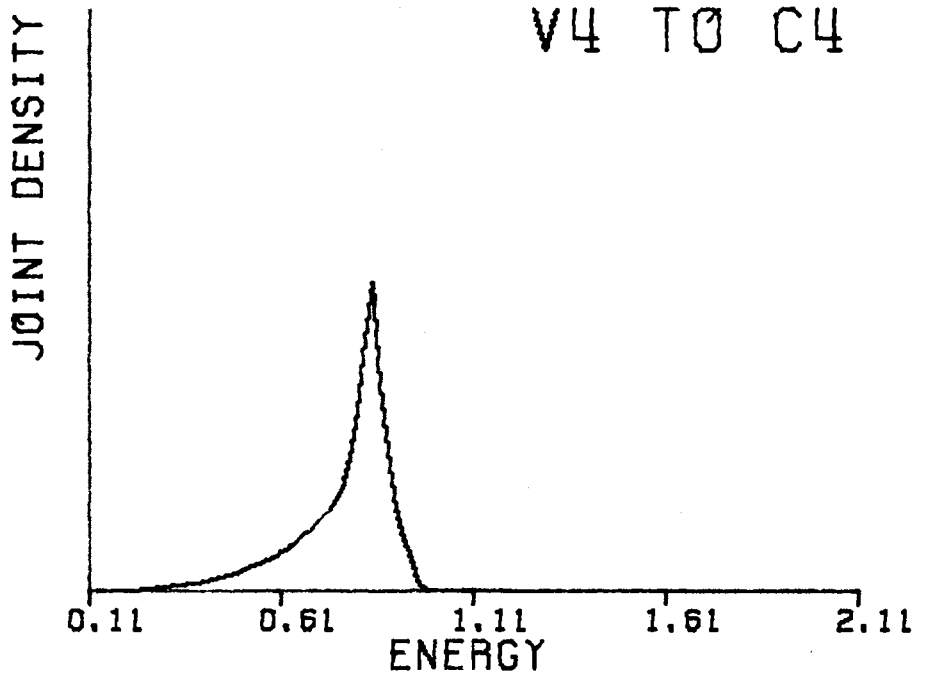
V4 TØ C4
JØINT DENSITY
0.11
0.61
1.11
1.61
2.11
ENERGY

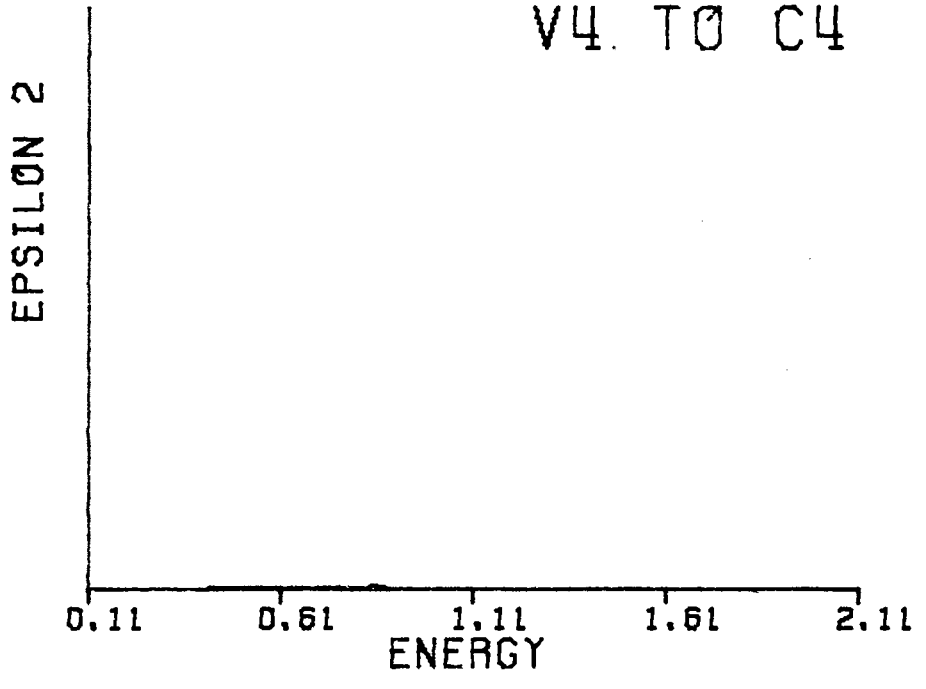
V4 TØ C4
EPSILØN 2
0.11
0.61
1.11
1.61
2.11
ENERGY

APPENDIX C

REDUCTION OF TRANSITION MATRIX ELEMENT MULTI-CENTER INTEGRALS TO OVERLAP INTEGRALS

The multi-center integrals to be reduced are taken from equation (3-11) and are given by

$$I'_{ij} = \int \phi_i(\bar{r}_A)\, \vec{\vec{\nabla}}\, \phi_j(\bar{r}_B)\, d\tau$$

where $\bar{r}_B = \bar{r}_A - \bar{R}$. The orbitals, ϕ_i, are defined in Chapter II by equation (2-17). By inserting the expressions for the orbitals and dropping the numerical coefficients, we have the type of integral to be done. For a particular i and j value the form of the integrals is given by

$$\vec{I} = \int x_A^{l} y_A^{m} z_A^{n} e^{-\alpha r_A^2}\, \vec{\vec{\nabla}}\, x_B^{l'} y_B^{m'} z_B^{n'} e^{-\beta r_B^2}\, d\tau$$

The necessary vector relationships are shown in figure 14.

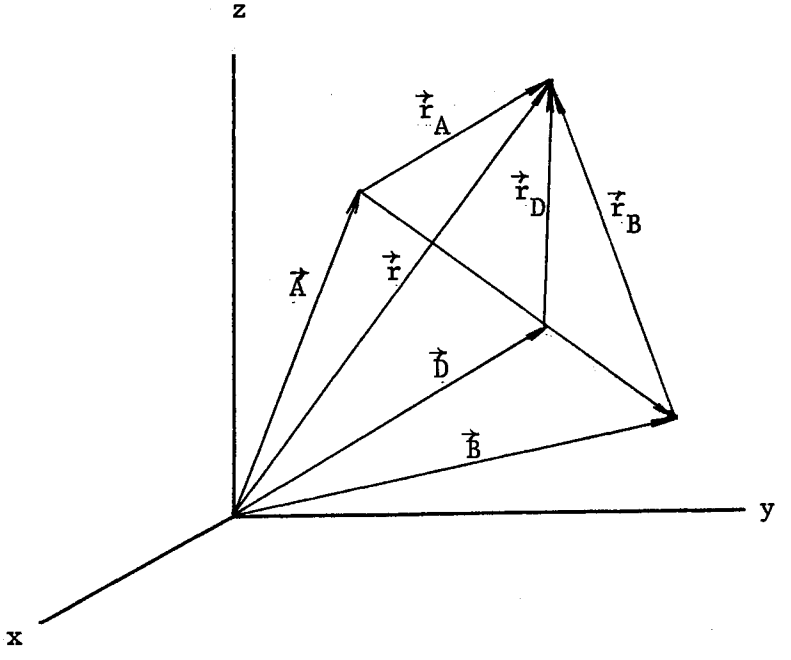

Figure 14. Relations between various vectors in the reduction of the gaussian orbitals.

Expanding the gradient operator into cartesian coordinates and then performing the operation, a sum of integrals is obtained such that

$$\vec{I} = I_x \hat{x} + I_y \hat{y} + I_z \hat{z},$$

where, for example, the x component is given by

$$I_x = l' \int X_A^{l} Y_A^{m} Z_A^{n} e^{-\alpha r_A^2} X_B^{l'-1} Y_B^{m'} Z_B^{n'} e^{-\beta r_B^2} d\tau$$
$$-2\beta \int X_A^{l} Y_A^{m} Z_A^{n} e^{-\alpha r_A^2} X_B^{l'+1} Y_B^{m'} Z_B^{n'} e^{-\beta r_B^2} d\tau$$

Using the following vector relationships,

$$e^{-\alpha r_A^2} e^{-\beta r_B^2} = e^{-H \overline{AB}^2} e^{-(\alpha+\beta) r_D^2}$$

where

$$H = \frac{\alpha+\beta}{\alpha\beta}, \quad \vec{D} = \frac{\alpha\vec{A}+\beta\vec{B}}{\alpha+\beta}, \quad \vec{r}_D = \vec{r} - \vec{D},$$

the x component integral then becomes

$$I_x = e^{-H\overline{AB}^2} \int X_A^{l} Y_A^{m} Z_A^{n} (l' - 2\beta X_B^2) X_B^{l'-1} Y_B^{m'} Z_B^{n'} e^{-(\alpha+\beta) r_D^2} d\tau.$$

The components of the vectors $\overline{A}$ and $\overline{B}$ can be expressed in terms of the $\overline{D}$ vector in the following manner,

$$X_A = X - A_x = X_D + D_x - A_x = X_D + \overline{AD}_x,$$
$$X_B = X - B_x = X_D + D_x - B_x = X_D + \overline{BD}_x.$$

The integral can now be expressed in terms of the components of the $\overline{r}$

and $\overline{D}$ vectors. The integral for the x component becomes

$$I_x = l' e^{-H\overline{AB}^2} \int (x+\overline{AD}_x)^{l} (y+\overline{AD}_y)^{m} (z+\overline{AD}_z)^{n} (x+\overline{BD}_x)^{l'-1} (y+\overline{BD}_y)^{m'} (z+\overline{BD}_z)^{n'} e^{-(\alpha+\beta) r_D^2} d\tau$$

$$- 2\beta e^{-H\overline{AB}^2} \int (x+\overline{AD}_x)^{l} (y+\overline{AD}_y)^{m} (z+\overline{AD}_z)^{n} (x+\overline{BD}_x)^{l'+1} (y+\overline{BD}_y)^{m'} (z+\overline{BD}_z)^{n'} e^{-(\alpha+\beta) r_D^2} d\tau.$$

This integral and similar one for the y and z components are overlap integrals of the type found in the secular equation. The gradient matrix elements can now be written as a sum of overlap integrals.

The overlap integrals have traditionally been found by taking derivatives of overlap integrals involving lower angular momentum states, with the 1s-1s overlap integral being done analytically. But because evaluation of the gradient matrix elements involves an overlap integral of angular momentum one level higher than is found in the corresponding secular equation, another method of calculating overlap integrals has been devised.

The overlap integrals needed are of the form

$$I_s = \int (x+\overline{AD}_x)^{l} (y+\overline{AD}_y)^{m} (z+\overline{AD}_z)^{n} (x+\overline{BD}_x)^{l'} (y+\overline{BD}_y)^{m'} (z+\overline{BD}_z)^{n'} e^{-\gamma r_D^2} d\tau.$$

By using the binomial expansion of the type

$$(x+y)^N = \sum_M \binom{N}{M} y^{N-M} x^M$$

on each term yields

$$I_s = \sum_{\substack{r,s,t \\ r',s',t'}} \binom{l}{r}\binom{m}{s}\binom{n}{t}\binom{l'}{r'}\binom{m'}{s'}\binom{n'}{t'} (\overline{AD}_x)^{l-r} (\overline{AD}_y)^{m-s} (\overline{AD}_z)^{n-t}$$

$$(\overline{BD}_x)^{l'-r'} (\overline{BD}_y)^{m'-s'} (\overline{BD}_z)^{n'-t'} \int x^{r+r'} e^{-\gamma x^2} dx$$

$$\int y^{s+s'} e^{-\gamma y^2} dy \int z^{t+t'} e^{-\gamma z^2} dz \; e^{-H\overline{AB}^2}.$$

The integral portions can now be solved analytically, the solutions being

$$Z_N = \int x^N e^{-\gamma x^2} dx = \frac{1 \cdot 3 \cdot 5 \cdots (N-1)}{(2\gamma)^{N/2}} \sqrt{\frac{\pi}{\gamma}}.$$

Then using the vector relations

$$\overrightarrow{AD} = \frac{\beta}{\alpha+\beta} \overrightarrow{AB}, \qquad \overrightarrow{BD} = \frac{-\alpha}{\alpha+\beta} \overrightarrow{AB},$$

the overlap integral can be written as

$$I_s = \left(\frac{\beta}{\alpha+\beta}\right)^{l+m+n} \left(\frac{-\alpha}{\alpha+\beta}\right)^{l'+m'+n'} \overline{AB}_x^{\,l+l'} \overline{AB}_y^{\,m+m'} \overline{AB}_z^{\,n+n'} e^{-H\overline{AB}^2}$$

$$\sum_{r,s,t,r',s',t'} \binom{l}{r}\binom{m}{s}\binom{n}{t}\binom{l'}{r'}\binom{m'}{s'}\binom{n'}{t'} \overline{AB}_x^{-(r+r')} \overline{AB}_y^{-(s+s')} \overline{AB}_z^{-(t+t')}$$

$$\left(\frac{\beta}{\alpha+\beta}\right)^{-(r+s+t)} \left(\frac{\alpha}{\alpha+\beta}\right)^{-(r'+s'+t')} Z_{r+r'}(\gamma)\, Z_{s+s'}(\gamma)\, Z_{t+t'}(\gamma).$$

The sum indices are changed by letting

$$\lambda_1 = r + r' \quad , \quad \lambda_2 = s + s' \quad , \quad \lambda_3 = t + t'$$

to eliminate r',s' and t'. The defining a set of B values in the following manner

$$B_\lambda^{jj'}\left(\frac{\beta}{\alpha+\beta}\right) = \sum_\sigma \binom{j}{\sigma}\binom{j'}{\lambda-\sigma}(-1)^{\lambda-\sigma}\left(\frac{\alpha}{\beta}\right)^\sigma\left(\frac{\alpha+\beta}{\alpha}\right)^\lambda$$

enables one to write the overlap integral as

$$I_s = \left(\frac{\beta}{\alpha+\beta}\right)^{l+m+n}\left(\frac{-\alpha}{\alpha+\beta}\right)^{l'+m'+n'}\overline{AB}_x^{\,l+l'}\,\overline{AB}_y^{\,m+m'}\,\overline{AB}_z^{\,n+n'}\,e^{-H\overline{AB}^2}$$

$$\sum_{\lambda_1,\lambda_2,\lambda_3} B_{\lambda_1}^{ll'}\left(\frac{\beta}{\alpha+\beta}\right) B_{\lambda_2}^{mm'}\left(\frac{\beta}{\alpha+\beta}\right) B_{\lambda_3}^{nn'}\left(\frac{\beta}{\alpha+\beta}\right)$$

$$\overline{AB}_x^{-\lambda_1}\,AB_y^{-\lambda_2}\,AB_z^{-\lambda_3}\,Z_{\lambda_1}(\gamma)\,Z_{\lambda_2}(\gamma)\,Z_{\lambda_3}(\gamma)\,.$$

This expression for the overlap integrals can be easily evaluated for all values of angular momentum.

VITA

Doyle Frank Fouquet

Candidate for the Degree of

Master of Science

Thesis: FIRST PRINCIPLES CALCULATION OF THE IMAGINARY PORTION OF THE DIELECTRIC FUNCTION FOR DIAMOND AND SILICON

Major Field: Physics

Biographical:

Personal Data: Born in Lincoln County, Oklahoma, October 9, 1943, the son of Mr. and Mrs. Frank Fouquet, Jr.

Education: Graduated from Prague High School, Prague, Oklahoma, in 1961; received the Bachelor of Science degree from Oklahoma State University, Stillwater, Oklahoma, with a major in Physics, in January, 1970; completed requirements for the Master of Science degree in July, 1973.